CONSTRAINING THE NORTHERN HEMISPHERE MID-LATITUDE JET RESPONSE TO CLIMATE CHANGE USING THE DIFFERENCE BETWEEN ARCTIC AND SUBTROPICAL WARMING

by

Rachel Maya Robinson

A thesis submitted to the faculty of
The University of North Carolina at Charlotte
in partial fulfillment of the requirements
for the degree of Master of Science in
Earth Science

Charlotte

2021

Approved by:

_____
Dr. Jacob Scheff

_____
Dr. Casey Davenport

_____
Dr. Brian Magi

ABSTRACT

RACHEL MAYA ROBINSON. Constraining the Northern Hemisphere Mid-Latitude Jet Response to Climate Change Using the Difference Between Arctic and Subtropical Warming
(Under the direction of DR. JACOB SCHEFF)

Greenhouse gases' continuously increasing emissions have a variety of implications for the future of our climate patterns. This includes potential changes in the northern hemisphere jet strength and location, which are influenced by the warming in the subtropics and the Arctic. Many climate models disagree on the northern jet response to climate change. Some predict a strengthened jet with a poleward shift in response to increased subtropical warming, and others predict a weakened jet with an equatorward shift in response to increased Arctic warming. This results in the "tug-of-war" hypothesis, which states that whichever part of the atmosphere, the subtropics or the Arctic, "wins" the tug-of-war by warming more will control the future jet response. This study applies the newer Coupled Model Intercomparison Project Phase 6 (CMIP6) simulations to replicate previous analysis that used the correlation of the difference between upper-tropospheric subtropical warming and Arctic warming with zonal wind speed to predict models' future jet response. This study also furthers previous research by comparing reanalysis and microwave sounding unit (MSU) observations over the satellite era to the historical CMIP6 output to determine how well individual models capture the recent historical trends in Arctic minus subtropical warming and the change in jet speed. By understanding how each model performs over the satellite era, the validity of their warming and jet response is determined, illuminating the models that are more trustworthy and allowing predictions of the future jet response to be refined.

The findings of this study show that CMIP6 follows the same pattern as previous research, further showing that the Arctic minus subtropical warming difference and the zonal wind change are strongly correlated, and the warming difference is useful as a predictor of future jet response. Repeating this analysis over the satellite era from 1980-2014 shows the correlation exists over recent modeled history as well. The CMIP6 historical simulations are capturing the recent trends in the warming difference between the Arctic and the subtropics better than earlier CMIP generations. However, they still fail to capture the magnitude of this difference by continuing to underestimate the warming in the Arctic. Comparing the historical simulations to reanalysis output and satellite MSU data allows us to discard 8 out of 45 models based on the methods of this study. With so few of the models discarded, this further emphasizes that the models appear to be performing better than they were before. However, many of the same models that show increased warming in the Arctic over the satellite era still tend to produce more warming in the tropics and subtropics in the future, suggesting that a future where the tropics win the tug-of-war may be consistent with the current trends that the Arctic is winning the tug-of-war.

DEDICATION

This thesis work is dedicated to the memory of my dad, Rev. Randall Craig Robinson. Although he helped inspire a love for the wonders of nature in me from a young age, he was unable to witness my graduation with my Masters. I will always carry his unconditional support and love in my heart.

I also dedicate this work to my mom, Brenda Robinson, for always loving and supporting me and providing words of encouragement when I needed them the most. She is the most kind, understanding, and strong woman I've ever met, and her example has helped me grow into a person who never gives up, no matter how hard things get.

ACKNOWLEDGEMENTS

We would like to acknowledge the modeling groups that participated in the World Climate Research Program's CMIP6 project and made their model output available. We would also like to acknowledge Stephen Po-Chedley of Lawrence Livermore National Laboratory for providing satellite MSU and synthetic MSU temperature data. I would like to thank my advisor, Dr. Scheff, for his guidance on my thesis work, as well as his support and encouragement through all the ups and downs of the past two years. I would also like to thank my committee members, Dr. Davenport and Dr. Magi, for their support in this process. I would also like to thank my significant other, Jan Ising, for his love, support, and especially his patience. I wouldn't have finished this study if it weren't for his help pushing me to keep going. I would also like to thank my friends Caitlin, Charlie, and Daniel for never letting me forget my worth, that I could do this, and helping me keep my confidence up to follow through.

TABLE OF CONTENTS

LIST OF TABLES

LIST OF FIGURES

CHAPTER ONE: INTRODUCTION AND BACKGROUND

The Northern Hemisphere mid-latitude jet stream is driven in large part by the equator-pole temperature gradient and is responsible for the extratropical cyclones that provide essential precipitation to the mid-latitudes and drive heat, momentum, and moisture transport throughout the atmosphere (Harvey et al. 2015). However, these cyclones often generate extreme weather events as well, such as winter storms, floods, droughts, heat or cold waves, and severe outbreaks. Indisputably, the strength and location of the jet are anticipated to change in a warmed climate, but how these changes will manifest is not well defined. Due to the jet's high impact on mid-latitude weather, understanding the future jet response is crucial (Francis and Vavrus 2015, Francis 2017, Matsumura 2019).

A few possible responses of the jet to climate change have been found throughout climate model studies. One response is a poleward shift of the jet, with a similar shift of the mid-latitude storm track (Butler et al. 2010, Ceppi and Hartmann 2016, Deser et al. 2015, Yim et al. 2016, Shaw and Tan 2018, Peings et al. 2018). This response is often associated with an increase in zonal wind speed, resulting in a less wavy jet pattern. The poleward shift, increase in jet strength, and decrease in waviness are also signatures of a positive North Atlantic Oscillation (NAO)/Arctic Oscillation (AO) (Feldstein and Lee 2014).

In contrast, another response of the jet to climate change is an equatorward shift of the jet and mid-latitude storm track (Butler et al. 2010; Barnes and Polvani 2015; Deser et al. 2015; Ceppi and Hartmann 2016; Yim et al. 2016; Shaw and Tan 2018;

Peings et al. 2018). As expected, this response exhibits features opposite to those mentioned above. In accordance with a negative NAO/AO, it is accompanied by a decrease in zonal wind speed, leading to a wavier jet pattern (Feldstein and Lee 2014; Barnes and Polvani 2015, Francis and Vavrus 2015).

The poleward shift and strengthening of the mid-latitude jet have been attributed to increased warming aloft in the tropical upper troposphere (Butler et al. 2010; Ceppi and Hartmann 2016; Deser et al. 2015; Yim et al. 2016; Shaw and Tan 2018; Peings et al. 2018), though Shaw and Tan (2018) found the subtropical upper troposphere plays a larger role than the tropics. Lower-stratospheric cooling in the Arctic has also been shown to cause a poleward shift of the jet (Butler et al. 2010; Deser et al. 2015; Yim et al. 2016; Shaw and Tan 2018; Peings et al. 2018). Conversely, the equatorward shift and weakening of the mid-latitude jet has been attributed to increased warming near the Arctic surface (Butler et al. 2010; Barnes and Polvani 2015; Deser et al. 2015; Ceppi and Hartmann 2016; Yim et al. 2016; Shaw and Tan 2018; Peings et al. 2018). This increased warming in relation to the rest of the planet is known as Arctic Amplification (Francis and Vavrus 2012).

The waviness of the jet, its link to Arctic Amplification, and its effect on mid-latitude weather are points of contention among the climate science community. As noted above, Arctic Amplification is thought to drive the equatorward shift and weakening of the jet. Some studies have shown that this scenario increases the waviness of the jet. This causes increased blocking events which lead to an increasing number of prolonged extreme weather events in the mid-latitudes. The opposite scenario caused by increased tropical warming would result in a less wavy jet, with less blocking events to incite

extreme weather (Barnes and Screen 2015, Coumou et al. 2014, Francis and Vavrus 2012). However, some studies such as Trenberth et al. (2014) have not found evidence of a robust connection between Arctic Amplification and mid-latitude weather. Various studies have found that Arctic Amplification actually has the opposite effect on mid-latitude weather, decreasing chances of extreme events, particularly in the winter (Wallace et al. 2014, Schneider et al. 2014, Screen 2014, Screen et al. 2014). Other studies determined that the apparent connection between Arctic Amplification and mid-latitude weather cannot be distinguished from internal variability (Barnes et al. 2014, Sun et al. 2016, Screen et al. 2018, Staten et al. 2018). Though the equatorward (poleward) shift and weakening (strengthening) of the jet is often associated with a negative (positive) NAO, Hassanzadeh and Kuang (2015) caution against using the phase of the NAO to determine trends in the waviness of the jet due to Arctic Amplification. They warn that the link between the phase of the NAO and atmospheric blocking is still not well understood and should not be mistaken for a causal relationship.

The balance between the warming of the tropical upper troposphere and the Arctic lower troposphere is the premise of the tug-of-war hypothesis. It states that whichever part of the atmosphere warms more in the future, the tropical upper troposphere or the Arctic lower troposphere, should determine the future jet response. With both jet responses having different possible effects on the weather, the tug-of-war hypothesis has significant implications for the future of mid-latitude weather patterns. Thus, accurately projecting the future jet change in climate models is important for our understanding of the effects of climate change on mid-latitude weather. However, there is evidence that the behavior of the jet in climate models is at odds with observations. Most climate models

project a jet shift consistent with the tropics warming more (Yin 2005, Butler et al. 2010, Delcambre et al. 2013, Lorenz 2014, Lachmy and Shaw 2018, Screen et al. 2018), but observational studies indicate that the Arctic may be warming more (Graversen et al. 2008, Santer et al. 2013, Feldstein and Lee 2014, Francis and Vavrus 2015, Manney and Hegglin 2018, Santer et al. 2018).

Most model-based studies find a poleward shift and/or strengthening of the jet in response to climate change, associated with the tropics winning the tug-of-war. As an early example, Yin (2005) examined storm tracks in 15 coupled climate models. Storm tracks were found to shift poleward, typically coinciding with a poleward shift in momentum flux convergence that should result in a similar shift in the jet. Lorenz and DeWeaver (2007) found a strengthening and poleward shift of the jet in the models prepared for the Intergovernmental Panel on Climate Change Fourth Assessment Report. They found a similar jet response in a simple general circulation model (GCM) after increasing the height of the tropopause. More recently, Barnes and Polvani (2013) investigated the changes in jet position, speed, and variability using 26 models from phase 5 of the Coupled Model Intercomparison Project (CMIP5). They found a 1˚ poleward shift in the Northern Hemisphere jets, but little change in the jet speed. Variability in jet speed and wobbling changes as the jet shifts poleward, but the changes are region dependent. In modeling the impact of cloud radiative effects on the future jet, both Ceppi and Hartmann (2016) and Li et al. (2019) ran simulations of a future climate that produced a poleward shift in the jet, which was strengthened by the inclusion of cloud radiative effects. Harvey et al. (2020) compared the response of the jet to climate

change in CMIP3, CMIP5, and CMIP6, showing that they all exhibit a similar poleward shift in the jet.

However, studies based on observations and reanalysis of the satellite era reveal evidence that the Arctic may be winning the tug-of-war. Feldstein and Lee (2014) noted that the AO had been positive for about 20 years prior to the 1990's, consistent with the tropics warming more. After that, the AO started to decline, finally becoming negative around 2010 which is consistent with the Arctic warming more. This coincided with a sharp decline in sea ice, a significant driver of the Arctic Amplification that is hypothesized to cause the equatorward shift in the jet stream (Feldstein and Lee 2014, Francis and Vavrus 2015). Manney and Hegglin (2018) analyzed jet changes for 1980-2014 in five different reanalyses. They found an equatorward shift and weakening of the mid-latitude jet, though the speed was seasonally and regionally dependent. These results are consistent across the reanalyses, indicating the trends are robust.

The discussion surrounding the competition between the Arctic and the tropics has focused specifically on the warming of the Arctic near the surface and of the upper troposphere in the tropics. The Arctic upper troposphere is typically not considered, as most of the warming in the Arctic occurs near the surface (Lorenz 2014, Barnes and Screen 2015, Matsumura et al. 2019). However, some other reanalysis and observational based studies indicate that the Arctic upper troposphere is also warming significantly. Graversen et al. (2008) used the ERA-40 reanalysis to analyze the vertical structure of warming in the Arctic and found warming throughout the depth of the Arctic troposphere. The warming throughout the Arctic troposphere is generally larger than the warming in the lower latitudes in most seasons. However, this study is controversial because ERA-40

can not necessarily be applied for climate reanalysis (Thorne 2008). Santer et al. (2013, 2018) use microwave sounding unit (MSU) data that shows greater warming in the mid to upper tropospheric Arctic over the satellite era than the tropical upper troposphere. Additionally, both studies show that most CMIP5 models overestimate tropical warming and underestimate Arctic warming in the mid to upper troposphere compared to the MSU data. Jansen et al. (2020) compared various Representative Concentration Pathways (RCP's) from CMIP5 – RCP2.5, RCP4.5, and RCP8.5 – to ERA-Interim, and found the models largely fail to capture the abrupt Arctic warming of recent decades, with RCP8.5 performing better than the other two RCP's. Though this study focuses on the Arctic surface instead of the Arctic upper troposphere, it provides additional evidence that the models and observations disagree.

Additionally, while the multi-model means of the climate model-based studies tend to produce a poleward shift and strengthening of the jet, individual models have been shown to produce a wide variety of jet response patterns (Yim et al. 2016). Several studies have utilized the tug-of-war framework to understand differences in the jet response between different climate models. Barnes and Polvani (2015) analyzed output from 27 CMIP5 RCP8.5 models and found a -0.7 correlation between Arctic Amplification and zonal wind change in the winter, and an even stronger correlation of almost -1 from May to August. This shows that stronger Arctic Amplification would lead to weaker zonal winds, which is consistent with the tug-of-war framework. Yim et al. (2016) used 34 CMIP5 RCP4.5 models to highlight the difference in jet response between models. This study found an equatorward shift in the jet when there was stronger warming at the Arctic surface, and a poleward shift when the upper tropical troposphere

warmed more, again compatible with the tug-of-war idea. Using 36 CMIP5 historical and RCP8.5 climate models as well as 40 ensemble members from the Community Earth System Model Large Ensemble (CESM-LENS), Peings et al. (2018) also found results that support the tug-of-war framework. Most significantly, they found a strong correlation of 0.84 between the change in the zonal index (ZON) with global warming, where ZON is used to indicate jet strength, and the "ratio between upper- troposphere tropical and Arctic warming (RUTAW)" (Peings et al. 2018). The correlation between ZON and RUTAW offers the benefit of being able to qualitatively predict the jet response in climate models.

Golden (2020) used output from 42 RCP8.5 and historical simulations from CMIP5. This study further refined the metric developed by Peings et al. (2018) and incorporated historical simulations to determine if the correlation exists over the modeled satellite era as well. This also sets up the possibility of comparing observations to the modeled satellite era to determine if any models can be ruled out due to inaccurate representations of reality. While Peings et al. (2018) computed a warming ratio between the Arctic and the tropics, Golden (2020) instead subtracted the subtropical warming from the Arctic warming. This alternative method was chosen to improve the original metric by Peings et al. (2018), as it specifies the magnitude of the warming and jet response. Golden (2020) computed the inter-model correlation between the Arctic minus subtropical warming and the zonal wind change over the future era and found a very strong, statistically significant correlation of around -0.92, compared to the 0.84 correlation found by Peings et al. (2018). Many combinations of latitude-pressure boxes for the Arctic, subtropics, and zonal wind were tested to find the most highly correlated

grouping. As noted above, the focus of the competition between the Arctic and the tropics is usually on the warming of the Arctic near the surface and of the upper troposphere in the tropics. However, Golden (2020) found that the highest correlation resulted from Arctic and subtropical boxes that extend from 850mb-300mb and 850mb-200mb, respectively. This implies that the warming throughout the depth of the free troposphere in both regions plays an important role in driving the latitudinal shift of the jet, instead of only the upper troposphere in the tropics and the lower troposphere in the Arctic. This increases the relevance of the recent observational and reanalysis-based studies that show the Arctic upper troposphere may be warming more rapidly than the tropics. Golden (2020) also computed the correlation between the Arctic minus subtropical warming and the zonal wind change over the modeled satellite era, which resulted in a weaker, but still statistically significant, correlation of -0.79. This correlation was produced with a slightly different Arctic box that starts in the mid-troposphere and extends to the upper troposphere instead of including the entire Arctic free troposphere, though the original box combination produced a similar correlation of -0.76.

Given the apparent disagreement between climate models and observations, as well as the disagreement between individual models, there is significant motivation to study the relationship between Arctic warming, tropical warming, and the mid-latitude jet. The studies so far have all used older versions of CMIP. The most recent iteration, CMIP6, is now publicly available (Eyring et al. 2016) and offers the opportunity to further the work of Golden (2020) and prior studies using a suite of state-of-the-art climate models. This new set of models will help us answer a variety of questions. Does the significant relationship between Arctic and subtropical warming and zonal wind

found by Golden (2020) hold in CMIP6 future and historical climate projections, and if so, is it stronger or weaker? Are climate models accurately capturing the satellite era mid-latitude jet change and warming pattern? Given the utility of the correlation between the Arctic minus subtropical warming and zonal wind change as a predictor of the future jet response, the goal is to use this relationship to determine if a model is useful or not. This objective is driven by the apparent disagreement between the models, which have tended to produce stronger tropical warming, and the observations, which indicate the Arctic may be warming more than the tropics. By comparing the ensemble members in a models' historical simulations to observations, models can be ruled out based on how well they match the observations.

CHAPTER TWO: DATASET

a) Future Era

The data used for the first part of this study are 45 climate models from Phase 6 of the Coupled Model for Intercomparison Project (CMIP6) (Eyring et al. 2016). CMIP6 has a wide selection of model output that is organized into activities, two of which were considered for this study, CMIP and ScenarioMIP. From CMIP, we considered using the idealized 1pctCO2 and abrupt4xCO2. The 1pctCO2 model experiments are forced by a 1% per year increase in CO2 for 150 years leading to a gradual quadrupling of CO2, while the abrupt4xCO2 experiments are forced by abruptly quadrupling CO2. The gradual forcing of the 1pctCO2 experiment is more realistic compared to the dramatic forcing used in the abrupt4xCO2 experiments. ScenarioMIP includes various even more realistic experiments with different levels of CO2 forcing (comparable to the RCP emissions scenarios of previous CMIP models) but has fewer available models than either of the CMIP experiments. Therefore, the 1pctCO2 experiment was chosen for its number of available models, as well as its more realistic, though idealized, forcing. By the end of the 150-year 1pctCO2 simulations, CO2 concentration has quadrupled, resulting in an average planetary temperature that is several degrees Celsius warmer than today's average. Only the first ensemble member of each model is used for this study because Golden (2020) found the other ensemble members' behaviors to be nearly identical to the first for the RCP8.5 simulations. A comparison of the first ensemble member of HadGEM3-GC31-LL and CNRM-ESM2-1 to their respective additional ensemble

members showed this to be a reasonable assumption for CMIP6 as well. The names of the models used for this study can be found in Table 1.

The variables analyzed in this study are the monthly air temperature (K) and zonal wind (m/s) on pressure levels, and a control and future period is identified for each variable. The control period is defined as model years 1 through 30 for each variable. The future period is defined as model years 121 through 150 for each variable. By the 150th year of the model, the CO2 concentration has quadrupled, and the average planetary temperature is several degrees Celsius warmer than that of years 1 through 30.

b) Satellite Era

The second part of this study uses the historical simulations from the same 45 models that were used for the future portion. Data for these simulations begin no later than 1979, though some start as far back as 1850, and they all end in 2014. This could be extended to 2019 using output from other simulations, but this study will only extend to 2014 due to time constraints. Unlike the 1pctCO2 simulations, multiple ensemble members are included where available to help account for internal variability, due to the smaller signal-to-noise ratio in the satellite era. There are 469 total ensemble members across 45 models included in this part of the study. The number of ensemble members for each models' historical simulations is also listed in Table 1. Again, the variables analyzed are the monthly temperature (K) and zonal wind (m/s), with a past and present period for each variable. Currently, only the data from 1980-2014 is considered. Starting in 1980 instead of 1979 allows for a more direct comparison with the reanalysis output later in this study, since output for MERRA-2 is only available starting in 1980. The historical simulation data is then halved into two 18-year segments to obtain the past (1980-1997)

and present (1997-2014) periods. It should be noted that due to the odd number of years there is one year of overlap between the time periods, with 1997 occurring in both.

c) Observations

The final two parts of this study use temperature and zonal wind output from six state-of-the-art global reanalyses (listed in Table 2), as well as Microwave Sounding Unit (MSU) data on free tropospheric temperature. The analysis of MSU data requires two datasets for a direct comparison to CMIP6 because MSU data is not output by models. The first dataset is the observational MSU satellite data, which shows tropospheric temperature observations for 1979-2019. This consists of data originating from over a dozen satellites, provided by Po-Chedley et al. (2021), that have been spliced together and interpreted by three different groups: Remote Sensing Systems, the National Oceanic and Atmospheric Administration (NOAA) Center for Satellite Applications and Research, and the University of Alabama at Huntsville (Po-Chedley et al. 2015, Spencer et al. 2017, Mears and Wentz, 2016). The second dataset is synthetic MSU data for the same time frame, developed by Po-Chedley et al. (2021). While the first dataset corresponds to observations of the real atmosphere, the synthetic dataset shows what a satellite would have observed in the atmosphere simulated by a CMIP6 climate model. There is synthetic MSU data for all of the CMIP6 models used in the previous two sections, except for IITM-ESM. The number of ensemble members for each model's synthetic MSU data is also listed in Table 1. For a more direct comparison to the CMIP6 analyses, only 1980-2014 will be considered.

Additionally, MSU instruments do not measure temperature at specific pressure levels. Instead, they have vertical channels that measure temperature in larger sections of

the atmosphere. There are many MSU channels to choose from and using two different channels for the Arctic and subtropics was considered. However, Golden (2020) found that the warming throughout the depth of the free troposphere in both the Arctic and the subtropics is significant for the jet response, so a single channel called TMT (the temperature of the mid-troposphere) was chosen for both. This channel aligns most closely with the pressure levels used in this study because it focuses on the mid to upper troposphere.

However, TMT includes some influence from stratospheric cooling that leads to a low bias in long-term trends. To account for this, Fu et al. (2011) implemented a weighting function to remove stratospheric contamination in the upper troposphere. This stratosphere-corrected TMT is also known as T24 or TTT, and the weighting function defined by Fu et al. (2011) for this channel can be found in Figure 1. This function was created by subtracting a portion of the lower-stratospheric temperature channel (TLS) from TMT. The most used formula for this function uses different coefficients in the Arctic than the tropics due to the lower height of the tropopause in the extratropics. The coefficients switch at 30 N/S, which results in a discontinuity that occurs in the region defined as the subtropics in this study (20 N to 40 N). This formula is known in the MSU community as tf2. To avoid this discontinuity, a slightly different weighting function is used for this study. Instead of switching from tropical to Arctic coefficients, the alternative weighting function used for this study employs only the tropical coefficients for the entire globe. This method is known as tf1. A weighting function that switches the coefficients at 40 N/S instead of 30 N/S was also considered (named “tf3”) but was less useful than using the tropical coefficients globally (tf1). Data for tf1, tf2, and tf3 for both

the observational MSU temperature and the synthetic MSU temperature are provided by Stephen Po-Chedley of Lawrence Livermore National Laboratory (Po-Chedley, pers. comm., 2021).

CHAPTER THREE: METHODS

a) Future Era

As in Golden (2020) and similar to Yim et al. (2016), the first step of this study is to calculate the zonal wind change and temperature change between the control and future period for the 1pctCO2 simulations. The first and last 30 years (years 1-30 and 121-150, respectively) yield two separate variables for temperature, control and future. The zonal and time means are then calculated for both the control and future periods. The change in temperature is found by subtracting the control period from the future period. The same process of separating the variables and calculating the differences is then performed with the first and last 30 years of the zonal wind data from each model to produce the zonal wind change. This process is repeated for each of the 45 1pctCO2 model runs, resulting in 45 sets of zonally and yearly averaged temperature and zonal wind variables. This results in two latitude-pressure plots per model that show the difference in the zonal wind and the temperature between the control and future period (Figures 2 through 11).

For the next part of the study, the general location of the tropics, Arctic, and mid-latitude jet must be defined. This is done by defining a latitude-pressure box for each variable, resulting in three latitude-pressure boxes. Golden (2020) tested various combinations of latitude-pressure boxes and found the boxes that will be used in this study to be the most highly correlated. The latitude-pressure box for the zonal wind difference extends from 30˚N to 70˚N and 1000mb to 200mb. For the Arctic temperature difference, the latitude-pressure box extends from 60˚N to 90˚N and 850mb to 300mb.

Finally, the latitude-pressure box for the tropical temperature difference extends from 20˚N to 40˚N and 850mb to 200mb. Golden (2020) chose this latitude range for the tropics based on Shaw and Tan (2018), which found that the jet is more sensitive to subtropical warming than tropical. A visual of each of these boxes can be found in Figures 12 and 13.

Once the tropics, Arctic, and mid-latitude jet have been defined, two variables must be created from the 45 sets of temperature and zonal wind change to use in the correlation analysis. The mean is first calculated over all three latitude-pressure boxes for each model to get a subtropical warming mean, an Arctic warming mean, and a zonal wind change mean. Then, the subtropical warming mean is subtracted from the Arctic warming mean to get the Arctic-subtropical warming difference. The result is two variables, Arctic-subtropical warming difference and zonal wind change, that each contain 45 values, which are then used for the correlation analysis to determine if the difference in warming between the Arctic and the subtropics can be used to predict the future jet response. The scatterplot for this correlation as well as the accompanying statistics can be found in Figure 14.

b) Satellite Era

The above process is repeated for the historical simulations of the satellite era. The only differences are the use of 18-year segments for the past and present (1980-1997 and 1997-2014, respectively), instead of the 30-year segments used in the future period, and the creation of two variables with 469 values instead of 45, which correspond to the number of ensemble members. Additionally, the correlation analysis is done twice – first with only the first run of each model, as a more direct comparison to the future era

correlation, and second with all ensemble members included. The inclusion of multiple ensemble members provides insight into how each model's ensemble is capturing the past changes in warming and the jet and helps account for internal variability. This lays the groundwork for comparison with observations to determine if some models can be ruled out with respect to their jet response to warming. Latitude-pressure plots for the first ensemble member of each model are shown in Figures 15 through 24, and the scatterplot for both correlation analyses can be found in Figures 25 and 26. The warming difference for the historical era is also plotted against the 1pctCO2 warming difference, and the historical zonal wind change is plotted against the 1pctCO2 zonal wind change. This allows for a comparison of how the models are portraying the temperature difference and the zonal wind change over the satellite era versus the future. This scatterplot for each variable can be found in Figures 27 and 28.

c) Observations – Reanalysis

The next part of this study incorporates reanalysis output for 1980-2014. The reanalysis output is analyzed in the same way the climate model output is analyzed for the satellite era, resulting in latitude-pressure plots for each reanalysis (Figures 29 and 30). Unlike the modeled satellite era analysis, a correlation is not computed between the reanalyses. There are so few reanalyses to correlate, and the reanalysis only serves as an estimate of reality, so a correlation between them would not be useful for this study. The reanalysis results are overlaid first on the scatterplot with all ensemble members from the modeled satellite era (Figure 31), then on the scatterplot with the ensemble members for each model. This results in a separate scatterplot for each model with the reanalysis overlaid, for a total of 45 plots that can be found in Figures 32 through 36. The goal of

this comparison is to determine which climate models are accurately capturing the patterns found over the modeled satellite era, thus increasing confidence that they are more reliable for simulations of the future. Each model's ensemble can be compared to the reanalysis points to determine if the model should be kept or discarded for the purpose of this study based on whether it is consistent with the pattern of warming and jet change shown by the reanalyses.

To quantify which models can be discarded based on the reanalysis output, a two-sample t-test is used for both the warming difference and zonal wind change to compare each model to reality as estimated by reanalysis. The average warming difference for all five reanalyses is calculated, resulting in a single estimate of reality that is used as one of the samples for the t-test. The collection of warming differences for all of the ensemble members of a model is used as the other sample. While the sample based on reality will only have a single value, the sample for the model will have multiple values, depending on the number of ensemble members. If there is only one ensemble member available for a model, as is the case for 5 of the 45 models, the two-sample t-test will not work. Thus, these models will not be included in the t-test analysis. This process is then repeated for the zonal wind change.

The two-sample t-test will evaluate the null hypothesis that the average reanalysis warming difference or zonal wind change could be a reasonable member of the ensemble population. If the test produces a p-value less than 0.05, the null hypothesis can be rejected, and the model can be discarded. In this case, the reanalysis does not fall within the ensemble population, so that model is not producing values that are consistent with reality. Similarly, if the test produces a p-value greater than 0.05, the null hypothesis

cannot be rejected, and the model cannot be discarded. In this case, the reanalysis does fall within the realm of possibility for the ensemble population, so the model is producing values that are consistent with reality. Table 3 shows the results of the t-test for the reanalysis warming difference and the zonal wind change.

d) Observations – Satellite MSU Data

In addition to reanalysis, satellite MSU data is also analyzed, though slightly differently than the above. For both the observational MSU data and the synthetic climate model MSU data, the average temperature of the first 18 years and the last 18 years is calculated, and the difference between them. However, instead of defining latitude-pressure boxes for the Arctic and subtropics, latitude is used in tandem with the stratosphere-corrected mid to upper tropospheric temperature channel (TTT) to create Arctic and subtropical boxes. As discussed above, this channel is used because it corresponds the closest to the pressure levels used for the latitude-pressure boxes in the previous analyses. As in the previous analyses, the subtropical box is then subtracted from the Arctic box. The synthetic climate model MSU temperature difference is correlated with the climate model zonal wind change over the satellite era for each model. As with the reanalysis, all members from each model are combined into a single scatterplot with the observational MSU temperature data overlaid as vertical lines to determine the utility of the synthetic climate model MSU Arctic minus subtropical warming as a predictor of the modeled jet change (Figure 37). Then to determine their consistency with reality, each model's ensemble is plotted separately with the observational MSU temperature data overlaid as vertical lines as a reference point for comparison. As with the reanalysis, this will show which models are more accurately

capturing the satellite era and allow the less trustworthy models to be ruled out. These plots are shown in Figures 38 through 42.

As with the reanalysis, a two-sample t-test is used to quantify which models can be discarded based on the satellite MSU data. Like the reanalysis, the average of the observational MSU data is calculated, resulting in a single estimate of reality that is used as one of the samples for the t-test. The collection of warming differences for all the ensemble members of the synthetic climate model MSU output is used as the other sample. Like with reanalysis, the sample based on reality will only have a single value, and the sample for the model will have multiple values, depending on the number of ensemble members. If there is only one ensemble member available for a model, as is the case for 5 of the 44 models of synthetic MSU output, the two-sample t-test will not work, and these models will not be included in the t-test analysis. However, since there is no observational zonal wind data from MSU, the t-test can only be performed with the warming difference. Again, the two-sample t-test will evaluate the null hypothesis that the average observational MSU warming difference could be a reasonable member of the synthetic MSU ensemble population. If the test produces a p-value less than 0.05, the null hypothesis can be rejected, and the model can be discarded for not producing reasonable temperature changes. If the test produces a p-value greater than 0.05, the null hypothesis cannot be rejected, and the model cannot be discarded. The results of the t-test for the MSU warming difference can also be found in Table 3. Once the models that can be discarded are determined, either with the reanalysis or the satellite MSU observations, the 1pctCO2 scatterplot from Figure 14 is reproduced with the discarded models noted in different colors. This updated scatterplot can be found in Figure 43.

CHAPTER FOUR: RESULTS – FUTURE

a) Latitude-Pressure Plots

The latitude-pressure plots in Figures 2 through 10 (even numbers) show the temperature change between the control (years 1-30) and future (years 121-150) periods of the 1pctCO2 simulations. All models produce the expected increase in temperature throughout the Northern Hemisphere troposphere, and cooling in the stratosphere. They also show increased warming in the tropical upper troposphere and the lower tropospheric Arctic. An exception to this is CAMS-CSM1-0, which has significant upper tropospheric warming but lacks a warming "bullseye" in the near-surface Arctic (Figure 2). The warming "bullseye" in the Arctic is also very weak in SAM0-UNICON (Figure 10). The depth of the troposphere in the Arctic warms at a similar magnitude to the troposphere at other latitudes. As expected based on various studies (Barnes and Polvani 2015, Yim et al. 2016, Peings et al. 2018), the magnitude of warming in different locations throughout the atmosphere varies significantly between models. For example, MRI-ESM2-0 (Figure 10) features more warming in the tropical upper troposphere than the Arctic near-surface, while EC-Earth3 (Figure 4) shows more warming in the lower tropospheric Arctic.

The latitude- pressure plots in Figures 3 through 11 (odd numbers) show the zonal wind change between the control (years 1-30) and future (years 121-150) periods of the 1pctCO2 simulations. These plots also include the jet from the control period in black contours for comparison. Like the temperature change plots, there are a variety of responses found in the zonal wind change plots, with some exhibiting an increase in

zonal wind, and others exhibiting a decrease. When the temperature change plots are compared to the zonal wind change plots, it is found that models that tend to produce stronger Arctic (subtropical) warming also tend to produce a weaker (stronger) jet. However, the latitudinal shift of the jet does not follow the expected pattern as closely. Thus, focus is kept only on the jet strength. For example, EC- Earth3 (Figure 5) shows a significant decrease in jet speed, which is consistent with the enhanced Arctic warming noted before. However, EC-Earth3 shows no shift in the jet, though an equatorward shift would be expected based on the tug-of-war hypothesis. MRI-ESM2-0 (Figure 11) produces a significant increase in jet speed, again consistent with the enhanced subtropical warming noted before. A poleward shift of the jet would be expected in this case, but again there is no shift. There are also clear latitudinal shifts in the jet in many models, but they often don't follow expected patterns either. For example, there is an equatorward shift in CIESM (Figure 5), and a poleward shift in Nor-ESM2-LM (Figure 11). However, the Arctic and the subtropics warm by a similar amount in both models. Based on the tug-of-war hypothesis, an ambiguous warming difference would theoretically lead to a similarly ambiguous jet shift, but that is not the case in these models. Given this wide range of responses in the latitudinal shift of the jet, only the jet strength is considered for this study. These patterns in warming and jet change, and the variety of realizations between models, confirm the findings of Golden (2020), who found similar results in the RCP8.5 simulations from CMIP5.

b) Correlation Analysis

The correlation analysis allows for a more quantitative investigation of the patterns and relationships noted above to determine if the tug-of-war hypothesis can be a

useful predictor of the future jet response. The scatter plot between the Arctic minus subtropical warming and zonal wind change for the future period (Figure 14) shows a strong, very statistically significant negative correlation between the variables, with a correlation of -0.93. This is slightly stronger than the correlation found by Golden (2020) for CMIP5, -0.92. The negative correlation implies that as the Arctic warms more than the subtropics, the zonal wind tends to decrease, and as the subtropics warm more than the Arctic, the zonal winds tend to increase, consistent with the tug-of-war hypothesis. The slope of the line, also found in Figure 14, reveals that for every degree the Arctic warms more than the subtropics, the zonal wind should decrease by 0.46 m/s. In agreement with the previous model consensus, about 56% of models predict conditions that fall in the upper left quadrant of the scatter plot, which corresponds to the subtropics warming more, and the jet increasing. The strong correlation shows that the difference in warming between the Arctic and the subtropics is a useful predictor of the future jet response in climate models.

CHAPTER FIVE: RESULTS – MODELED SATELLITE ERA

a) Latitude-Pressure Plots

As previously found by Golden (2020), the latitude pressure plots for the historical simulations in Figures 15 through 24 also show a variety of outcomes. For example, the warming in the Arctic is stronger than the warming in the subtropics in CESM2 (Figure 15). As predicted by the tug-of-war hypothesis, there is a corresponding decrease in the jet strength, though there is no clear shift in the jet in CESM2 (Figure 16). CESM2-WACCM-FV2 shows increased warming in the Arctic (Figure 17) and a decrease in jet strength, but it also shows a poleward shift in the jet that would not be expected based on the tug-of-war hypothesis (Figure 18). Conversely, CIESM shows the subtropics warming more than the arctic (Figure 17), and correspondingly predicts the jet will increase in strength and shift poleward (Figure 18), again following the tug-of-war hypothesis. However, some models don't fit the patterns predicted by the tug-of-war hypothesis. For example, GISS-E2-1-G-p1 shows increased warming in the Arctic (Figure 19), but an increase in the jet strength (Figure 20).

b) Correlation Analysis

The correlation between the Arctic minus subtropical warming and zonal wind change for the first ensemble member of each model over the satellite era (Figure 25) also shows a very statistically significant negative correlation between the variables. The correlation is weaker than that over the future period, which is to be expected due to weaker forcing, but still fairly robust at -0.65. After all ensemble members are added to the calculation, the correlation increases slightly to -0. 71 (Figure 26). This is slightly

lower than the correlation found by Golden (2020) for the satellite era, -0.79. The slope is similar to the future analysis, showing that for every degree the Arctic warms more than the subtropics, the zonal wind should decrease by 0.42 m/s. Interestingly, about 59% of the models fall in the bottom right quadrant of the scatter plot, which corresponds to the Arctic warming more, and the jet decreasing. Some climate models have tended to warm the tropics more (Santer et al. 2013, 2018; Jansen et al. 2020), despite observational studies suggesting the Arctic is warming more in recent decades. This result indicates that the new CMIP6 climate models may be capturing the stronger warming over the satellite era in the Arctic better than the older generations of climate models (Jansen et al. 2020, Yin 2005, Butler et al. 2010, Delcambre et al. 2013, Lorenz 2014, Lachmy and Shaw 2018, Screen et al. 2018, Santer et al. 2013, 2018). Additionally, this suggests that the increased warming in the Arctic over the historical era may actually be consistent with the future model depiction of the tropics warming more and the jet increasing in strength.

c) Historical vs. 1pctCO2

To further examine this discrepancy between the historical era and the future in CMIP6 models, the historical warming difference and zonal wind change were plotted against the 1pctCO2 warming difference and zonal wind change, respectively. The plot of the warming difference in Figure 27 shows a large number of points in the bottom right quadrant compared to those in the top left quadrant, which indicates more warming in the Arctic over the historical era, but more warming in the tropics in the future throughout many of the models. Similarly, the zonal wind change plot in Figure 28 shows a large number of points in the top left quadrant compared to those in the bottom right quadrant, indicating the jet has slowed down more over the historical era, but will speed up more in

the future. All of this supports the idea that the warming difference in the future is inherently more tropical amplified than it has been over the satellite era, indicating that a future where the tropics warm more and the jet speeds up is consistent with a past where the Arctic warms more and the jet slows down.

CHAPTER SIX: RESULTS – USING OBSERVATIONS TO CONSTRAIN THE MODELS

a) Reanalysis Latitude-Pressure Plots

To determine which models could be ruled out based on the methods of this study, reanalysis is used as one estimate of reality, and satellite MSU data is used as another estimate. Focusing first on the reanalysis, the structure of the warming and the zonal wind change for each of the five reanalyses used in this study are shown in the latitude-pressure plots in Figures 29 and 30, respectively. All of the reanalysis products in Figure 29 show significant warming in the Arctic with weaker warming in the tropics and subtropics. CFSR does show significantly more warming in the tropical upper troposphere than the other four reanalyses, but it is still less than the warming in the Arctic. Additionally, while much of the warming in the Arctic is focused near the surface, all of the reanalyses show warming throughout the depth of the troposphere in the Arctic that is generally stronger than the warming found in the upper tropical or subtropical troposphere. This increases confidence in the previously mentioned studies that indicate the Arctic is warming significantly more than the tropics and winning the tug-of-war.

Looking at the corresponding latitude-pressure plots of the zonal wind change in Figure 30, four of the five reanalyses show an overall decrease in the zonal wind over the satellite era. Given the increased warming in the Arctic than the tropics in the reanalyses, this decrease in zonal wind is expected based on the tug-of-war hypothesis. As noted above, however, CFSR exhibits significantly stronger warming in the tropical upper troposphere than the other reanalyses, and the zonal wind change reflects this different

warming pattern. It is much more ambiguous whether the zonal wind is increasing or decreasing over the satellite era in this reanalysis, which is expected given the small difference in the warming between the Arctic and tropics. Overall, while CFSR does behave slightly differently than the other reanalyses, all five reanalyses produce a zonal wind change that is consistent with the tug-of-war hypothesis given their warming patterns.

b) Reanalysis Scatterplot Analysis – Full

The reanalyses are first included on the full scatterplot of warming difference versus zonal wind change for the CMIP6 historical simulations for comparison (Figure 31). As expected based on the latitude-pressure plots of the zonal wind change and the warming difference for each reanalysis, they all fall in the bottom right quadrant of the scatterplot which indicates more warming in the Arctic and a decrease in the zonal wind over the satellite era. Most of the reanalysis points (blue circles) are fairly close to one another, except one point located in the upper left part of the quadrant. This point represents the CFSR and is consistent with the stronger warming in the tropics and the ambiguous zonal wind change found in the latitude-pressure plots. However, much of the analysis going forward will focus on the average of the reanalyses, plotted as a red diamond on the scatterplot. This average falls within the point cloud of the models, providing evidence that at least some of the CMIP6 models are capturing the patterns over the satellite era. However, focusing solely on the bottom right quadrant, the reanalysis average is located further to the right relative to the models, so the models tend to produce a smaller difference between the Arctic warming and the subtropical warming than the reanalyses. This shows that even though many models appear to be capturing the

warming in the Arctic better than before, they are still underrepresenting the warming in the Arctic on average.

c) Reanalysis Scatterplot Analysis – Individual Models and T-test Analysis

Plotting the reanalysis on the full scatterplot of CMIP6 historical simulations is useful to compare how the models perform overall compared to an estimate of reality but attempting to discard models requires the reanalysis to be plotted with each model's ensemble, shown in Figures 32 through 36. A model can be discarded if its ensemble members (black dots) all fall far from the reanalysis average (red triangle). This shows that the model is not producing results that are consistent with reality (as estimated by reanalysis) over the satellite era. If the model doesn't produce reasonable results over the satellite era, it decreases confidence that it will produce reasonable predictions of the future climate and can be discarded. However, if the model's ensemble members fall close to the reanalysis average, the model is producing results that are realistic based on the estimate of reality provided by the reanalysis average. If the model can produce realistic results over the satellite era, this increases confidence that the model can produce plausible predictions of the future climate and should not be discarded.

Based on a qualitative visual analysis of Figures 32 through 36, most of the models produce results that are consistent with reanalysis. The models that could possibly be considered inconsistent with reality through visual analysis are CAMS-CSM1-0, CIESM, FIO-ESM-2-0, GFDL-ESM4, GISS-E2-1-G-p5, HadGEM3-GC31-MM, IITM-ESM, INM-CM4-8, NorCPM1, Nor-ESM2-MM, and SAM0-UNICON. All of the other models produce at least one point relatively close to the reanalysis average, showing that they have the potential to produce realistic values. However, it is important to note that

IITM-ESM, INM-CM4-8, and SAM0-UNICON all have only one ensemble member to compare to the reanalysis. While these members are all relatively far from the reanalysis average, there's nothing to guarantee that additional ensemble members wouldn't have fallen closer to the average, making the model more consistent with reality. This is the same reason these models are not included in the more quantitative t-test analysis. This results in CAMS-CSM1-0, CIESM, FIO-ESM-2-0, GFDL-ESM4, GISS-E2-1-G-p5, HadGEM3-GC31-MM, NorCPM1, and Nor-ESM2-MM being the primary models that could be considered inconsistent with reality.

However, deciding which models can be discarded solely based on examining the plots is qualitative and fairly subjective. To quantitatively determine which models can be discarded, a two-sample t-test is used, the results of which are listed in Table 3. As mentioned in the methods, a model can be discarded if it produces a p-value less than 0.05 and cannot be discarded if it produces a p-value greater than 0.05. The only models that can be ruled out based on the warming difference are GFDL-ESM4, GISS-E2-1-G-p5, HadGEM3-GC31-MM, MPI-ESM1-2-LR, and NorCPM1. Based on the zonal wind change, only CIESM can be ruled out. Interestingly, while some models can be ruled out based on either the warming difference or the zonal wind change, none of them can be completely discarded based on both variables. Some of the results of the t-test match what is expected from the qualitative analysis, with both analyses resulting in CIESM, GFDL-ESM4, GISS-E2-1-G-p5, HadGEM3-GC31-MM, and NorCPM1 being discarded. However, the quantitative analysis indicates that CAMS-CSM1-0, FIO-ESM-2-0, and Nor-ESM2-MM cannot be discarded, though the qualitative analysis indicates they should be. This is somewhat surprising considering the ensemble members for these

models are all a significant distance from the reanalysis average. However, each of these models only has two or three ensemble members. Despite their ensemble members being far from the average, the relationship does not appear to be significant enough with only a few members to allow these models to be discarded. Therefore, using reanalysis as the estimate of reality only results in 6 out of 45 models being discarded based either on the warming difference or the zonal wind change (note that 5 of the remaining 39 models only include one ensemble member, and by default are not discarded, rather than because of the t-test). With only 6 out of 45 models that can be ruled out, this increases confidence that CMIP6 models are better at capturing the trends in warming and zonal wind change over the satellite era than previous climate models.

d) Satellite MSU Correlation Analysis – Full

Satellite MSU temperature data is used as another estimate of reality for this study. As with the reanalysis, the observational satellite data is first included on the full regression of all ensemble members of the synthetic MSU warming difference versus the CMIP6 zonal wind change (Figure 37). Focusing first on the relationship between the synthetic MSU warming difference and the CMIP6 zonal wind change, there is a significant negative correlation of -0.77. This is slightly higher than the correlation of -0.71 for the CMIP6 historical simulations, so the synthetic MSU warming difference is a useful predictor of the modeled jet response. The average of the observed MSU temperature data falls within the point cloud of the models, but on the far right of the point cloud, as with the reanalysis. This provides additional evidence that while the models may be capturing the warming in the Arctic better than they were before, they are still underrepresenting the warming in the Arctic.

e) Satellite MSU Correlation Analysis – Individual Models and T-test Analysis

As with the reanalysis, the observational satellite data is overlaid on each model's ensemble to determine which models may be discarded. Based on a qualitative visual analysis of Figures 38 through 42, the models that could possibly be discarded are ACCESS-CM2, BCC-CSM2-MR, BCC-ESM1, CAMS-CSM1-0, CISEM, GFDL-ESM4, HadGEM3-GC31-MM, MPI-ESM1-2-HR, and NorESM2-LM. All of these models' ensemble members are located much farther from the observed satellite average than the other models. There are also quite a few models that could arguably be discarded as well, including CESM2-WACCM-FV2, EC-Earth3-Veg, FGOALS-g3, FIO-ESM-2-0, and GISS-E2-1-G-p5. The ensemble members for these models are still somewhat far from the observed satellite average but are closer than the ensemble members of the previously stated models. This results in up to 14 out of 44 models that could be discarded.

However, as noted with the reanalysis, the above is only a qualitative analysis, and a two-sample t-test can help quantify with more certainty which models can be discarded. The results of the two-sample t-test with satellite as the estimate of reality can be found in Table 3. Based on this, the models that can be discarded are BCC-CSM2-MR, EC-Earth3-Veg, GFDL-ESM4, GISS-E2-1-G-p5, HadGEM3-GC31-MM, and MPI-ESM1-2-LR. At only 6 out of 44 models that could be discarded, this is much less than the 14 models found with the qualitative analysis (again, note that 5 of the remaining 38 models only include one ensemble member, and by default are not discarded, rather than because of the t-test). As with the reanalysis, many of the models that looked like they could be discarded in the qualitative analysis only consist of two or three ensemble members. Thus, the relationship may not be strong enough to definitively rule many of

them out, though it might look like they should be. However, note that many of the same models that are quantitatively ruled out when reanalysis is used as the estimate of reality are the same as those quantitatively ruled out when satellite observations are used as the estimate of reality: GFDL-ESM4, GISS-E2-1-G-p5, HadGEM3-GC31-MM, and MPI-ESM1-2-LR. Overall, the models that can be discarded based on either the reanalysis or satellite analyses are BCC-CSM2-MR, CIESM, EC-Earth3-Veg, GFDL-ESM4, GISS-E2-1-G-p5, HadGEM3-GC31-MM, MPI-ESM1-2-LR, and NorCPM1.

f) Applying the T-test Results to the 1pctCO2 Scatterplot

The scatterplot of the 1pctCO2 simulations is reproduced with the models that can be discarded using either method noted by different colors in Figure 43. If the historical warming difference is a good predictor of the northern hemisphere mid-latitude jet, the models that are ruled out based on their historical simulations would ideally behave similarly in the 1pctCO2 simulations. Thus, the points corresponding to the ruled out models should fall in the upper left portion of the point cloud on the 1pctCO2 scatterplot. The models that are discarded with most confidence are those that are discarded by both the reanalysis and satellite MSU t-tests (GFDL-ESM4, GISS-E2-1-G-p5, HadGEM3-GC31-MM, MPI-ESMI-2-LR). These correspond to the green points in Figure 43, and all these points do fall more in the top left of the point cloud, as expected. However, many points also fall in the middle, or more to the bottom right of the plot. Additionally, only 8 out of 45 models are discarded, so most of the models aren't being ruled out. This further indicates that a future where the subtropics warm more than the Arctic and the jet strengthens is not necessarily inconsistent with a past where the Arctic warms more than the subtropics and the jet weakens. Therefore, the satellite era warming difference

between the Arctic and the subtropics may not be the most useful predictor of the jet's future response to climate change.

CHAPTER SEVEN: CONCLUSION

This study has shown that the strong correlation between Arctic minus subtropical warming and zonal wind change exists in both CMIP6 historical and future simulations. This relationship is consistent with the tug-of-war hypothesis, indicating that the Arctic minus subtropical warming difference is a useful predictor of the future jet response. The modeled future agrees with previous model consensus, tending to warm the subtropics more and increase jet strength, while the modeled past is more consistent with recent studies that show the Arctic warming more than the tropics. This indicates that the climate models can capture the historical Arctic warming better than before, and that the increased Arctic warming over the satellite era may actually be consistent with the future depicted by the models. However, while the models are performing better than before, they are still underestimating the magnitude of the warming in the Arctic over the satellite era. Comparing the modeled satellite era to reanalysis output and satellite MSU observations yields 8 models that can be discarded for not producing results that are consistent with the reanalysis and satellite MSU: BCC-CSM2-MR, CIESM, EC-Earth3-Veg, GFDL-ESM4, GISS-E2-1-G-p5, HadGEM3-GC31-MM, MPI-ESM1-2-LR, and NorCPM1. If these models don't perform well over the satellite era, it decreases confidence that they are accurately predicting the future climate. However, only 8 out of 45 models were discarded, showing that overall, the models are performing better than expected given previous model output that tended to show the tropics winning the tug-of-war instead of the Arctic over the satellite era (Jansen et al. 2020, Yin 2005, Butler et al. 2010, Delcambre et al. 2013, Lorenz 2014, Lachmy and Shaw 2018, Screen et al. 2018,

Santer et al. 2013, 2018). This performance over the satellite era increases confidence that their predictions of the future climate are still valid, and that the past warming in the Arctic may be consistent with the future warming in the tropics and subtropics. It also shows the satellite era warming difference between the Arctic and the subtropics may not be a particularly useful predictor of the future response of the northern hemisphere mid-latitude jet to climate change.

CHAPTER EIGHT: FUTURE WORK

There are several interesting ways to further this research, including performing a seasonal analysis and extending the analysis to 2019. As noted by various studies, changes in the future jet can be masked by using zonal or annual means due to the seasonal variability of the jet (Cattiaux et al. 2016, Manney and Hegglin 2018, Peings et al. 2018). Given that the jet changes throughout the year, with different consequences in different seasons, it is recommended that the analysis done so far be repeated with seasonal means instead of annual means to investigate any seasonality in the patterns observed in this study. While some studies may analyze all seasons (e.g., Barnes and Polvani 2015), many focus on the Northern Hemisphere winter season, when the hemispheric temperature gradient is stronger and the jet is more pronounced (e.g., Yim et al. 2016, Peings et al. 2018). By including a seasonal analysis, attention can be brought to seasonal variations that may exist and allow the results of this study to be more readily compared to prior research, regardless of what season(s) they focused on. Additionally, most of the CMIP6 models' historical simulations only extend through 2014, and another set of simulations is needed to extend through 2019 and capture the full extent of the satellite era. Due to time constraints, this study focused only on the historical simulations that extend through 2014. Future work could incorporate the additional simulations to include the full satellite era and improve the signal-to-noise ratio for this part of the analysis. The CMIP6 ssp simulations are recommended to extend the historical era to 2019. At the time of this study, ssp245 has the largest number of ensemble members available and is therefore the preferred set of simulations to use. However, the early years

of all the ssp simulations do not vary much from one to the other, so any ssp simulations could be used depending on which one has the most available ensemble members in the future. This future work will help reduce the signal-to-noise ratio over the satellite era and illuminate any seasonal patterns that may exist in the results found thus far.

Table 1: A list of all CMIP6 1pctCO2, historical, and synthetic MSU models used.

Model Number	Model Name	Number of Historical Ensemble Members	Number of MSU Ensemble Members
1	ACCESS-CM2	3	3
2	ACCESS-ESM1-5	30	20
3	AWI-CM-1-1-MR	5	5
4	BCC-CSM2-MR	3	3
5	BCC-ESM1	3	3
6	CAMS-CSM1-0	2	2
7	CESM2	11	11
8	CESM2-FV2	3	3
9	CESM2-WACCM	3	3
10	CESM2-WACCM-FV2	3	2
11	CIESM	3	3
12	CNRM-CM6-1	29	29
13	CNRM-CM6-1-HR	1	1
14	CNRM-ESM2-1	10	8
15	CanESM5	40	40
16	CanESM5-CanOE	3	3
17	EC-Earth3	18	6
18	EC-Earth3-Veg	9	5
19	FGOALS-f3-L	3	3
20	FGOALS-g3	6	3
21	FIO-ESM-2-0	3	3
22	GFDL-CM4	1	1
23	GFDL-ESM4	3	3
24	GISS-E2-1-G-p1	28	28
25	GISS-E2-1-G-p3	9	9
26	GISS-E2-1-G-p5	9	9
27	GISS-E2-1-H	15	15
28	HadGEM3-GC31-LL	5	4
29	HadGEM3-GC31-MM	4	3
30	IITM-ESM	1	N/A
31	INM-CM4-8	1	1
32	IPSL-CM6A-LR	32	32
33	KACE-1-0-G	3	3
34	MIROC6	50	50
35	MIROC-ES2L	30	10
36	MPI-ESM1-2-HR	10	10
37	MPI-ESM1-2-LR	10	10
38	MRI-ESM2-0	5	5
39	NESM3	5	5
40	NorCPM1	30	30
41	NorESM2-LM	3	3
42	NorESM2-MM	2	2
43	SAM0-UNICON	1	1
44	TaiESM1	2	1
45	UKESM1-0-LL	19	18

Table 2: A list of reanalysis products used.

Reanalysis	Years Available	Reference
Climate Forecast System Reanalysis (CFSR)	1979-Present	Saha et al. 2014
ECMWF Reanalysis Version 5 (ERA5)	1979-Present	Hersbach et al. 2020
ECMWF Interim Reanalysis (ERA Interim)	1979-Present	Berrisford et al. 2011
Japanese 55-year Reanalysis (JRA-55)	1958-Present	Kobayashi et al. 2015
Modern-Era Retrospective Analysis for Research and Applications, Version 2 (MERRA-2)	1980-Present	Gelaro et al. 2017

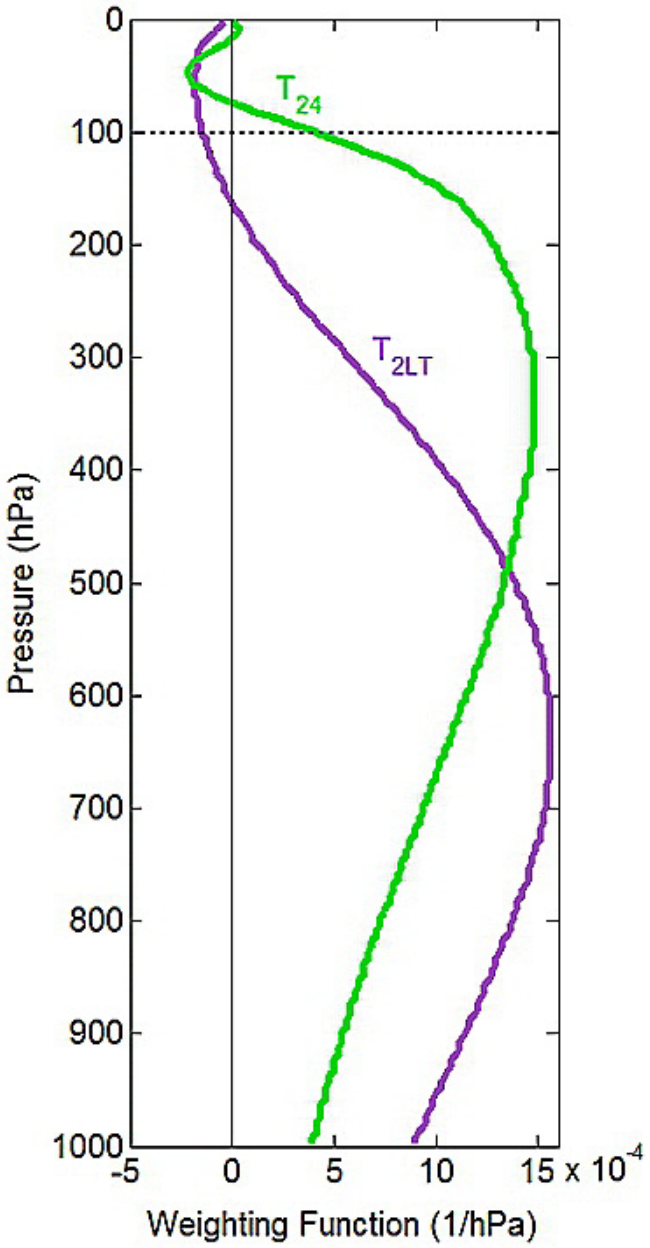

Figure 1: The effective weighting function of the stratosphere-corrected TMT (T24), represented by the green line, from Fu et al. 2011. The tropical tropopause is set at 100 hPa.

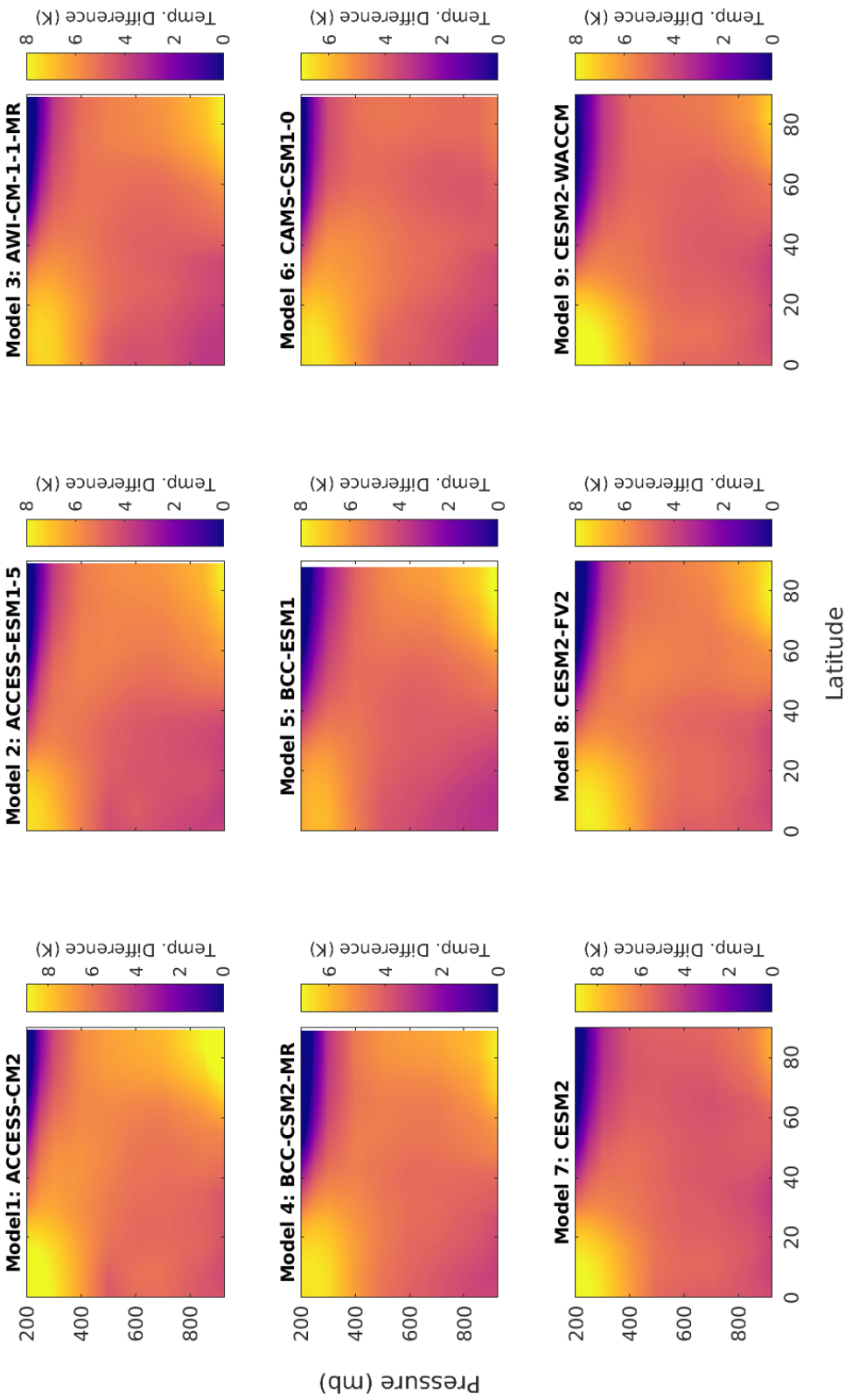

Figure 2: Warming between the future (years 121-150) and control (years 1-30) period of the 1pctCO2 simulations for models 1 through 9 of 45.

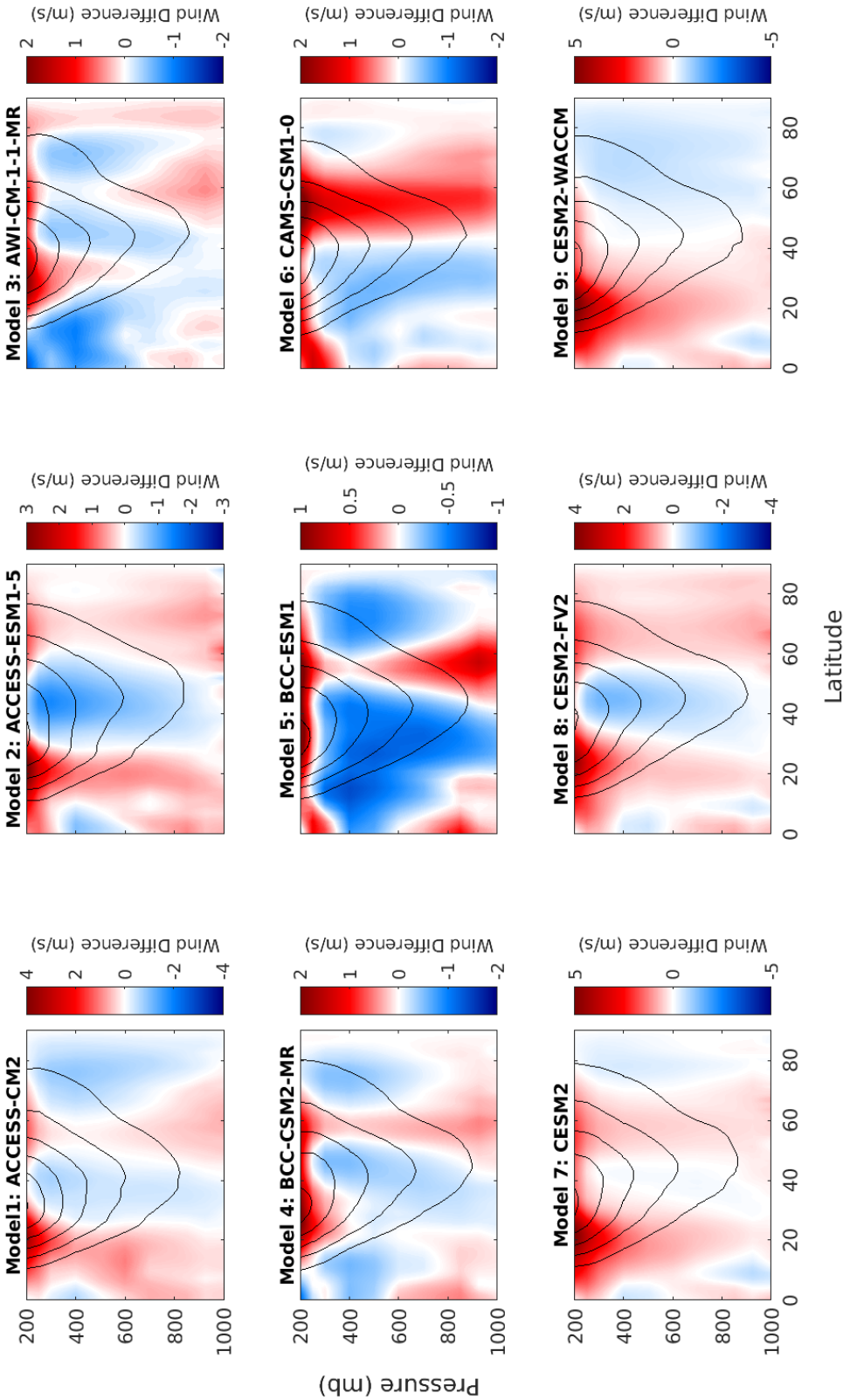

Figure 3: Zonal wind change between the future (years 121-150) and control (years 1-30) period of the 1pctCO2 simulations for models 1 through 9 of 45. The black contours are the zonal mean wind for the control period and are shown in 5 m/s intervals.

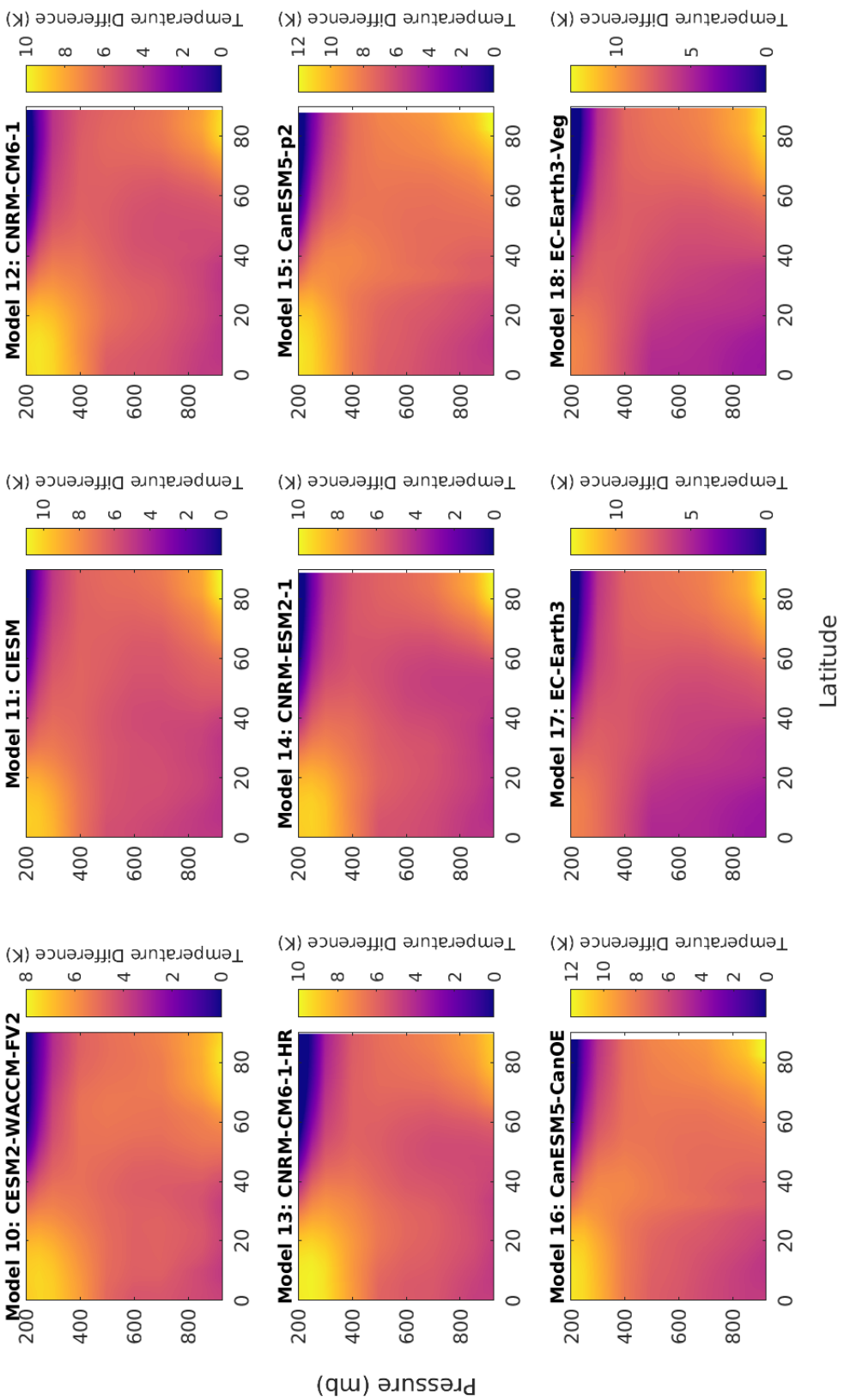

Figure 4: As in Figure 2, but for models 10 through 18 of 45.

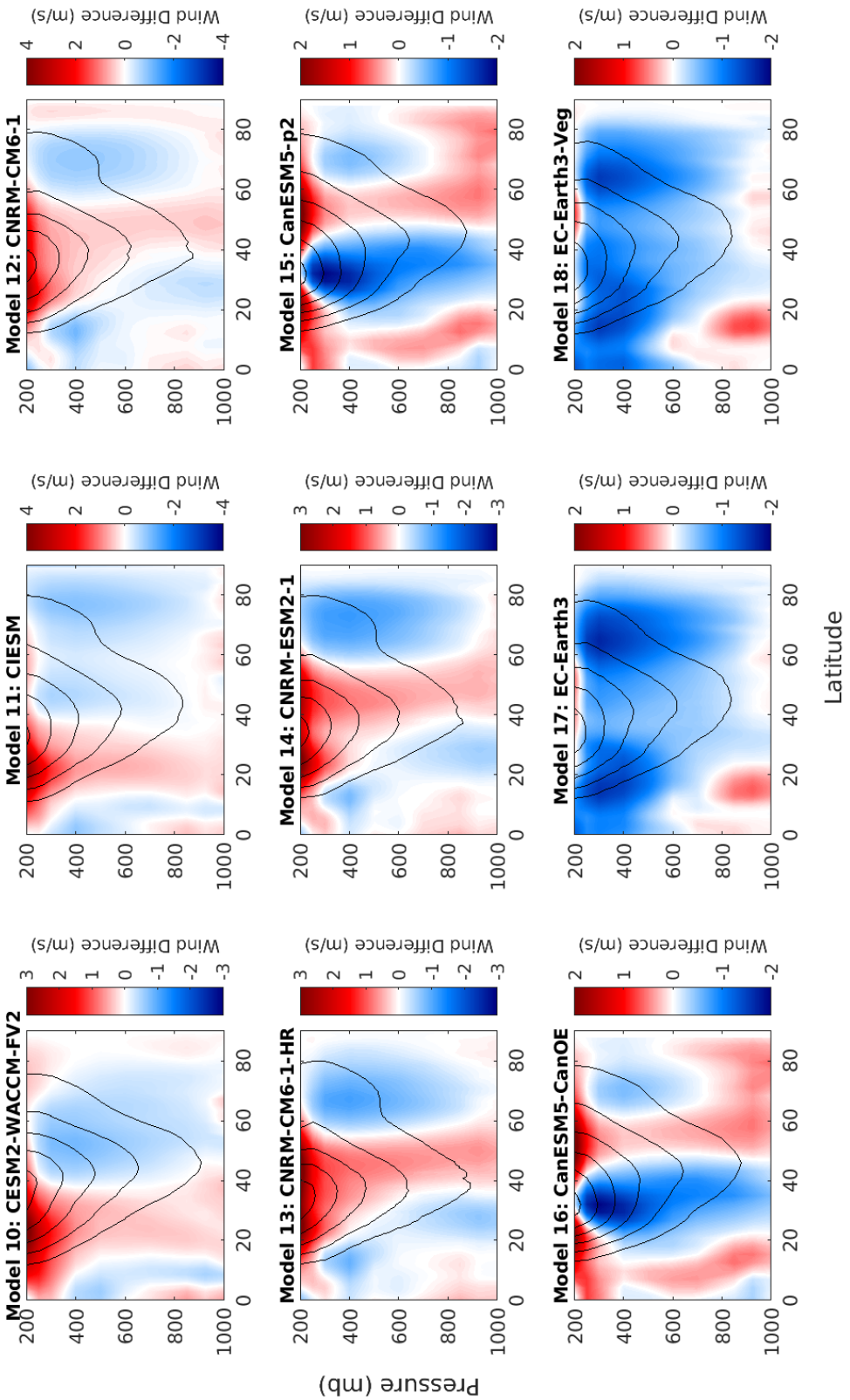

Figure 5: As in Figure 3, but for models 10 through 18 of 45.

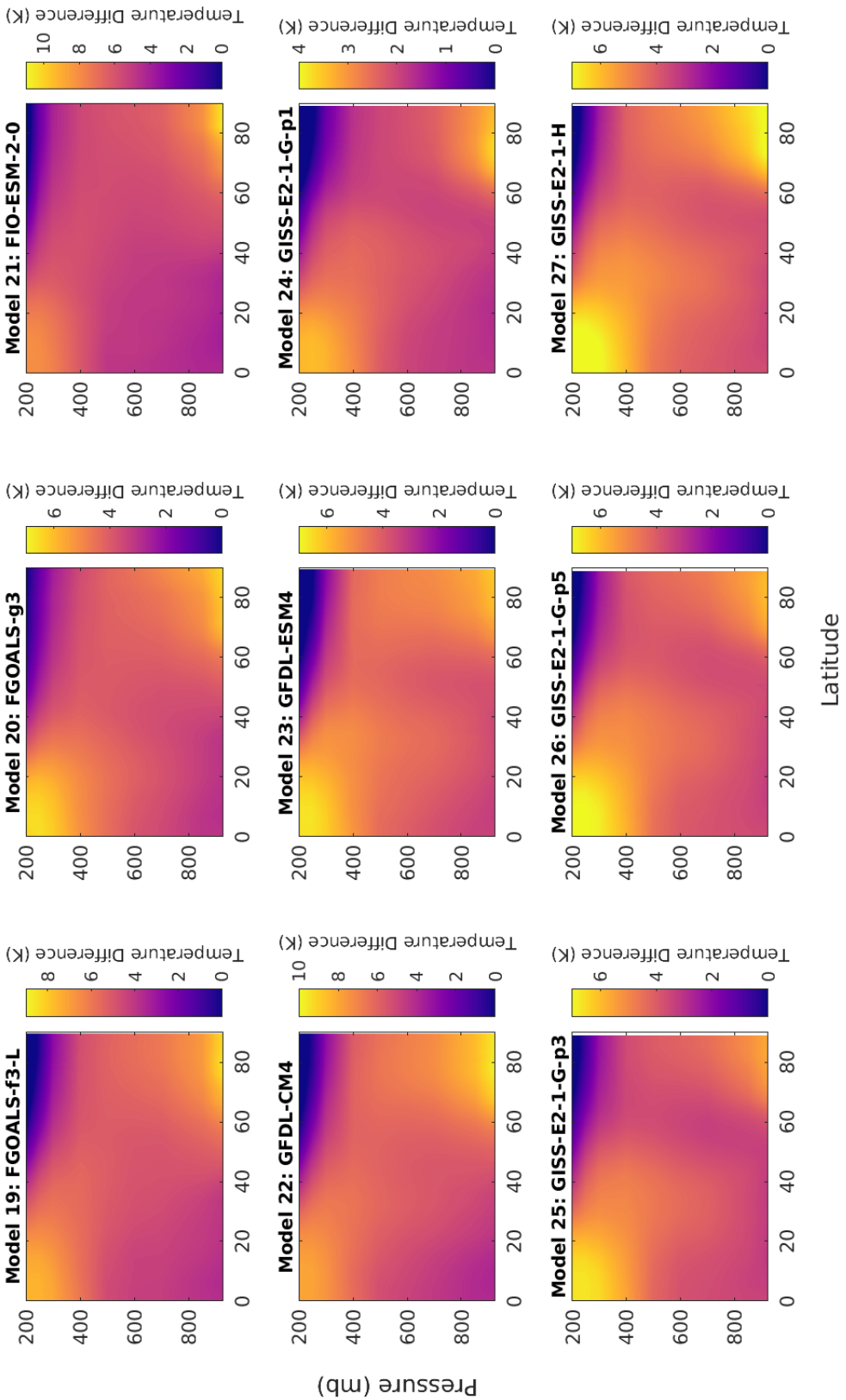

Figure 6: As in Figure 2, but for models 19 through 27 of 45.

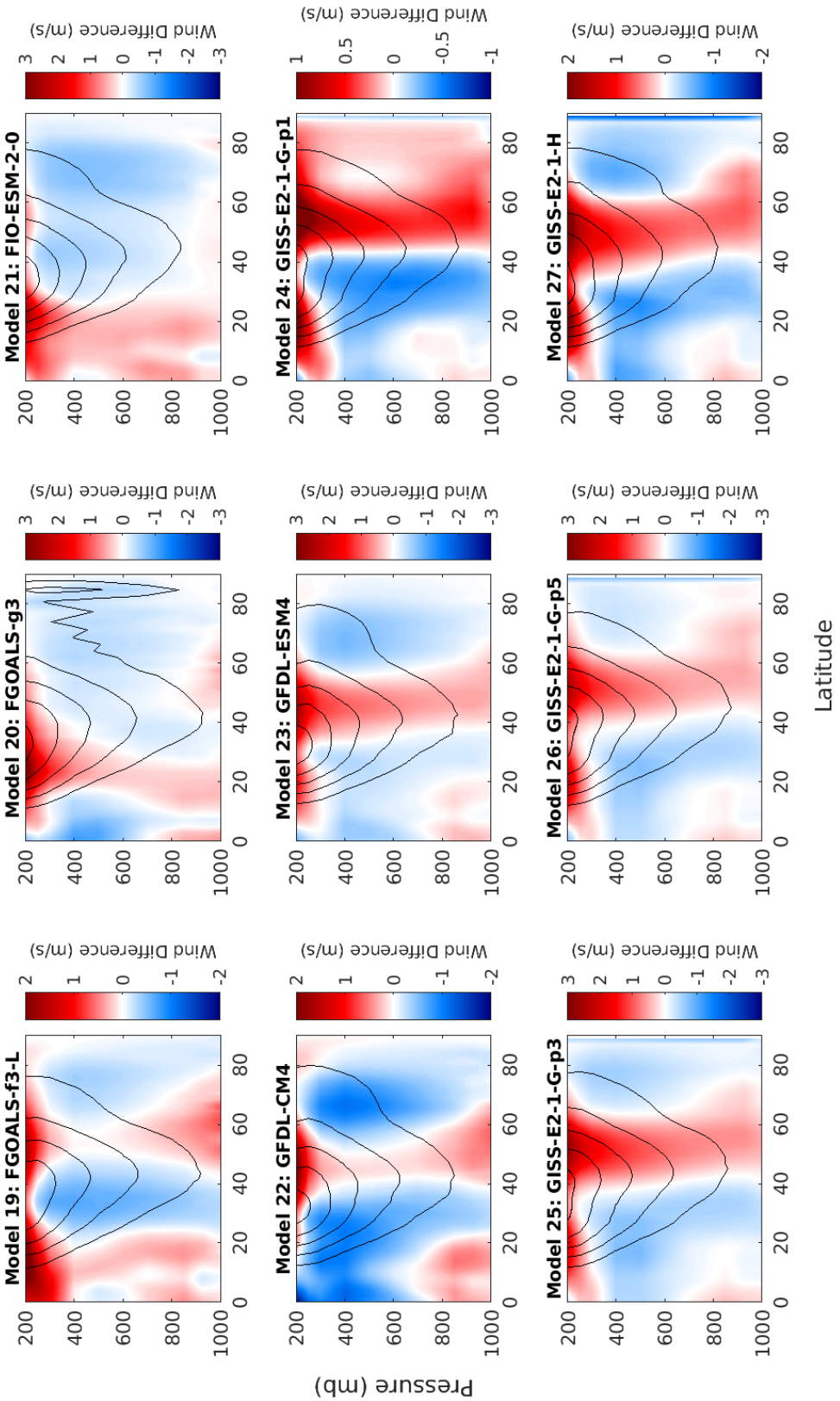

Figure 7: As in Figure 3, but for models 19 through 27 of 45.

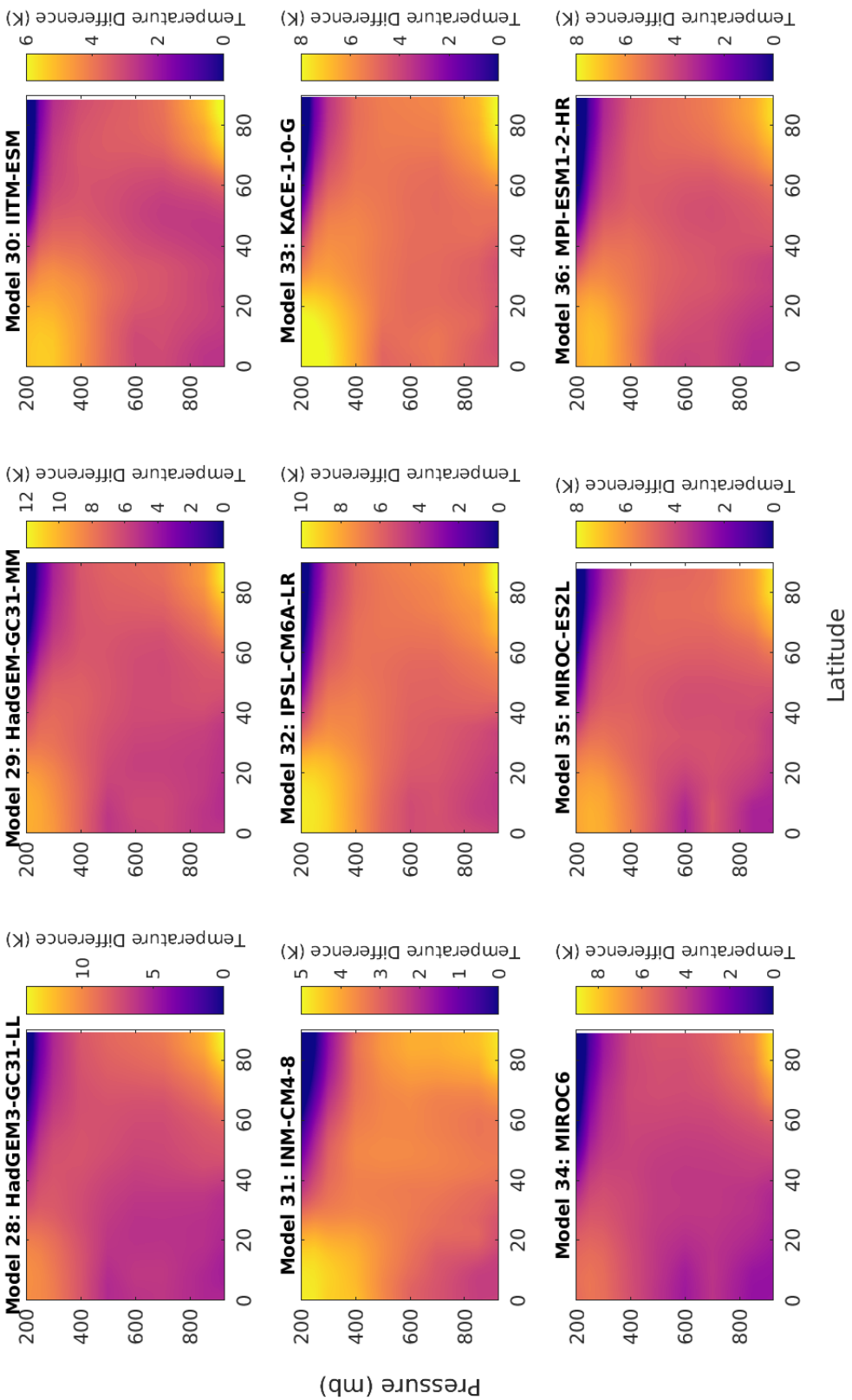

Figure 8: As in Figure 2, but for models 28 through 36 of 45.

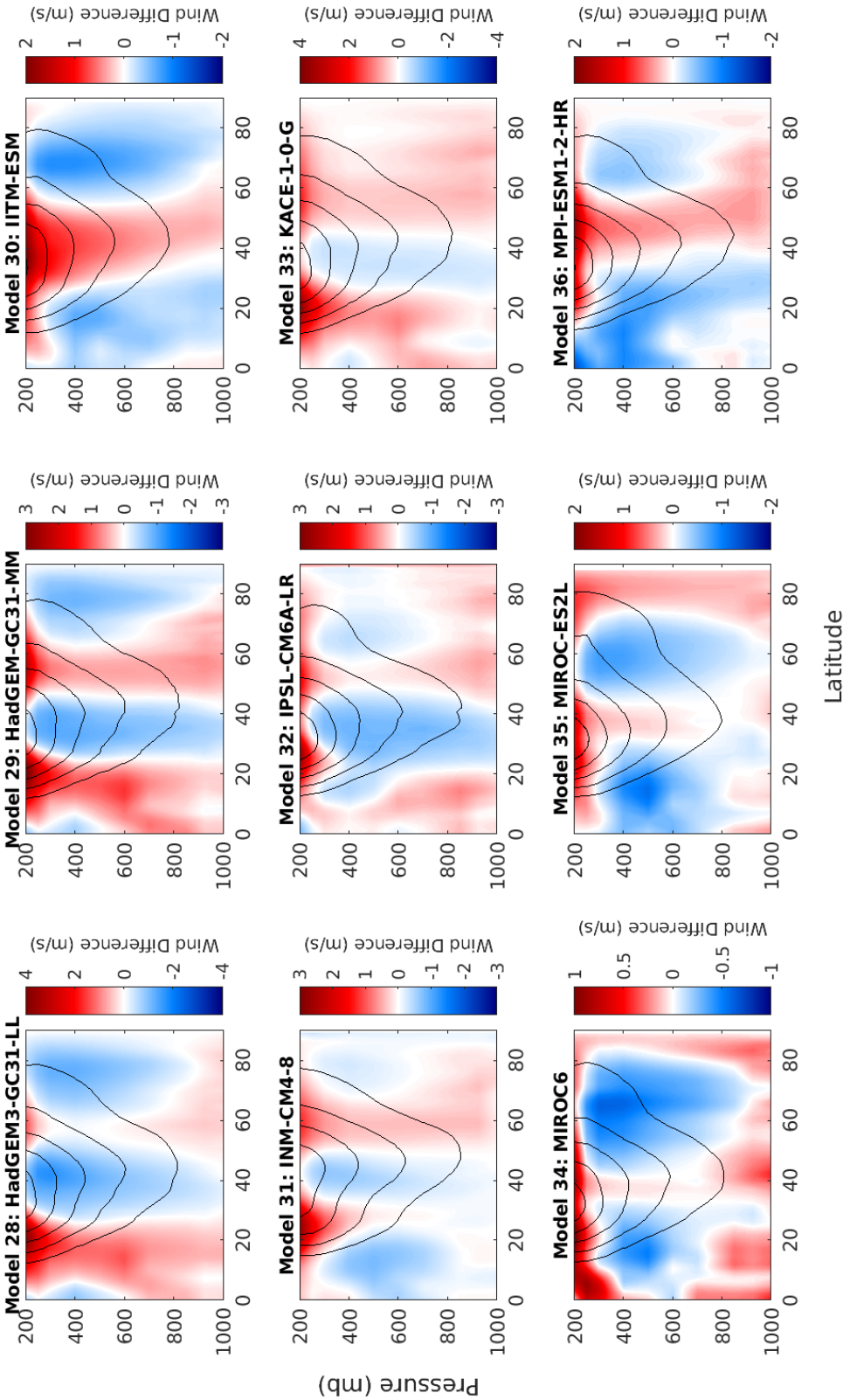

Figure 9: As in Figure 3, but for models 28 through 36 of 45.

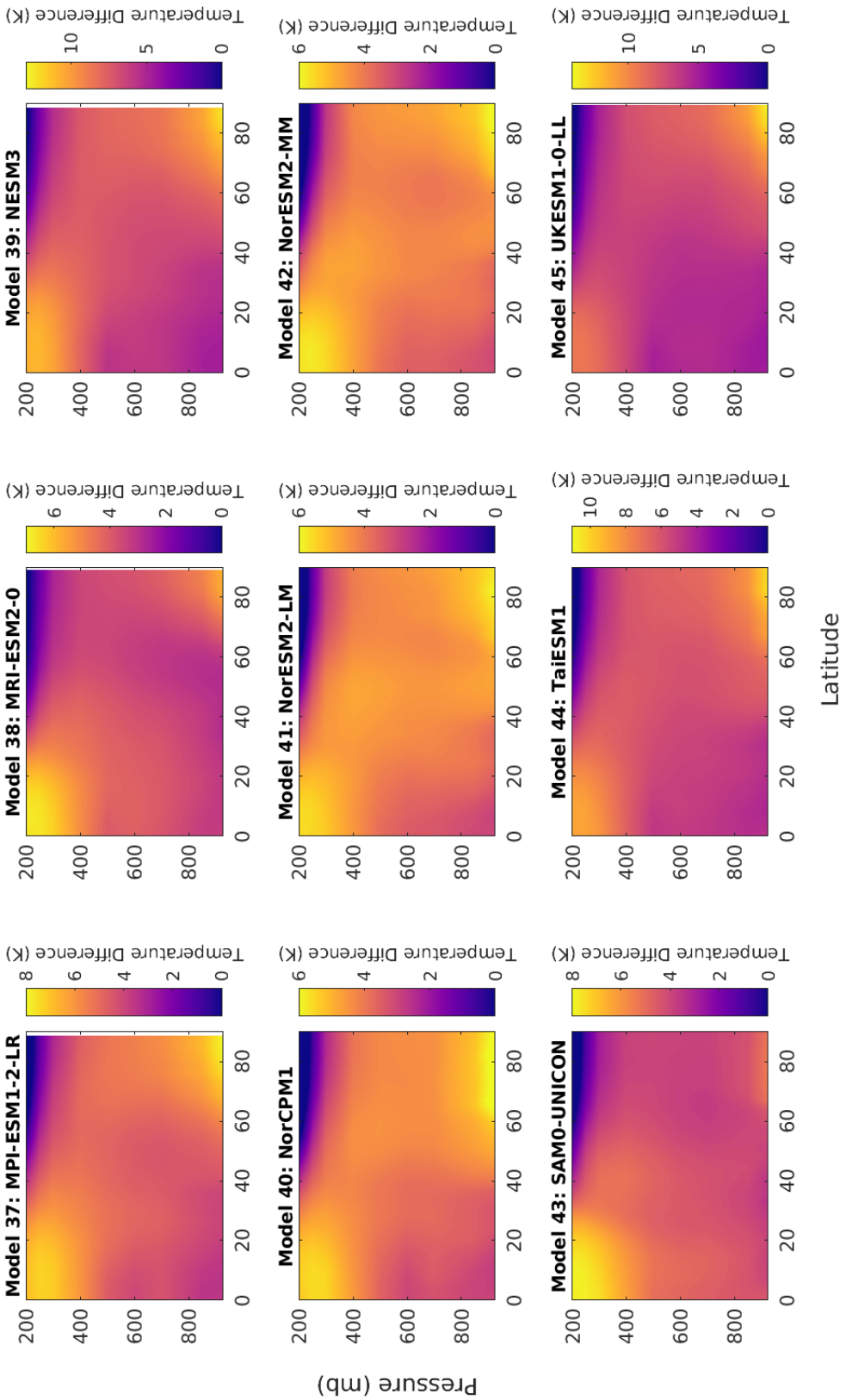

Figure 10: As in Figure 2, but for models 37 through 45.

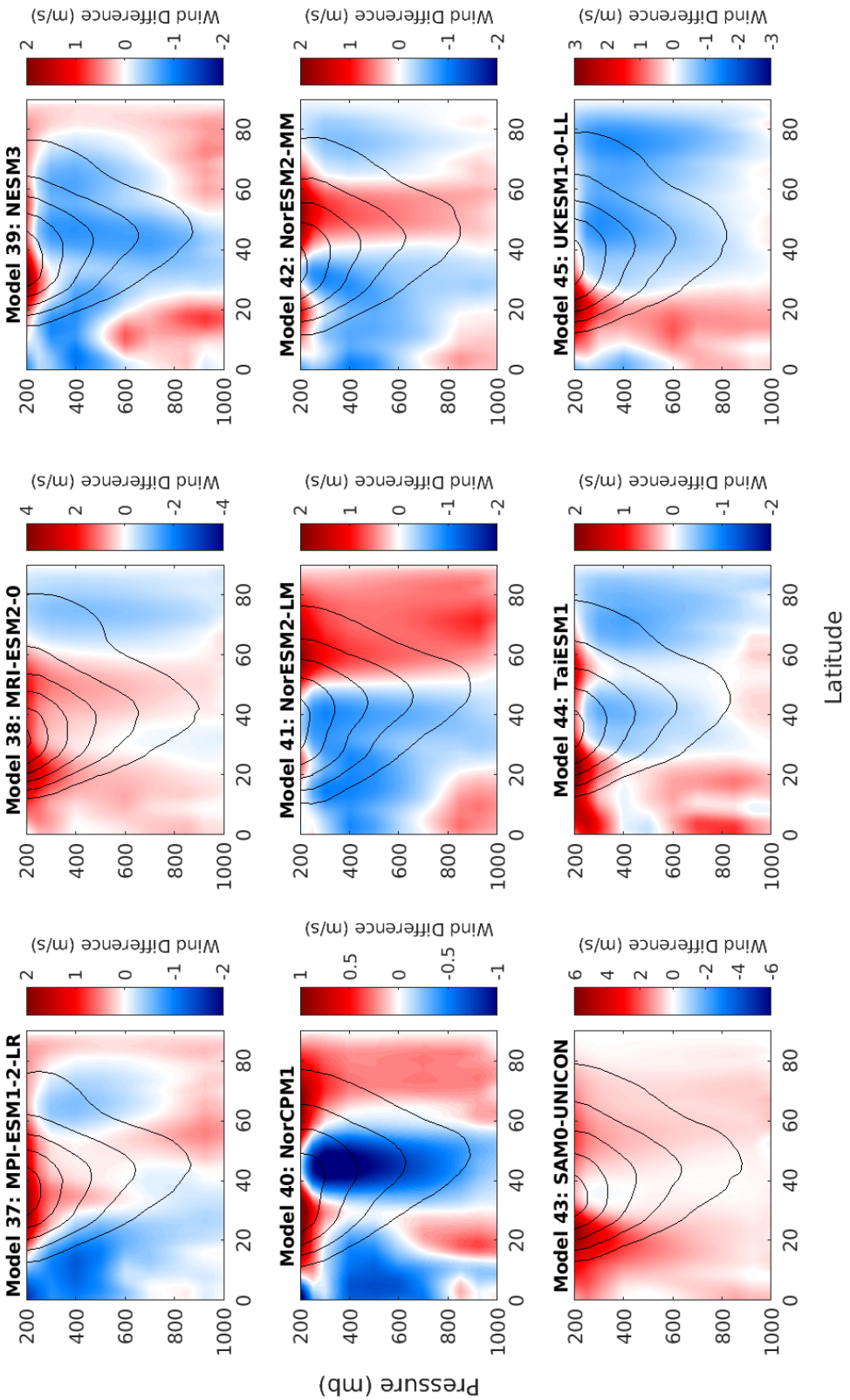

Figure 11: As in Figure 3, but for models 37 through 45.

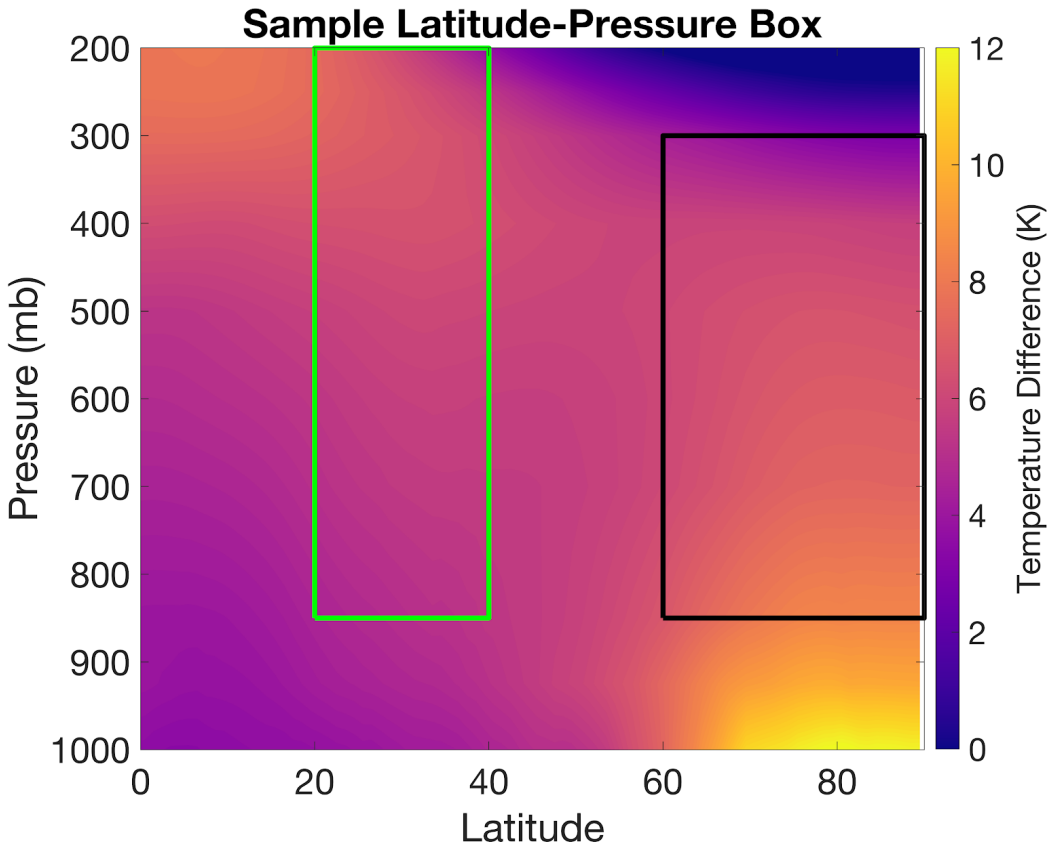

Figure 12: Visualization of the latitude-pressure boxes used to define the subtropics (green, 20˚N-40˚N, 850mb-200mb) and the Arctic (black, 60˚N-90˚N, 850mb-300mb).

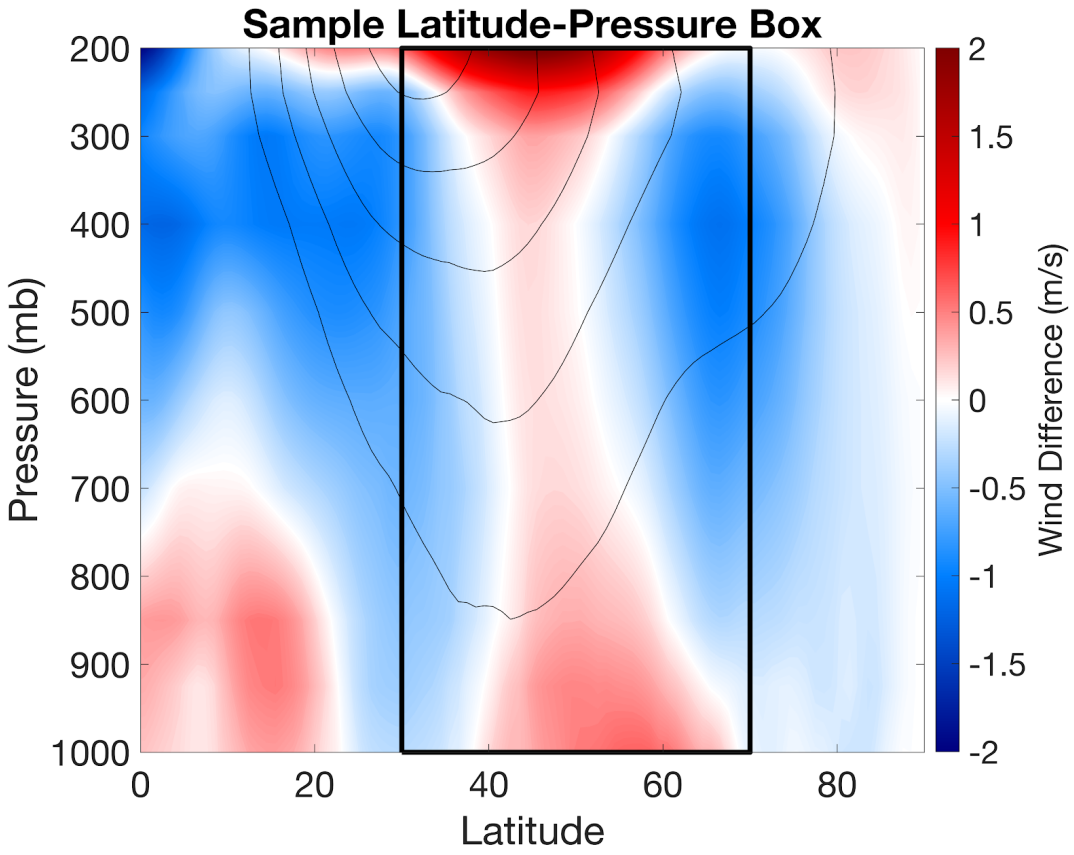

Figure 13: As in Figure 12, but for the mid-latitude jet (30˚N-70˚N, 1000mb-200mb).

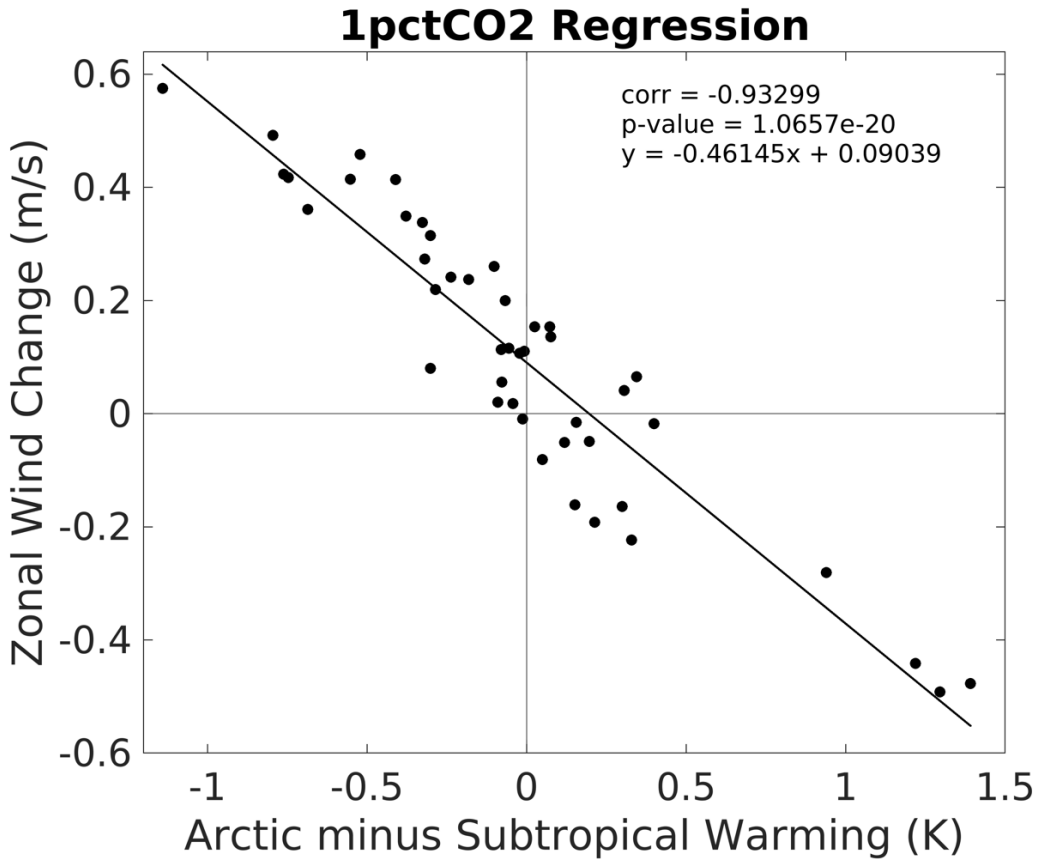

Figure 14: Scatterplot and regression line for the 1pctCO2 simulation analysis. Pearson correlation and p-value as well as the equation for the regression line are included on the plot.

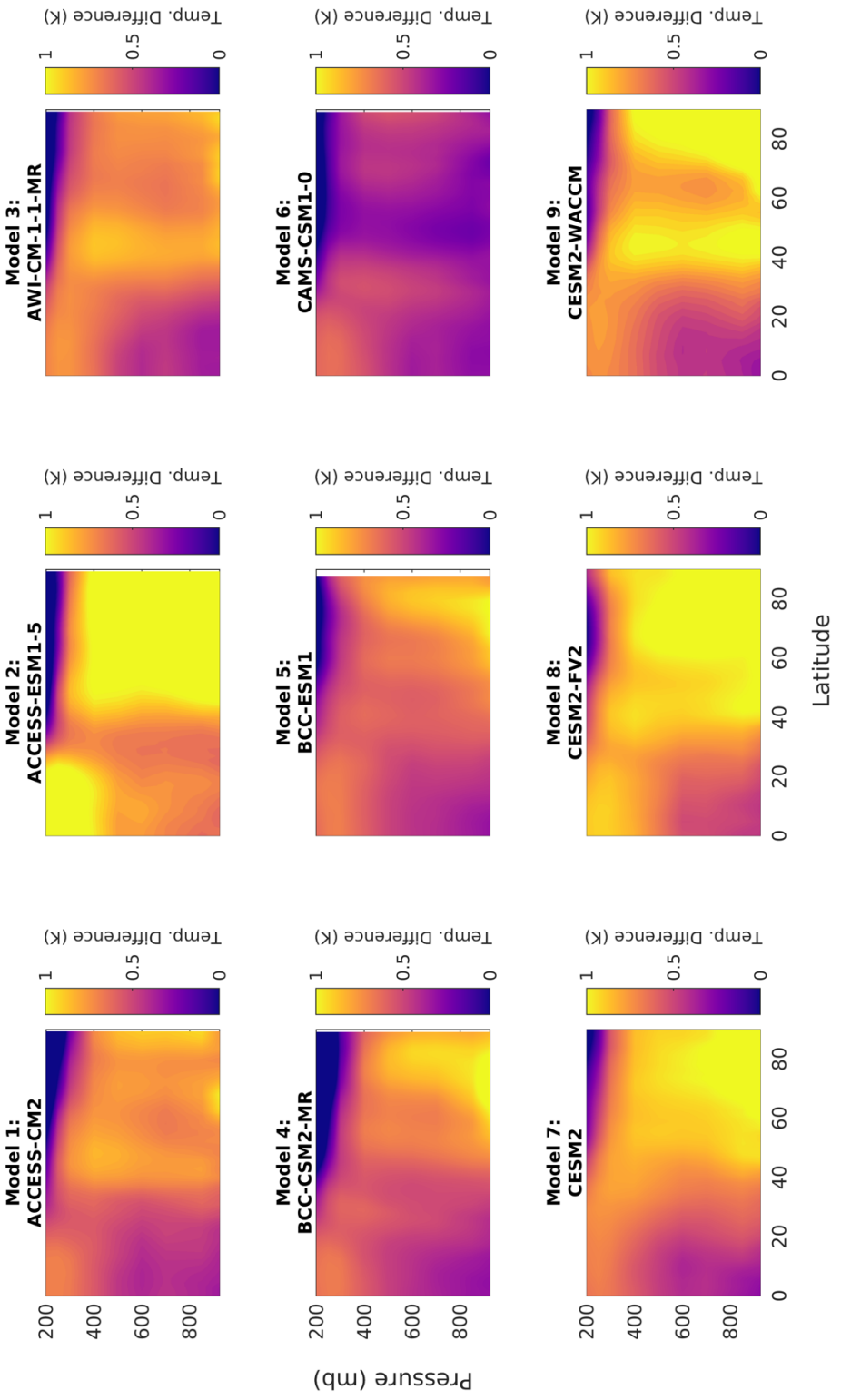

Figure 15: Warming between the present (1997-2014) and past (1980-1997) period of the historical simulations for models 1 through 9 of 45.

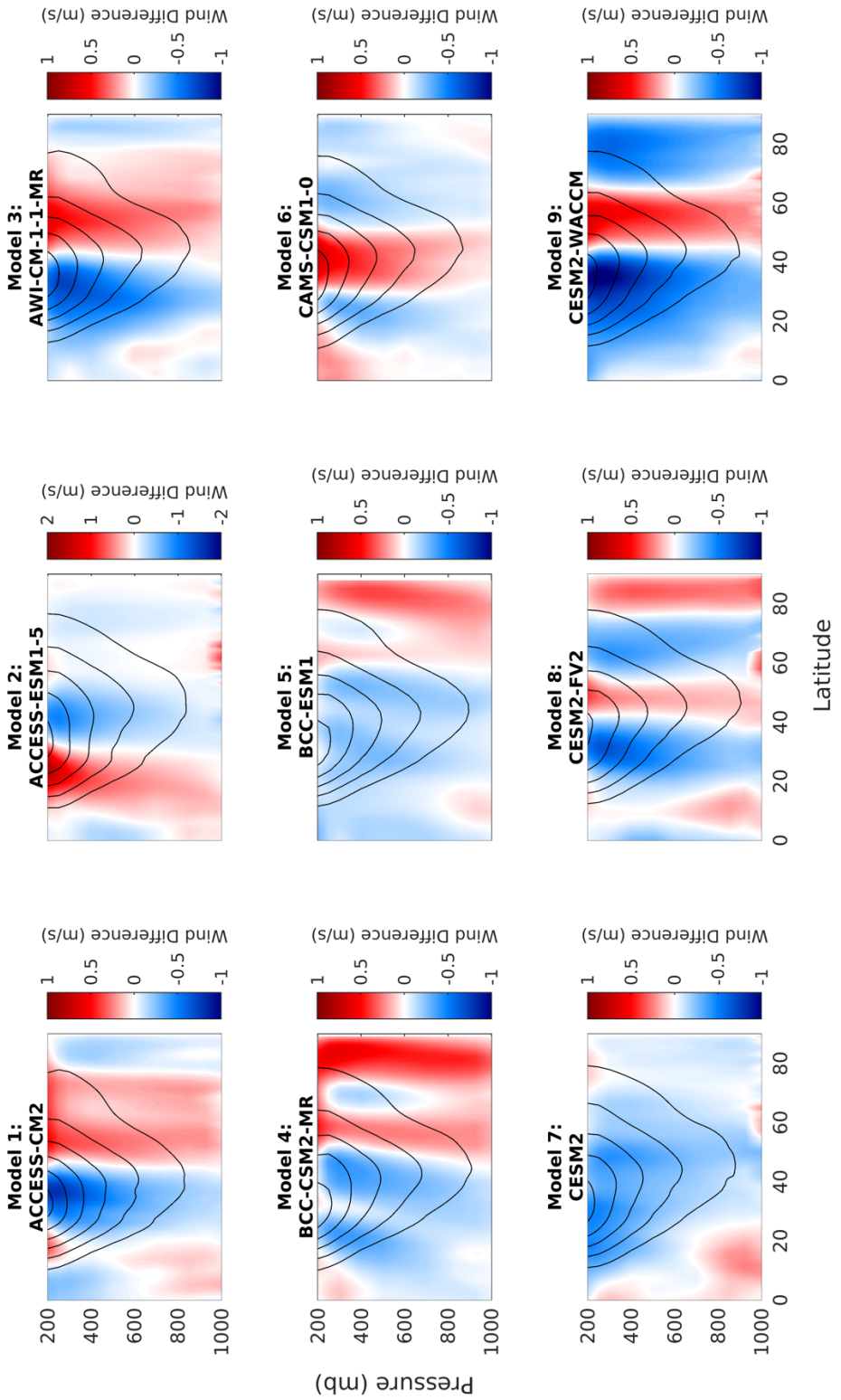

Figure 16: Zonal wind change between the present (1997-2014) and past (1980-1997) period of the historical simulations for models 1 through 9 of 45. The black contours are the zonal mean wind for the past period and are shown in 5 m/s intervals.

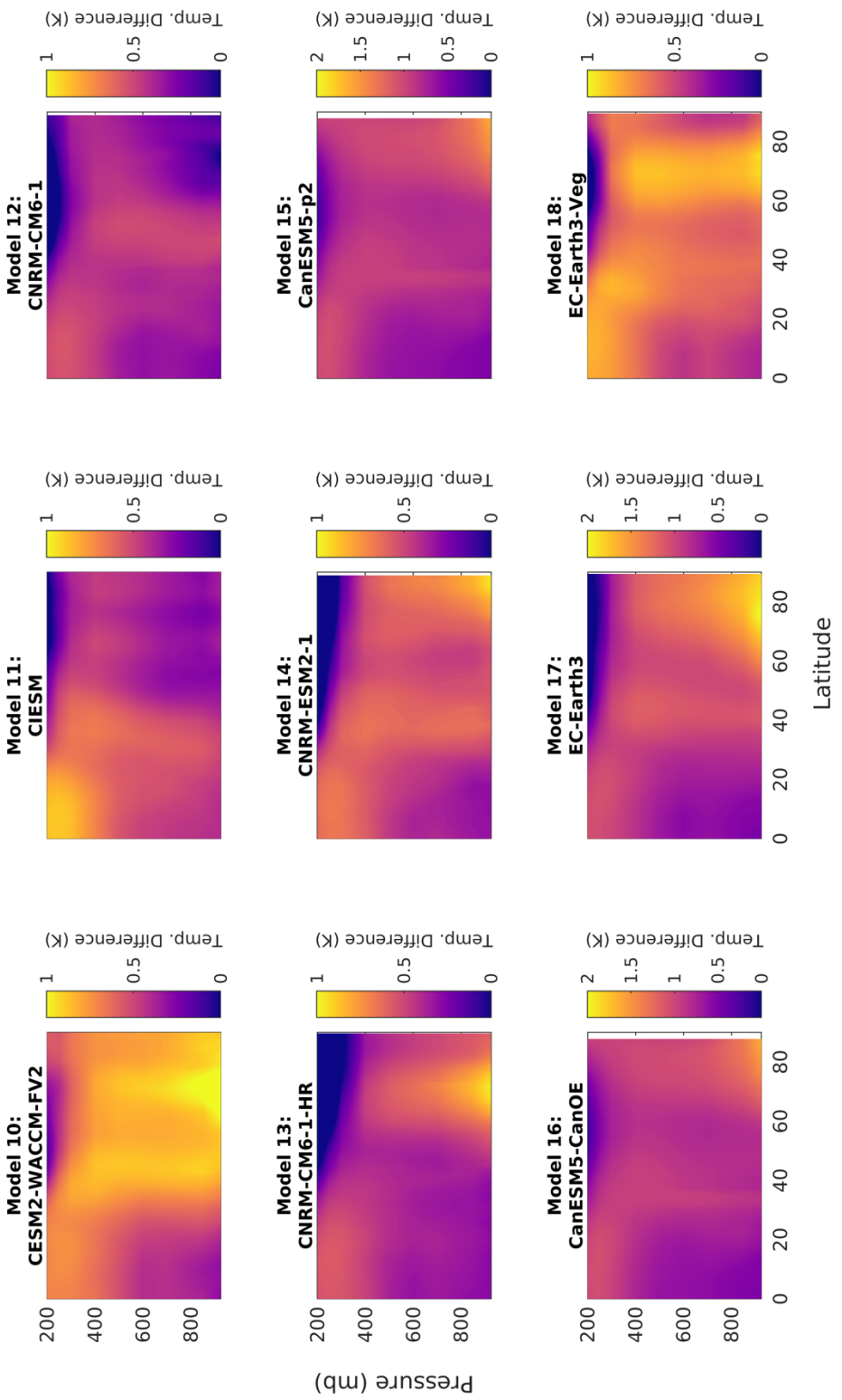

Figure 17: As in Figure 15, but for models 10 through 18 of 45.

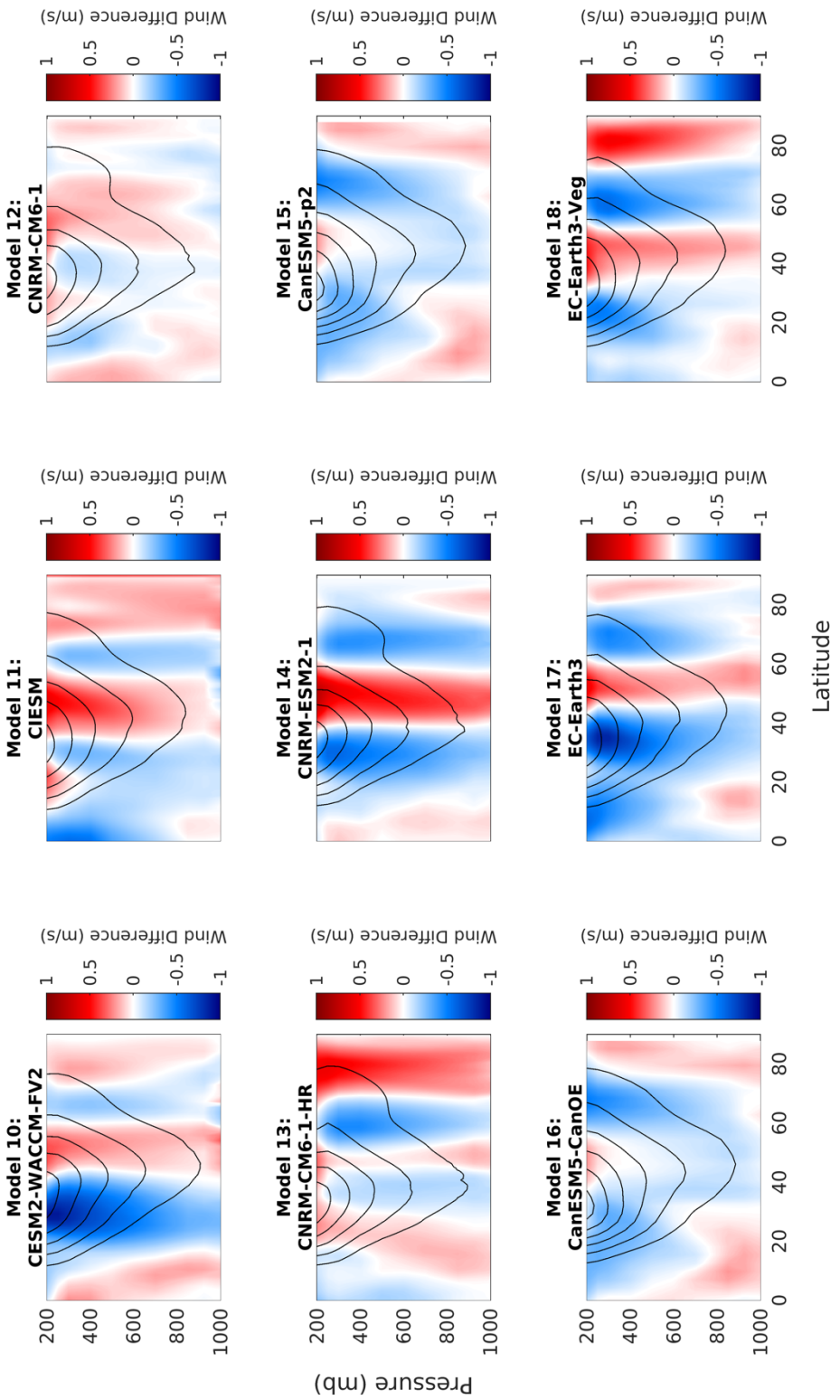

Figure 18: As in Figure 16, but for models 10 through 18 of 45.

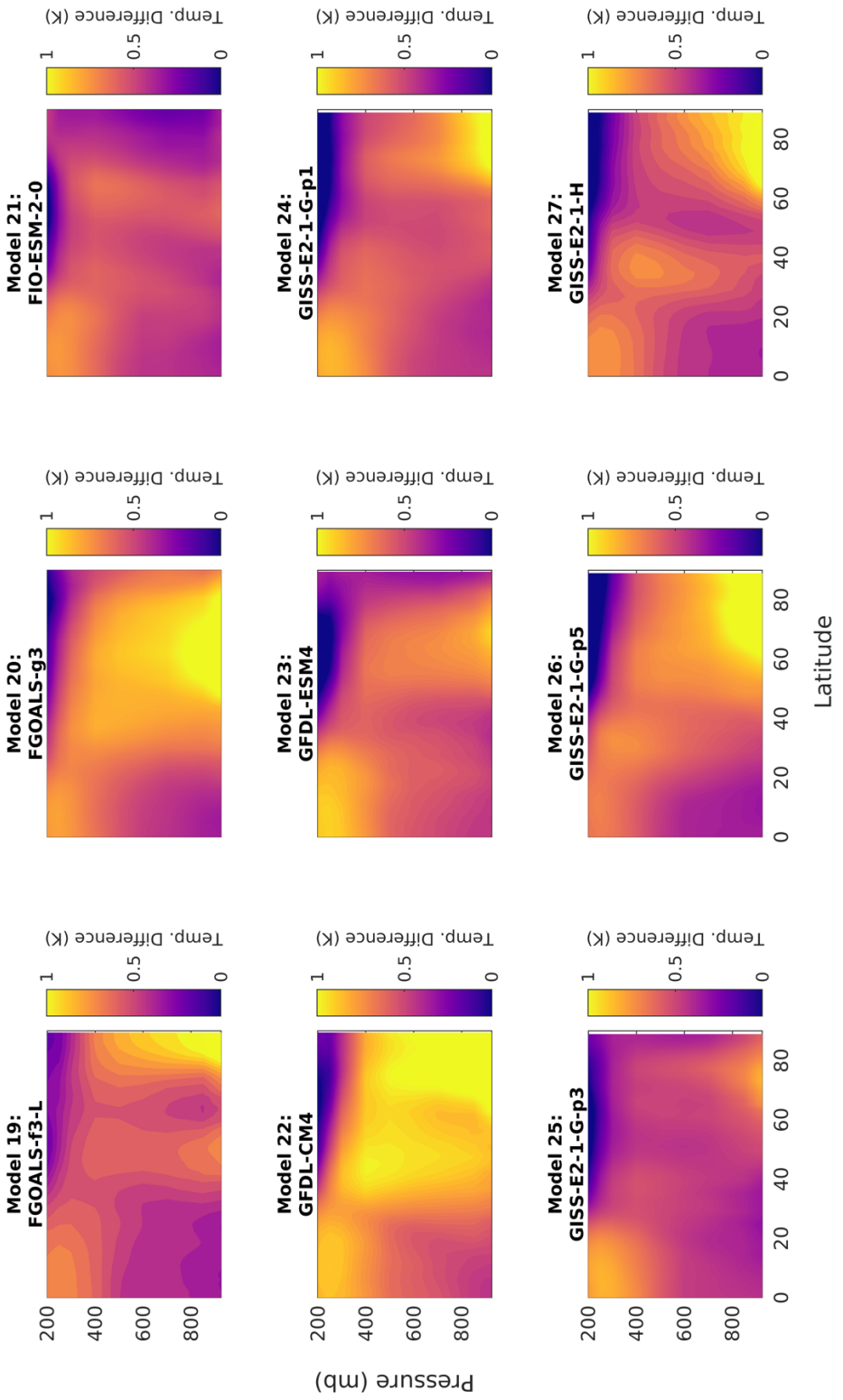

Figure 19: As in Figure 15, but for models 19 through 27 of 45.

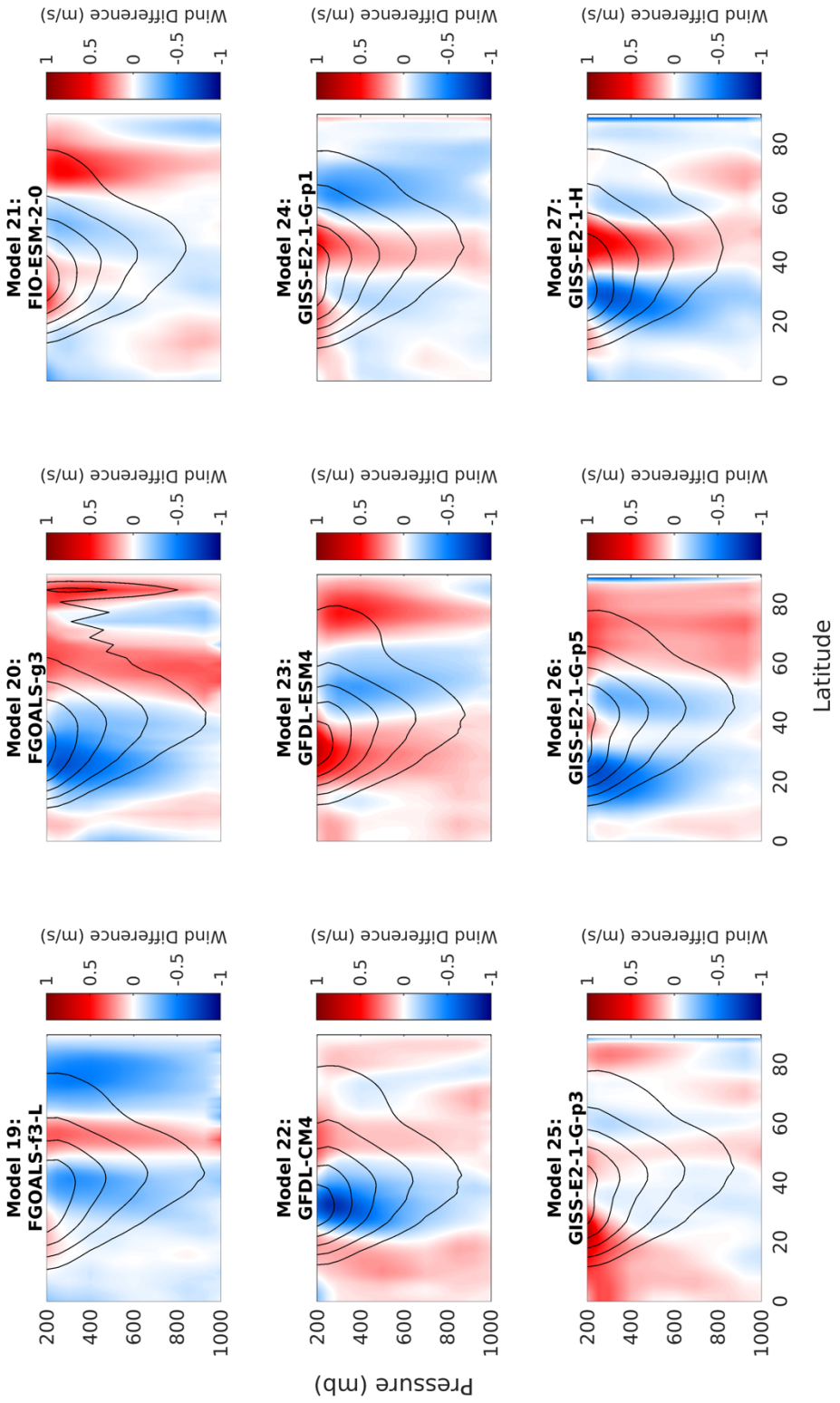

Figure 20: As in Figure 16, but for models 19 through 27 of 45.

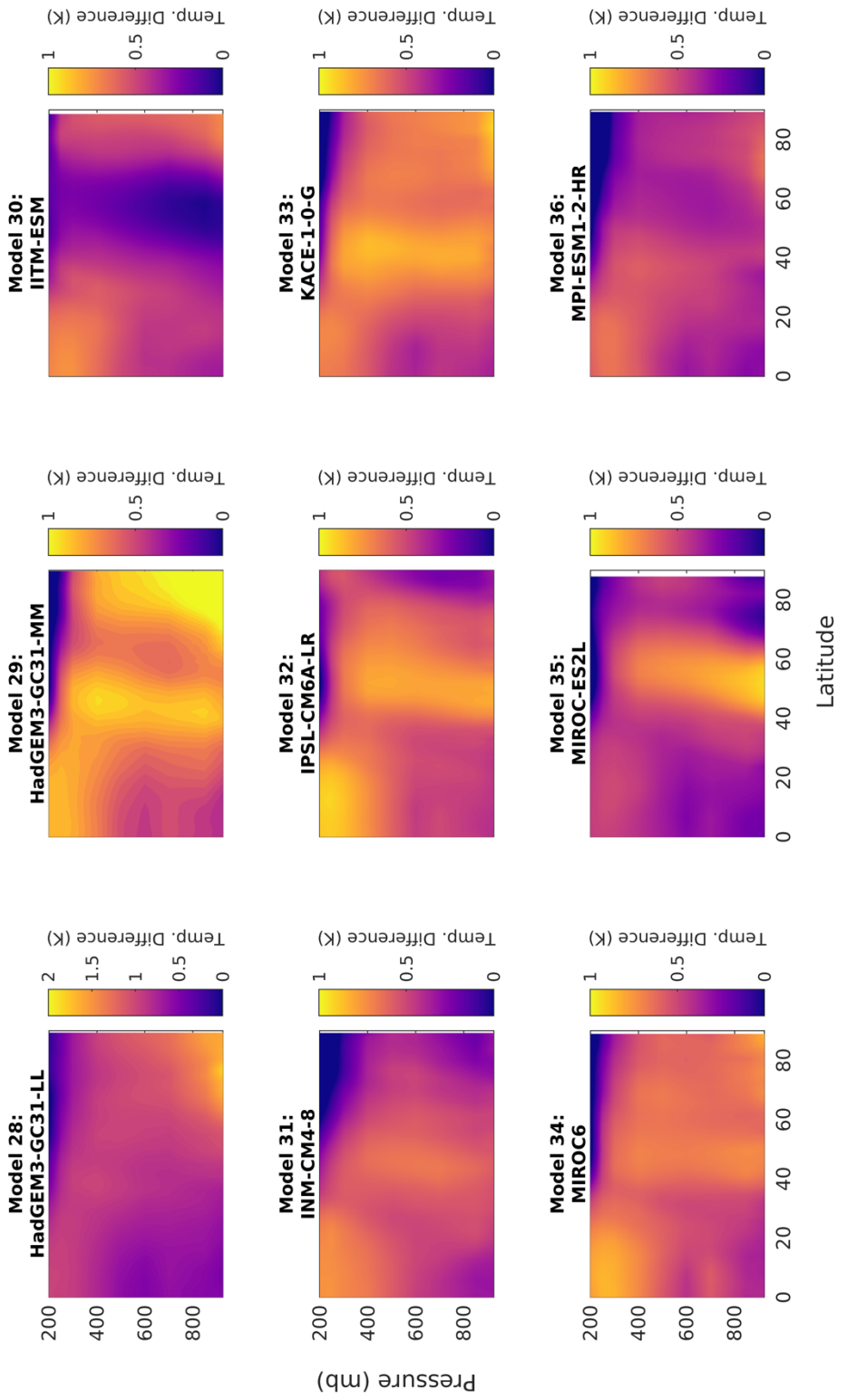

Figure 21: As in Figure 15, but for models 28 through 36 of 45.

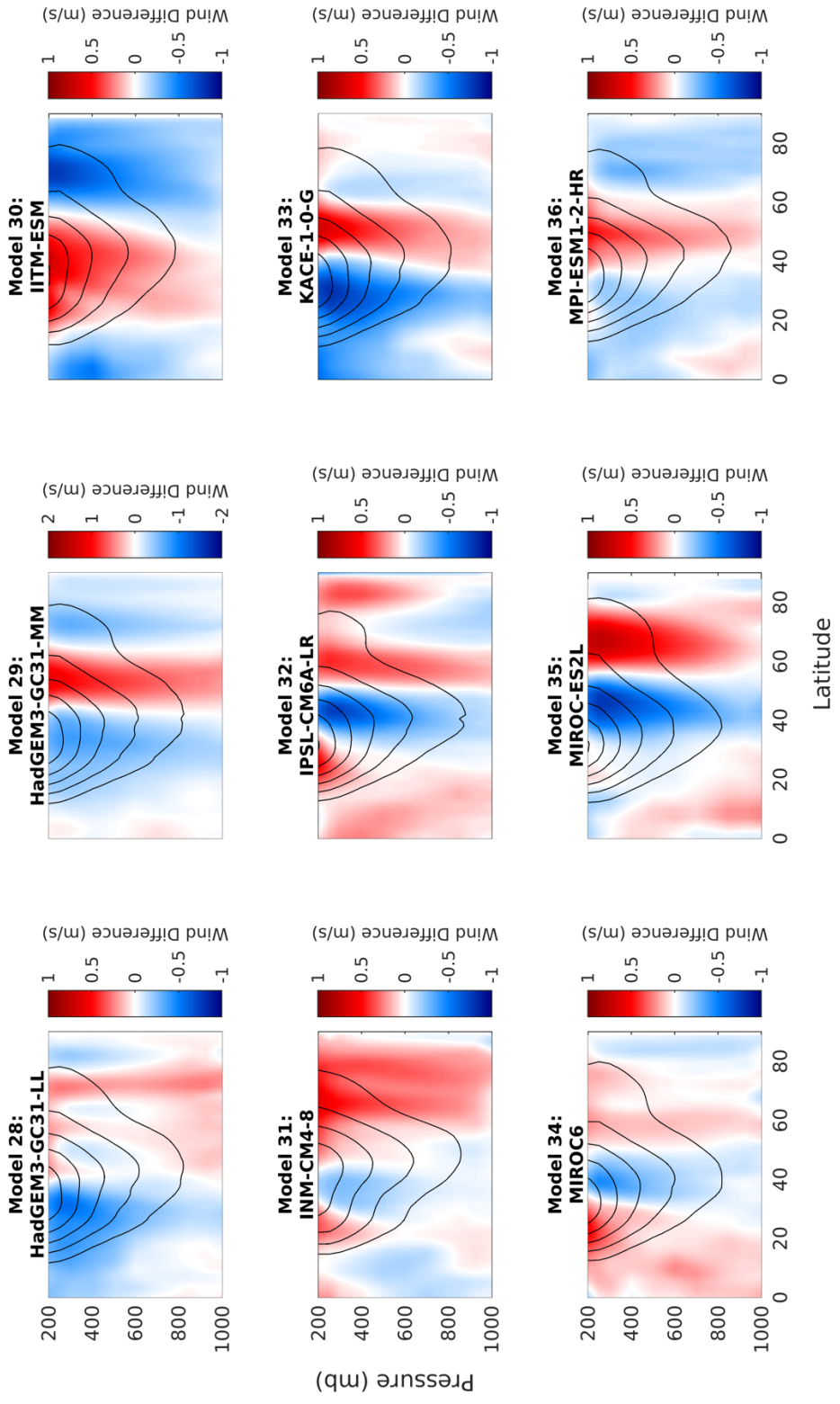

Figure 22: As in Figure 16, but for models 28 through 36 of 45.

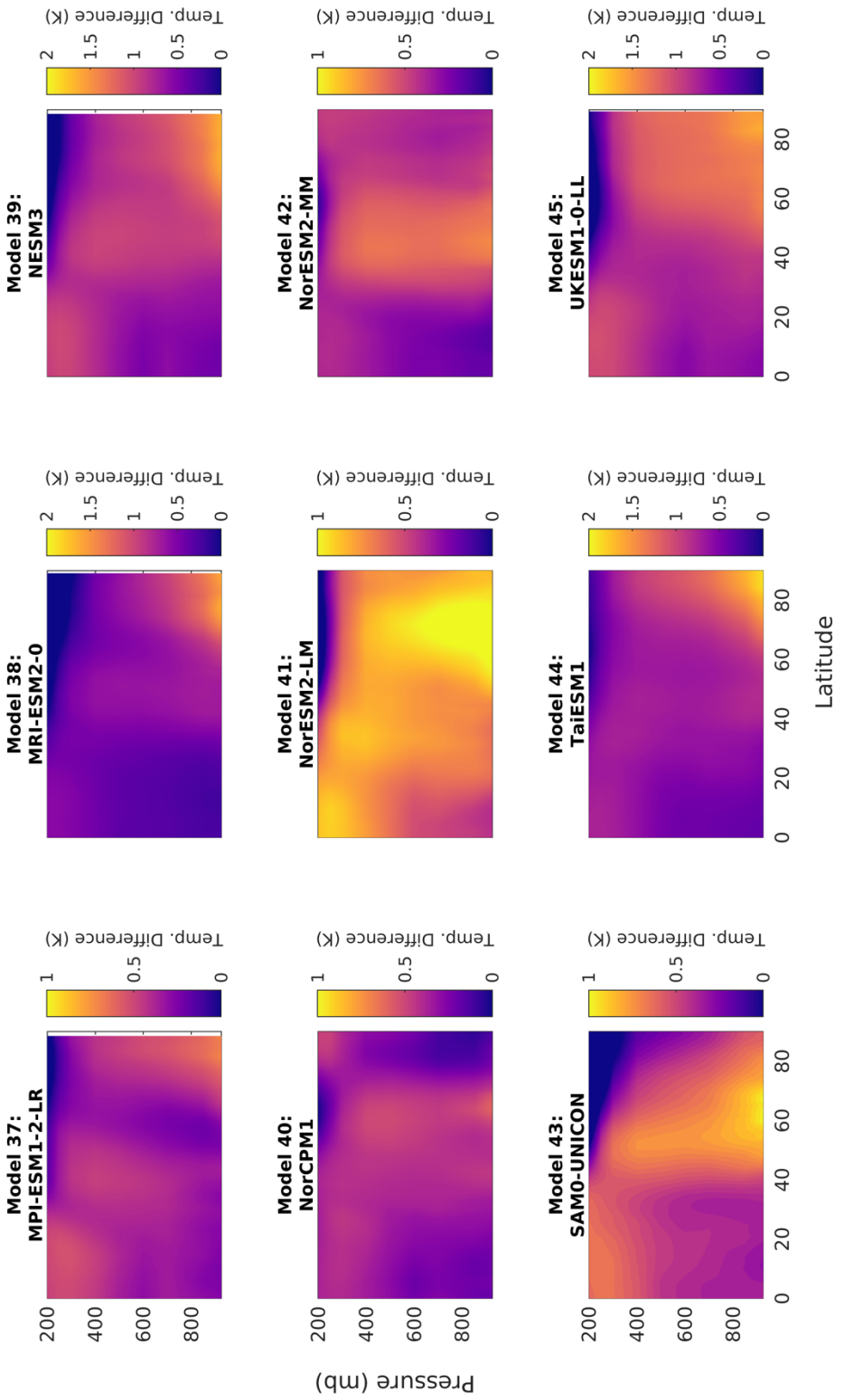

Figure 23: As in Figure 15, but for models 37 through 45.

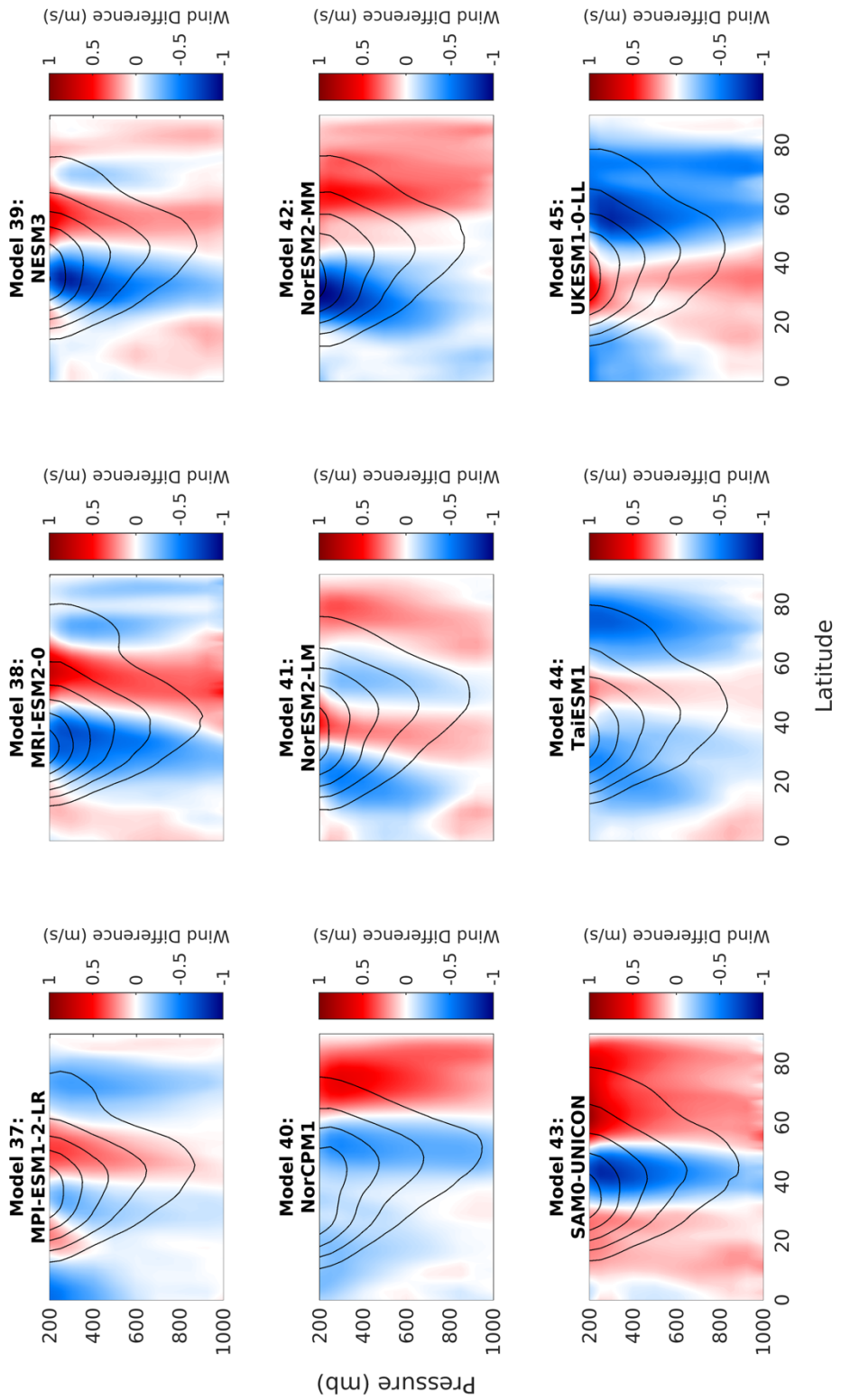

Figure 24: As in Figure 16, but for models 37 through 45.

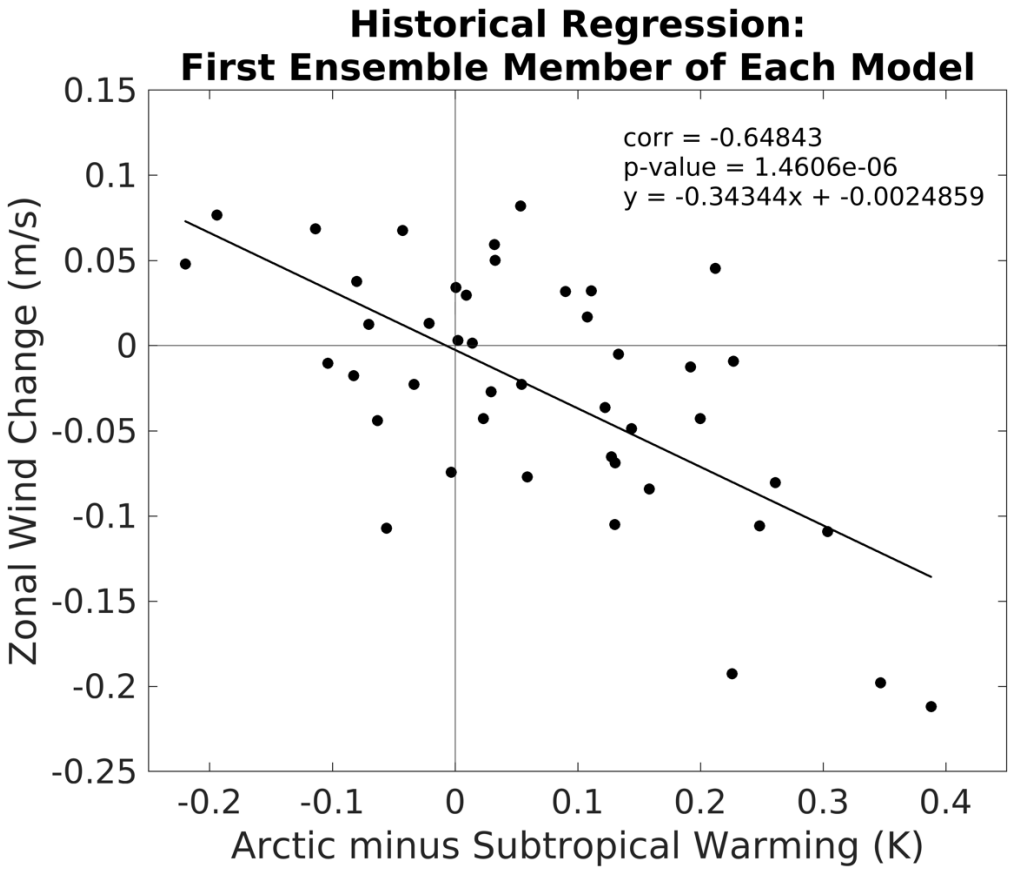

Figure 25: Scatterplot and regression line for the first ensemble member of each model for the historical simulation analysis. Pearson correlation and p-value as well as the equation for the regression line are included on the plot.

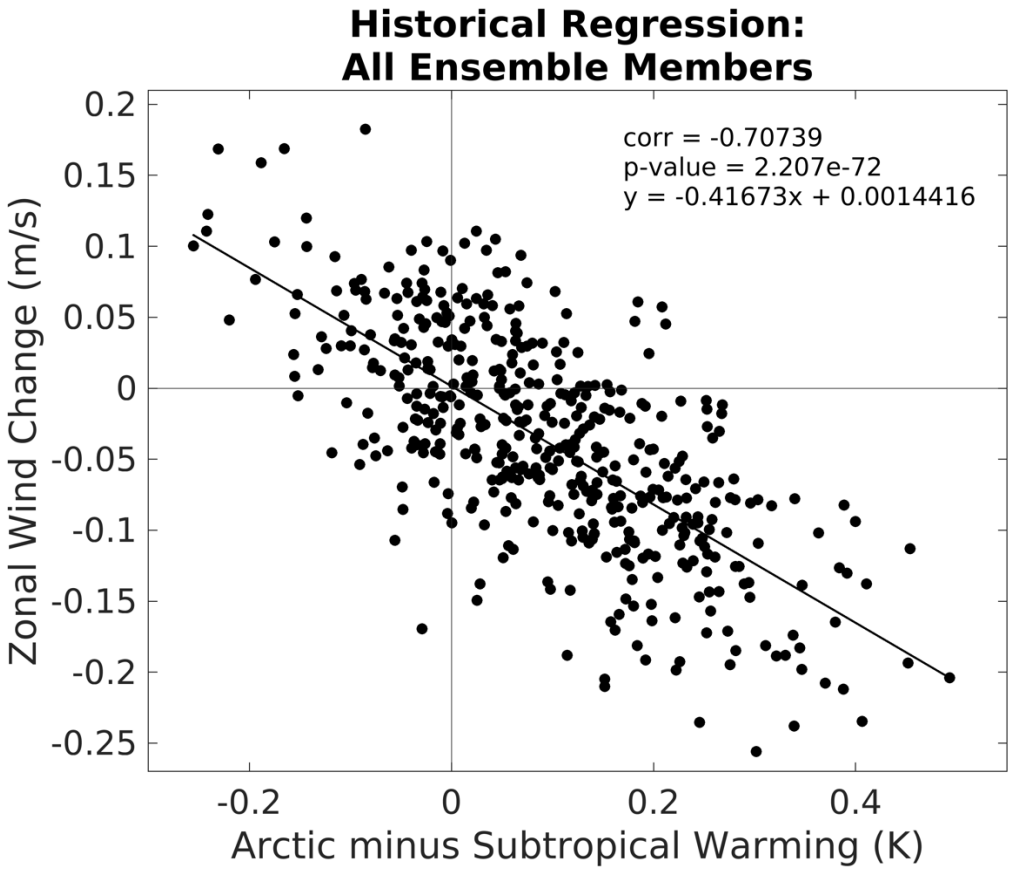

Figure 26: As in Figure 25, but for all ensemble members of the historical simulations.

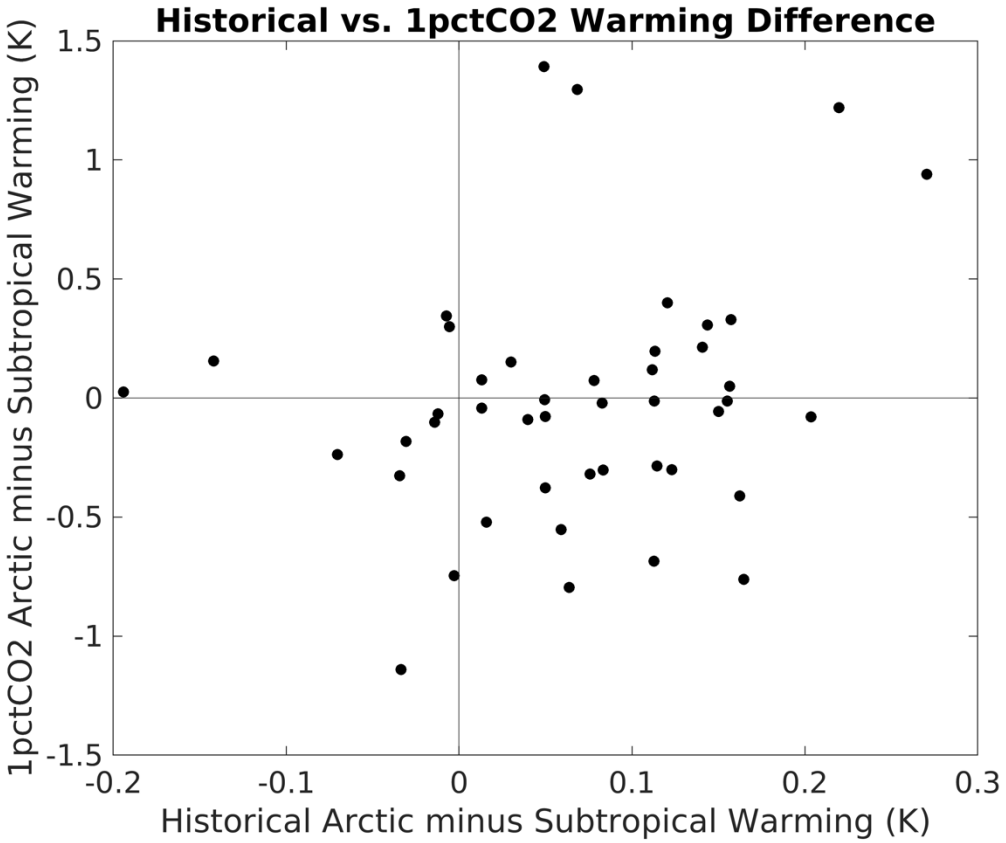

Figure 27: Scatterplot of the historical Arctic minus subtropical warming difference versus the 1pctCO2 Arctic minus subtropical warming difference.

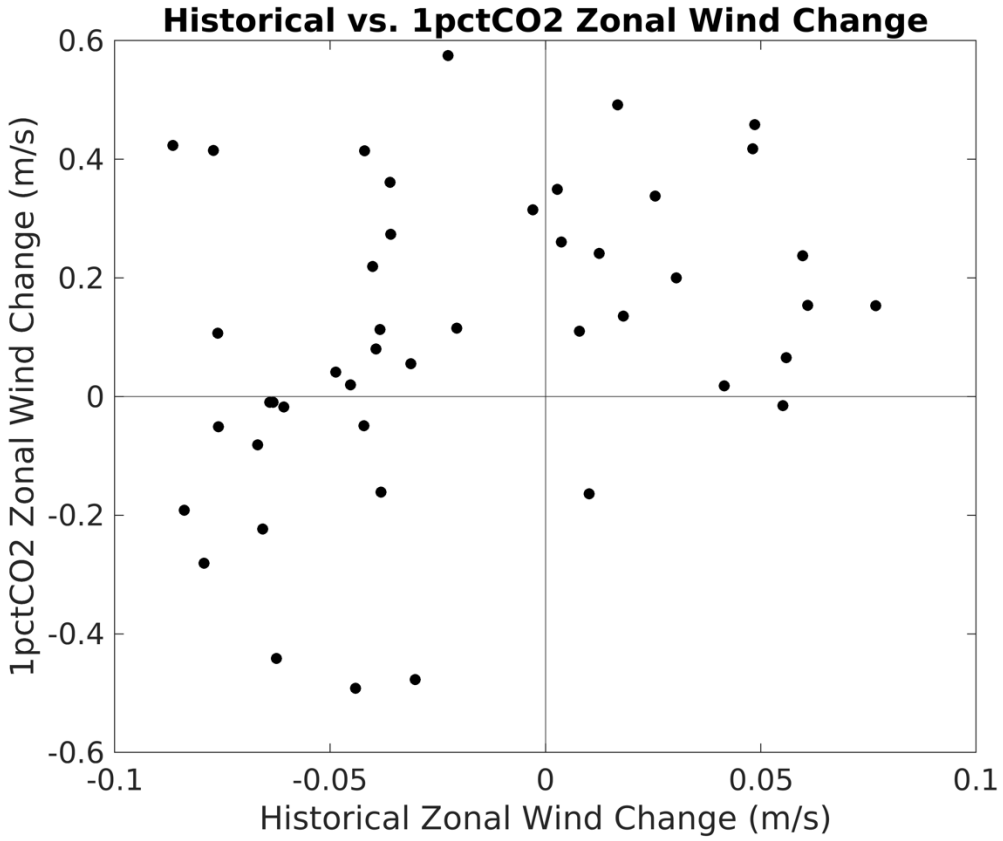

Figure 28: Scatterplot of the historical zonal wind change versus the 1pctCO2 zonal wind change.

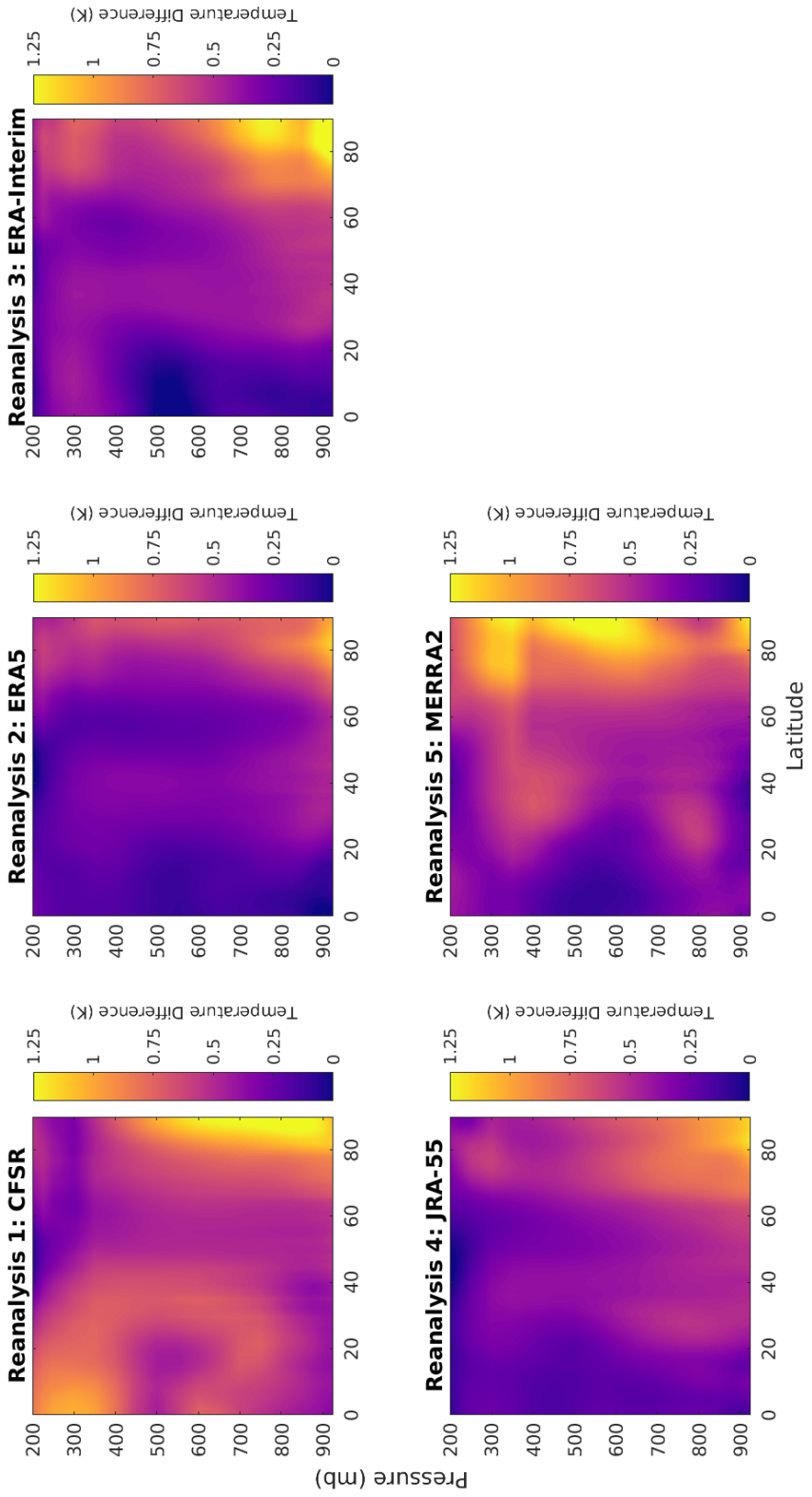

Figure 29: Warming between the last 18 years (1997-2014) and first 18 years (1980-1997) of each reanalysis.

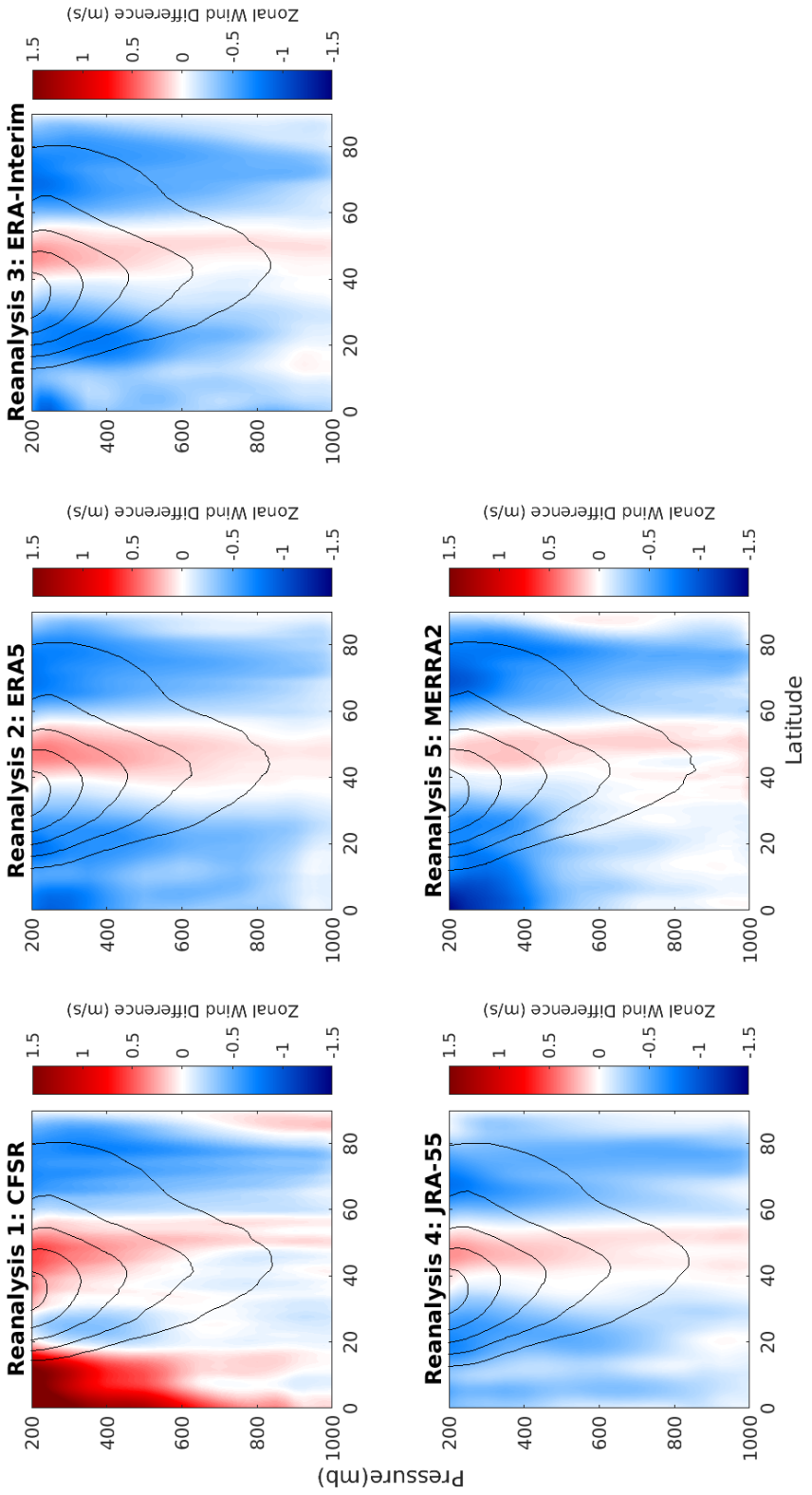

Figure 30: Zonal wind change between the last 18 years (1997-2014) and first 18 years (1980-1997) of each reanalysis. The black contours are the zonal mean wind for the first 18 years and are shown in 5 m/s intervals.

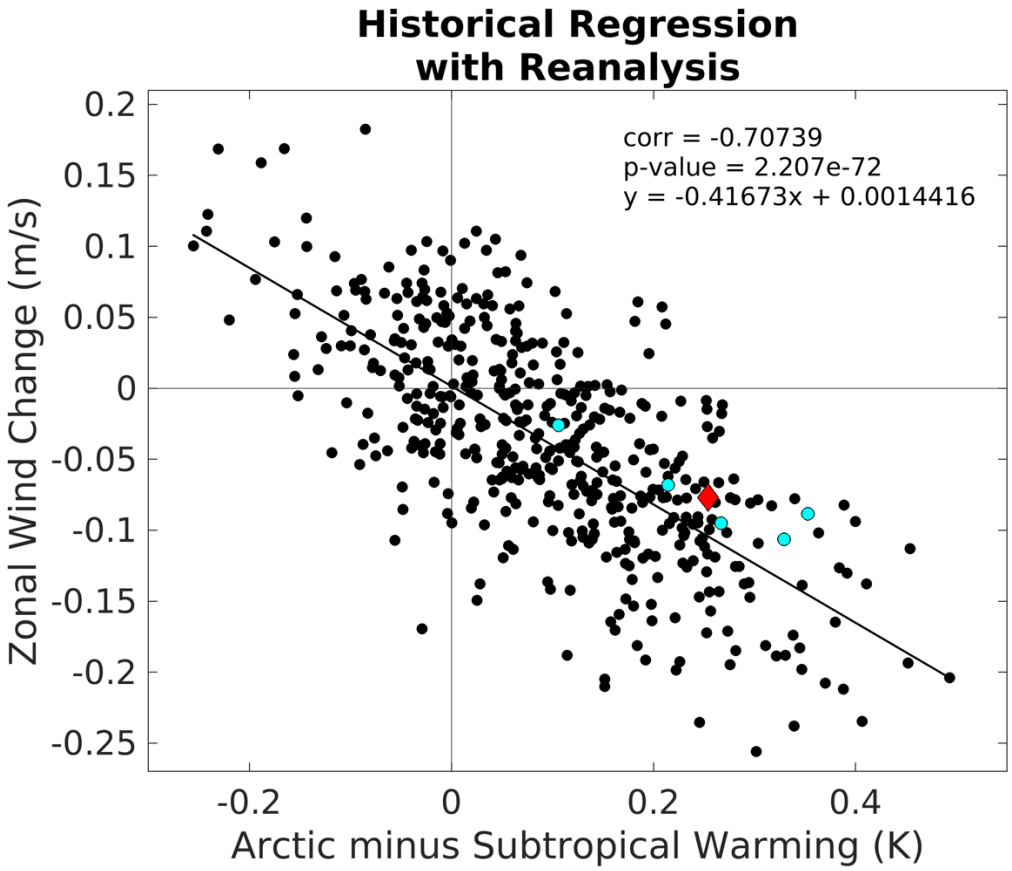

Figure 31: Scatterplot of all ensemble members of the historical simulations (as in Figure 16) with each reanalysis (blue circles) and the reanalysis average (red diamond) overlaid.

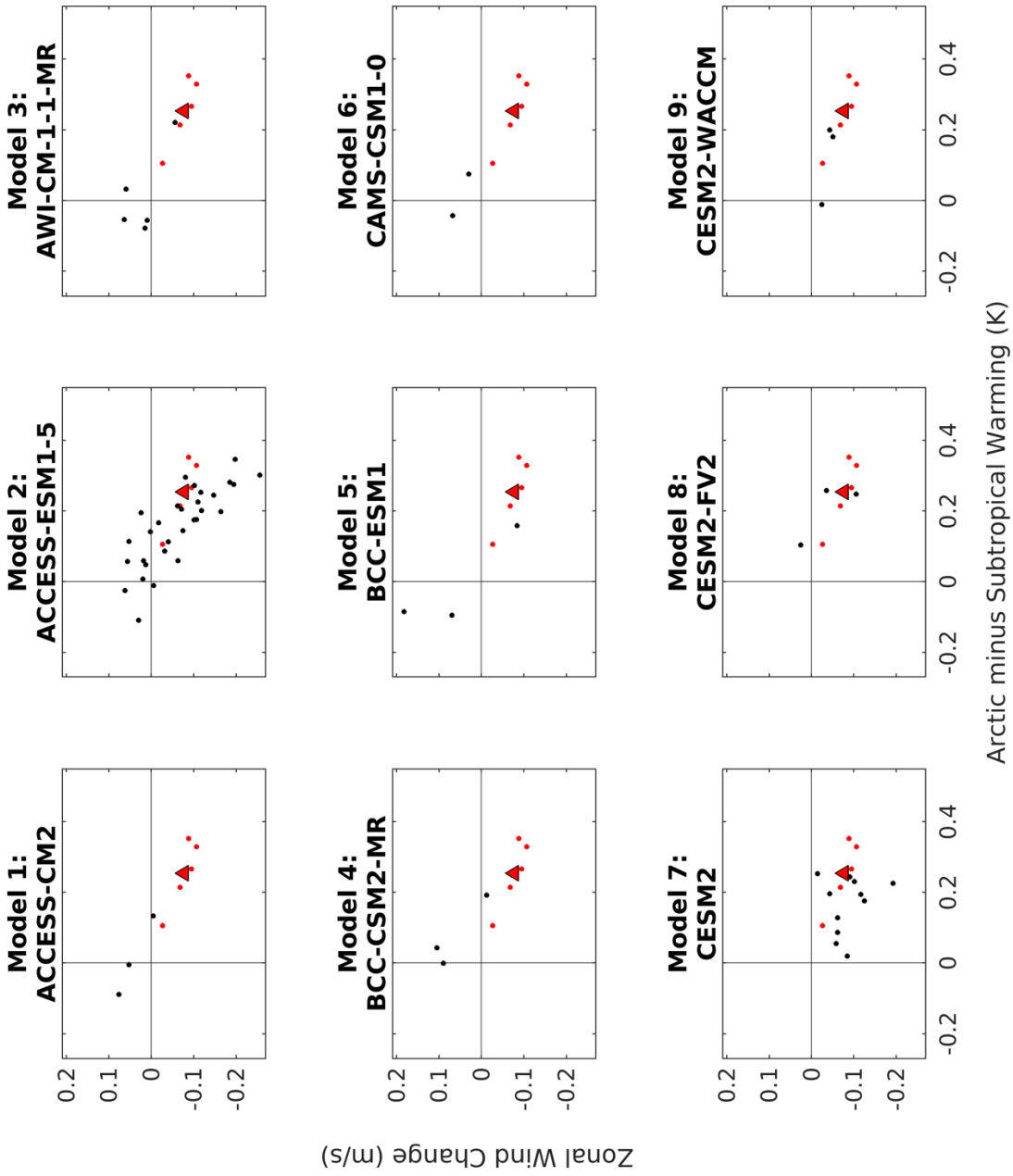

Figure 32: Each model's ensemble with the reanalysis average (red triangle) and each reanalysis (red dots) overlaid for models 1 through 9 of 45.

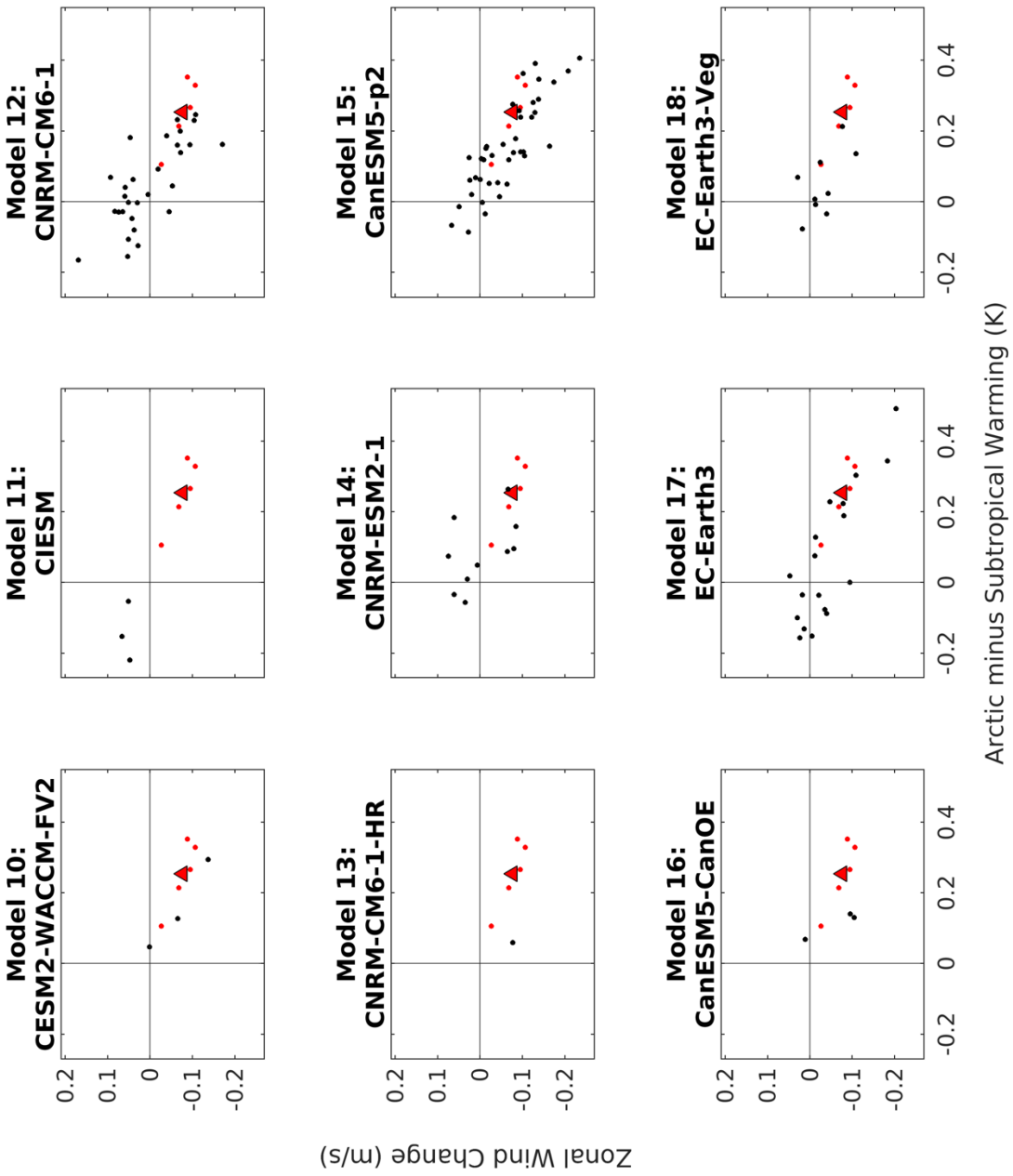

Figure 33: As in Figure 32, but for models 10 through 18 of 45.

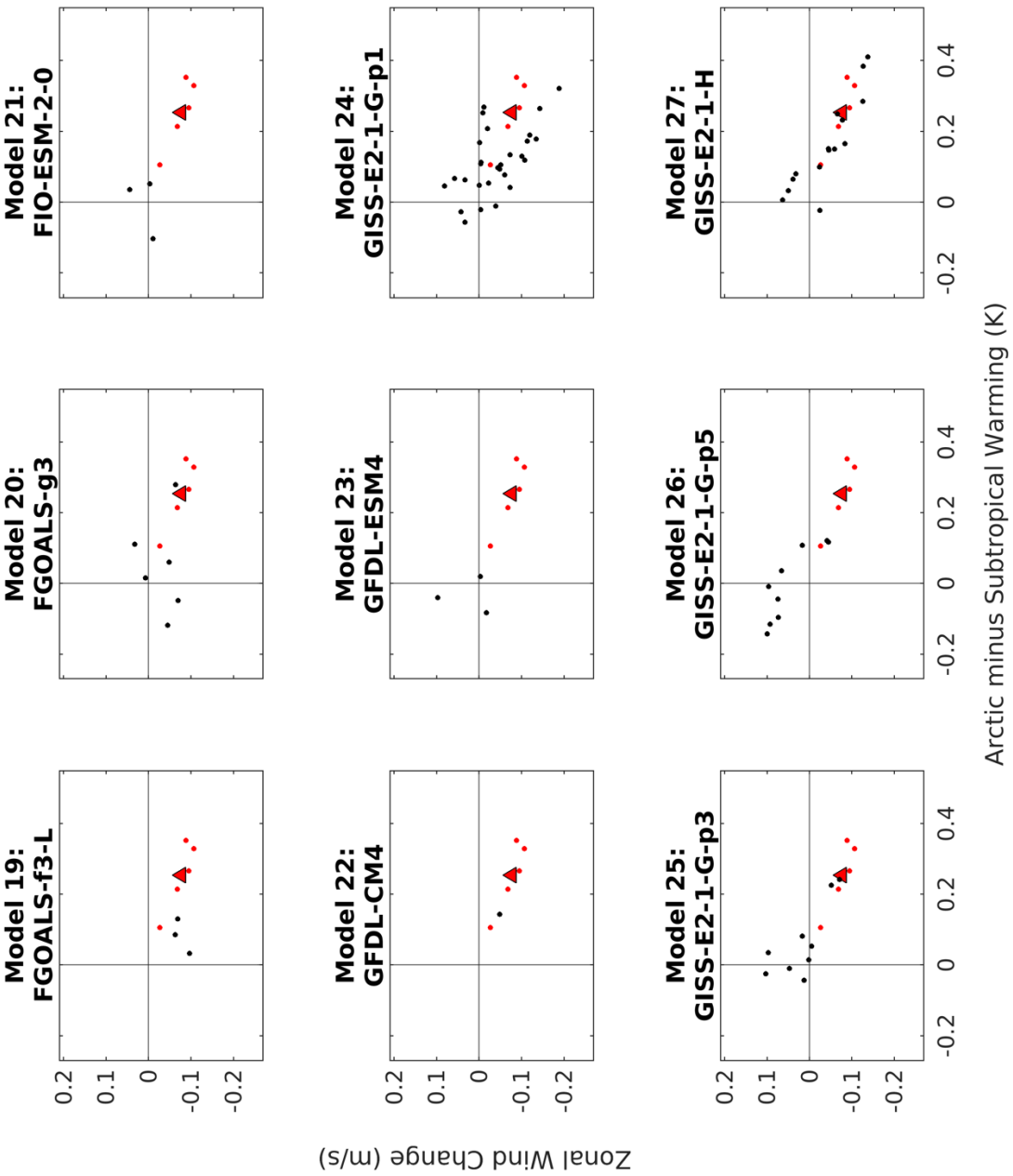

Figure 34: As in Figure 32, but for models 19 through 27 of 45.

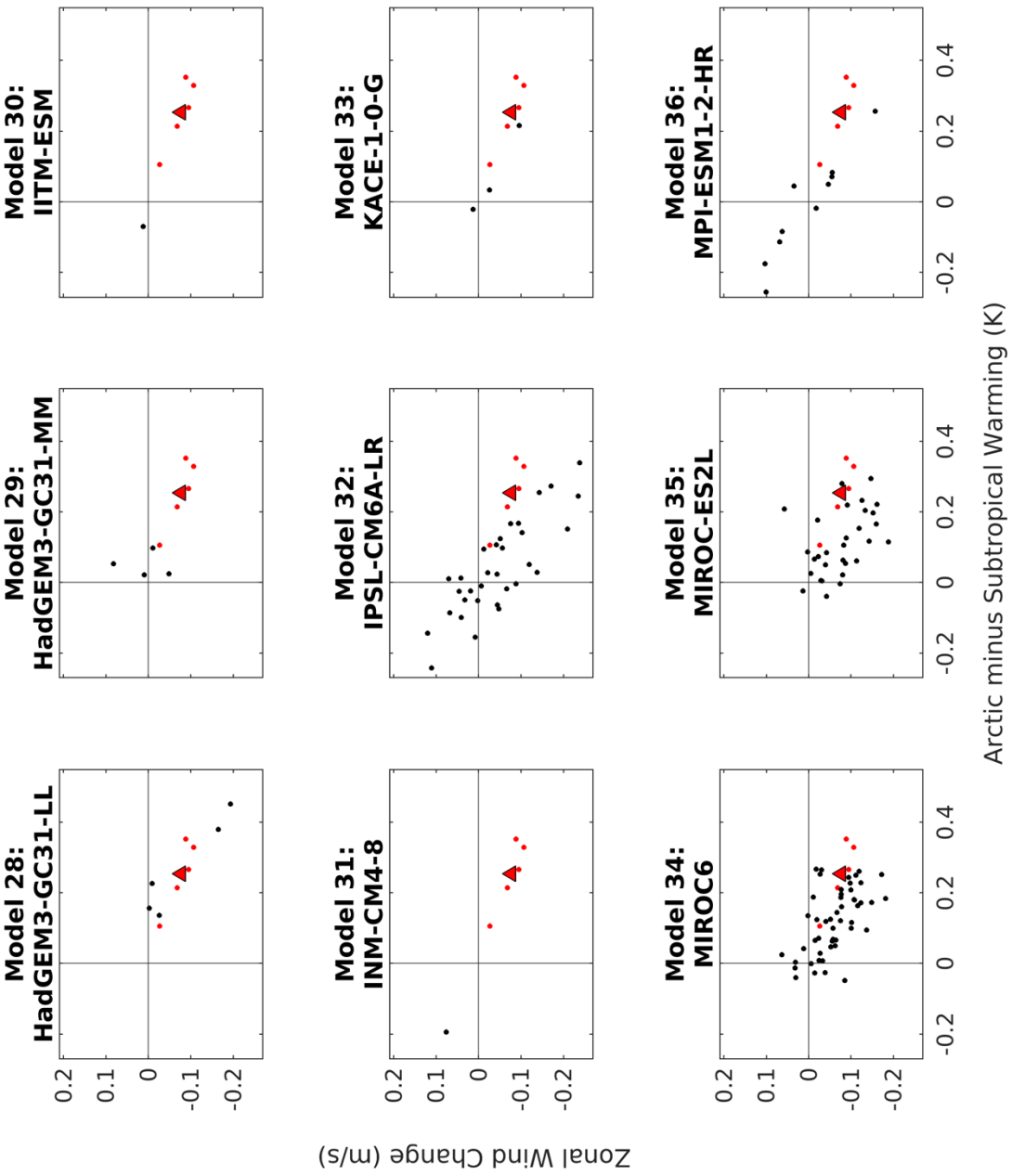

Figure 35: As in Figure 32, but for models 28 through 36 of 45.

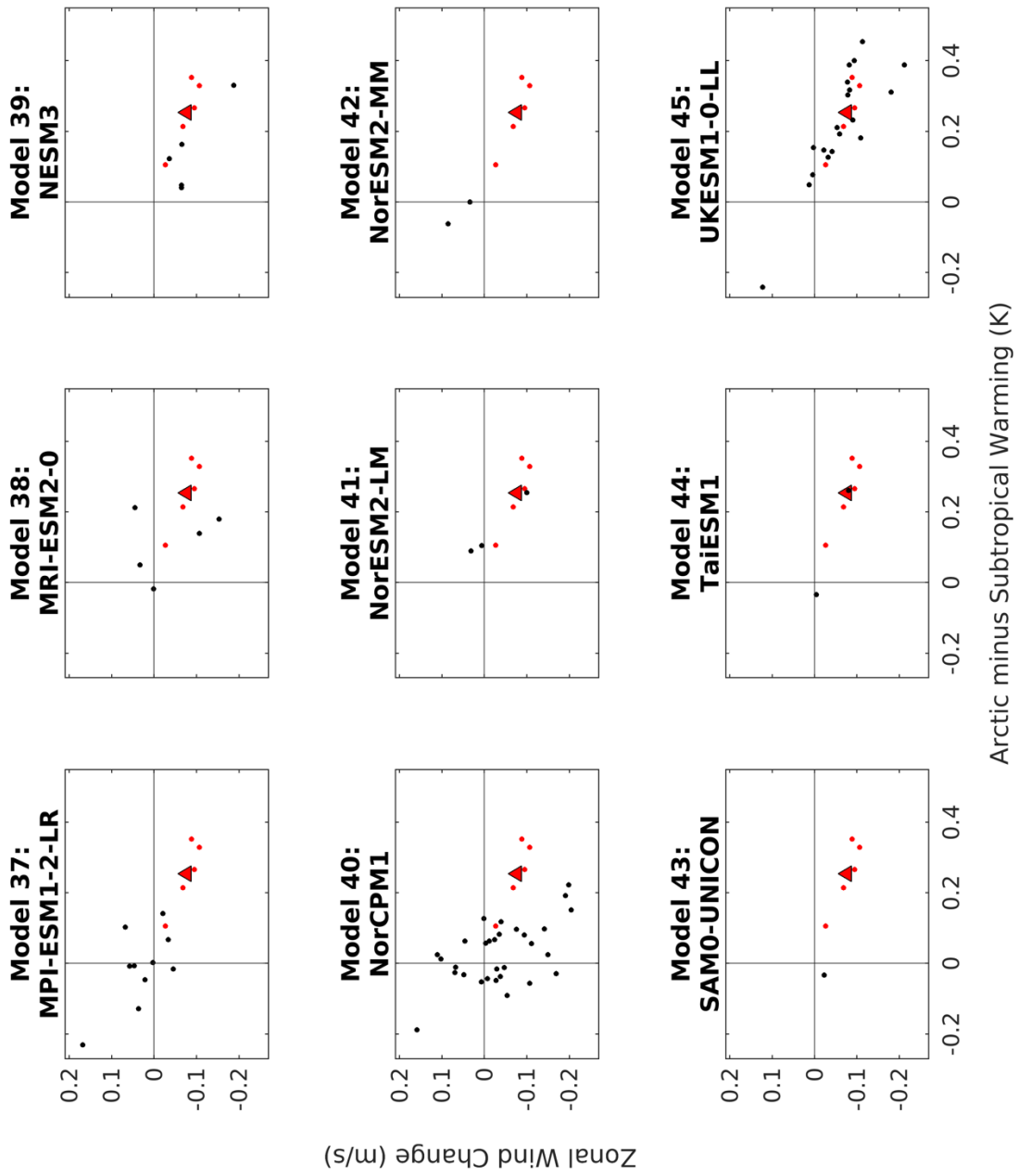

Figure 36: As in Figure 32, but for models 37 through 45.

Table 3: Results of the two-sample t-test for the reanalysis warming difference and zonal wind change, and for the observed satellite MSU warming difference. Models that can be discarded are highlighted red.

Model Name	Reanalysis warming difference p-values	Reanalysis zonal wind change p-values	Satellite MSU warming difference p-values
ACCESS-CM2	0.2043	0.1351	0.1043
ACCESS-ESM1-5	0.3994	0.8970	0.3678
AWI-CM-1-1-MR	0.1506	0.1478	0.1815
BCC-CSM2-MR	0.2712	0.2035	0.0380
BCC-ESM1	0.2559	0.4808	0.2035
CAMS-CSM1-0	0.2574	0.1625	0.0984
CESM2	0.3132	0.8517	0.1580
CESM2-FV2	0.6652	0.6629	0.1089
CESM2-WACCM	0.4332	0.1340	0.4415
CESM2-WACCM-FV2	0.5727	0.9116	0.3979
CIESM	0.0549	0.0070	0.0529
CNRM-CM6-1	0.1092	0.3131	0.0756
CNRM-CM6-1-HR	N/A	N/A	N/A
CNRM-ESM2-1	0.1367	0.3011	0.0544
CanESM5	0.4583	0.8598	0.4383
CanESM5-CanOE	0.0892	0.8714	0.3582
EC-Earth3	0.3586	0.6552	0.4459
EC-Earth3-Veg	0.0672	0.3369	0.0392
FGOALS-f3-L	0.0942	0.9715	0.0874
FGOALS-g3	0.2309	0.3536	0.1159
FIO-ESM-2-0	0.1193	0.1261	0.1479
GFDL-CM4	N/A	N/A	N/A
GFDL-ESM4	0.0396	0.2927	0.0226
GISS-E2-1-G-p1	0.1598	0.5865	0.0990
GISS-E2-1-G-p3	0.1203	0.1712	0.0733
GISS-E2-1-G-p5	0.0473	0.0727	0.0336
GISS-E2-1-H	0.5056	0.6126	0.2675
HadGEM3-GC31-LL	0.9179	0.9825	0.8188
HadGEM3-GC31-MM	0.0141	0.2622	0.0214
IITM-ESM	N/A	N/A	N/A
INM-CM4-8	N/A	N/A	N/A
IPSL-CM6A-LR	0.1241	0.7405	0.1846
KACE-1-0-G	0.3402	0.5855	0.3779
MIROC6	0.1618	0.7681	0.0826
MIROC-ES2L	0.1390	0.9882	0.1840
MPI-ESM1-2-HR	0.1180	0.3849	0.0668
MPI-ESM1-2-LR	0.0442	0.1340	0.0219
MRI-ESM2-0	0.2476	0.6962	0.0571
NESM3	0.4315	0.9204	0.2252
NorCPM1	0.0181	0.6893	0.0607
NorESM2-LM	0.4296	0.5569	0.3490
NorESM2-MM	0.1195	0.2003	0.2003
SAM0-UNICON	N/A	N/A	N/A
TaiESM1	0.6804	0.6925	N/A
UKESM1-0-LL	0.8398	0.8497	0.4543

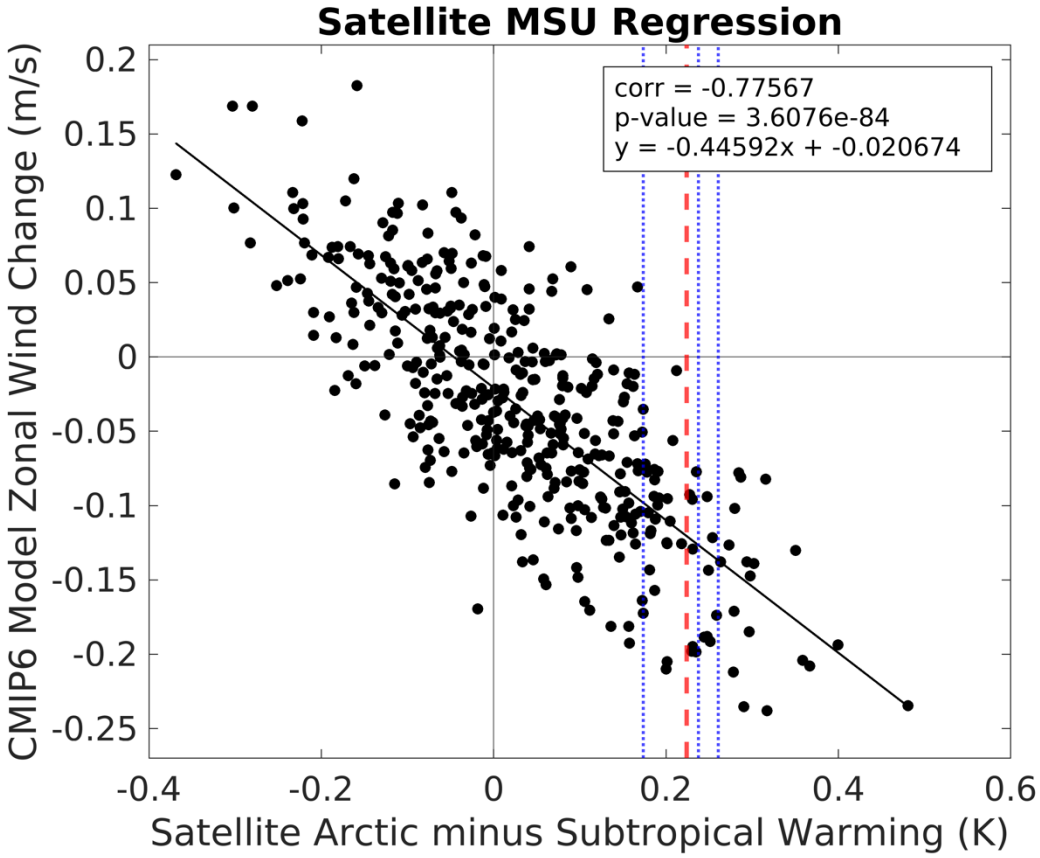

Figure 37: All ensemble members of synthetic MSU warming difference versus CMIP6 historical zonal wind change, with each observed MSU product (blue dotted lines) and the average of the observed MSU temperature data (red dashed line) overlaid.

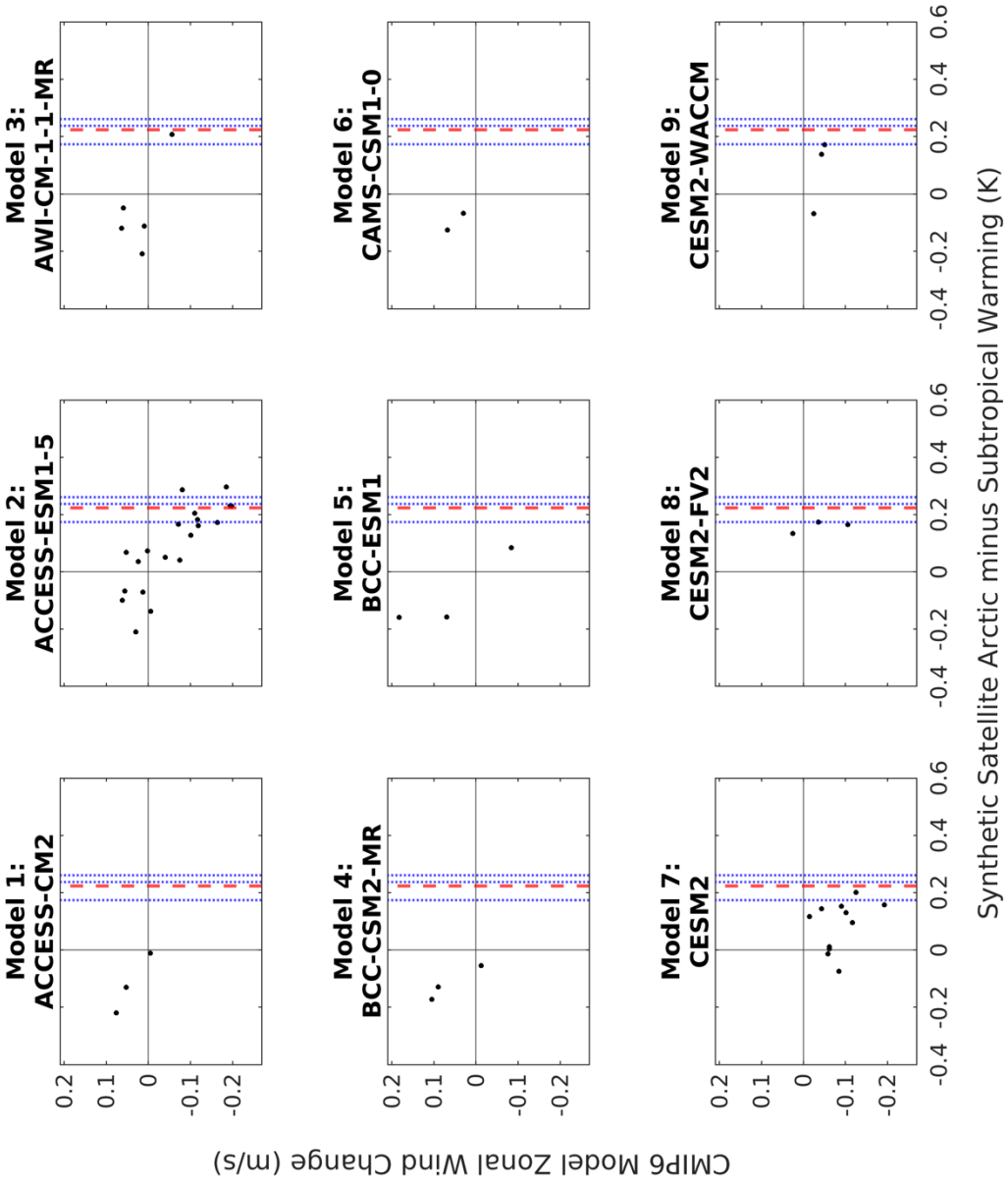

Figure 38: Each model's ensemble of synthetic MSU warming difference versus CMIP6 historical zonal wind change, with the average of the observed MSU temperature data (red dashed line) overlaid for models 1 through 9 of 44.

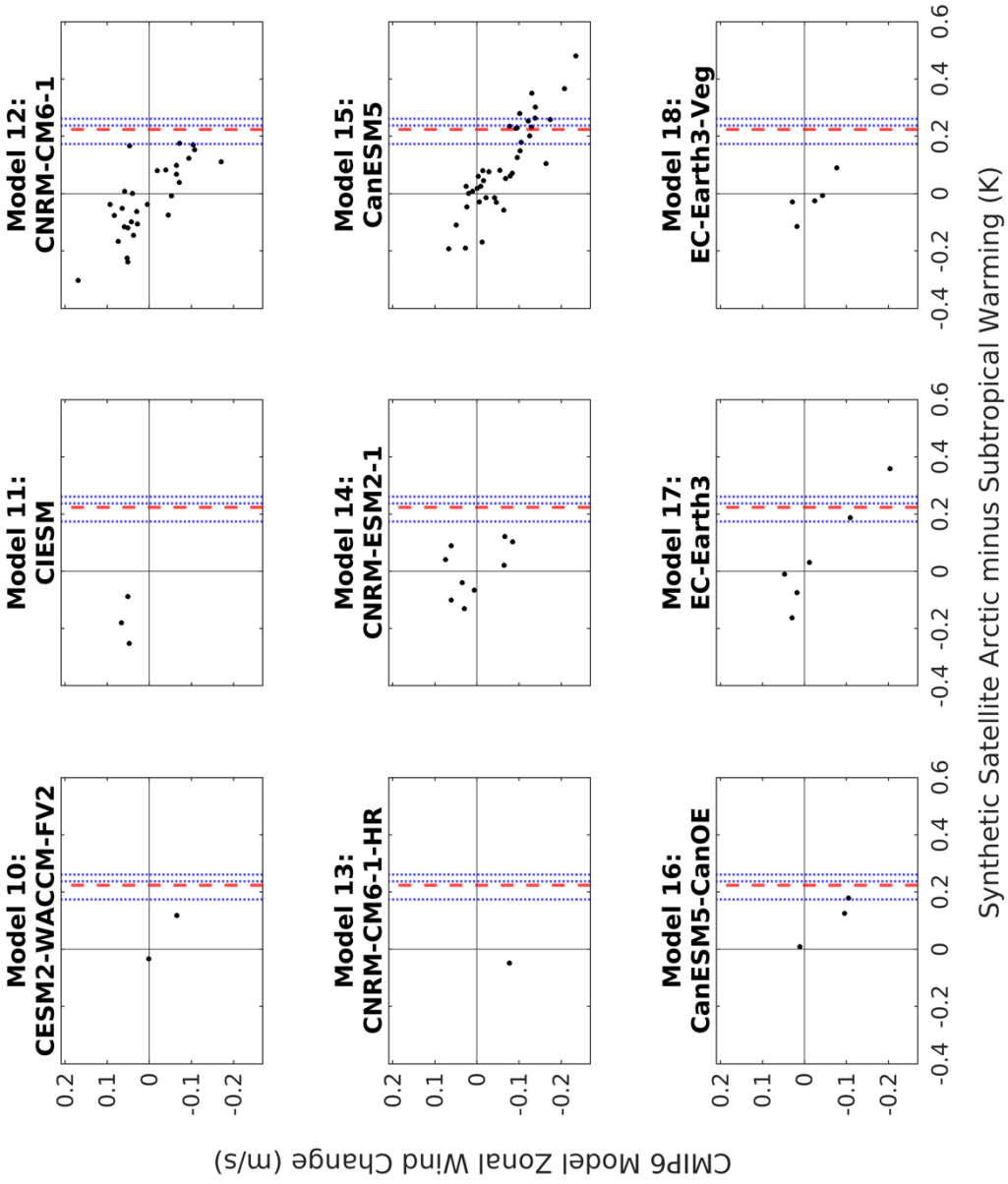

Figure 39: As in Figure 38, but for models 10 through 18 of 44.

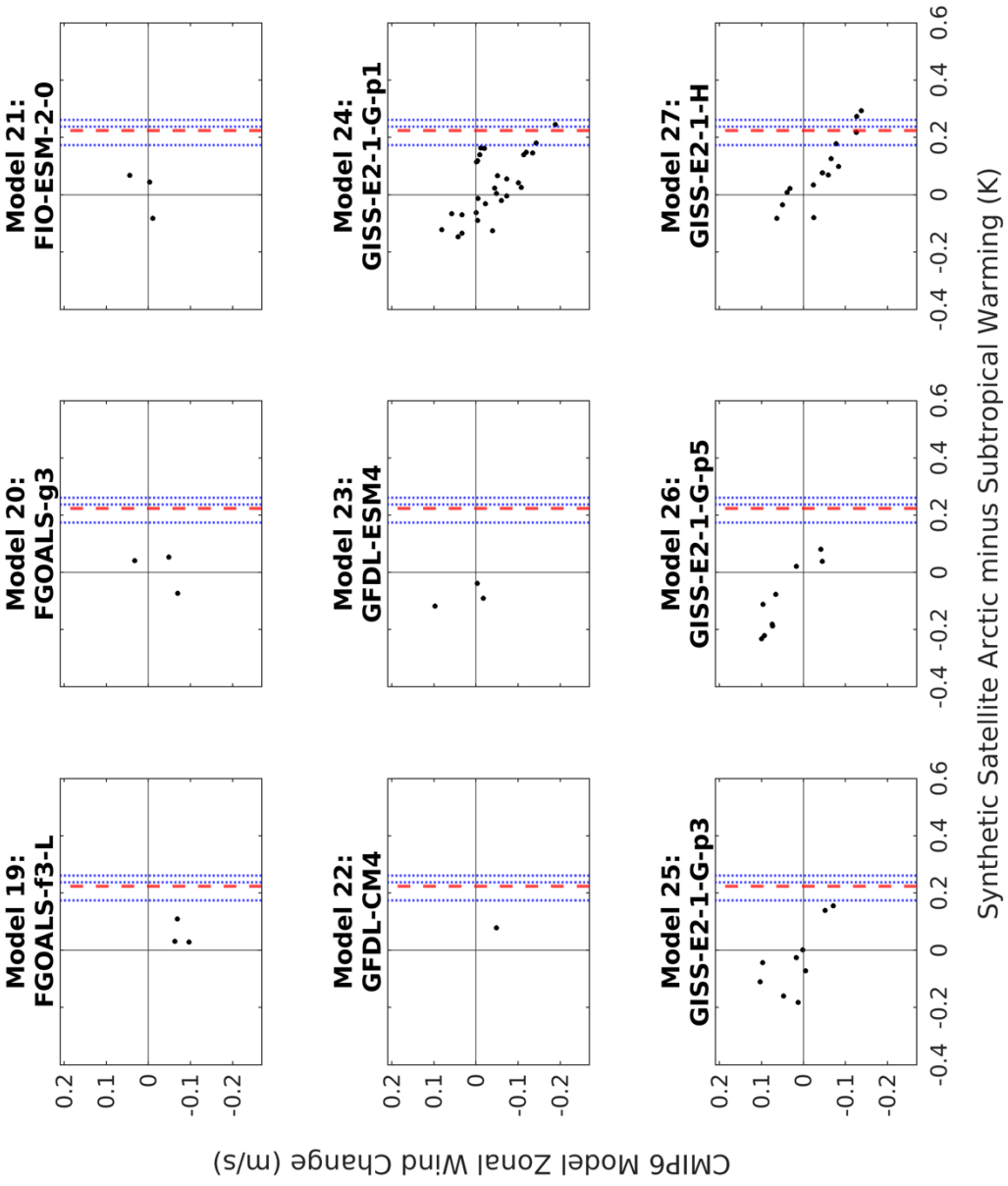

Figure 40: As in Figure 38, but for models 19 through 27 of 44.

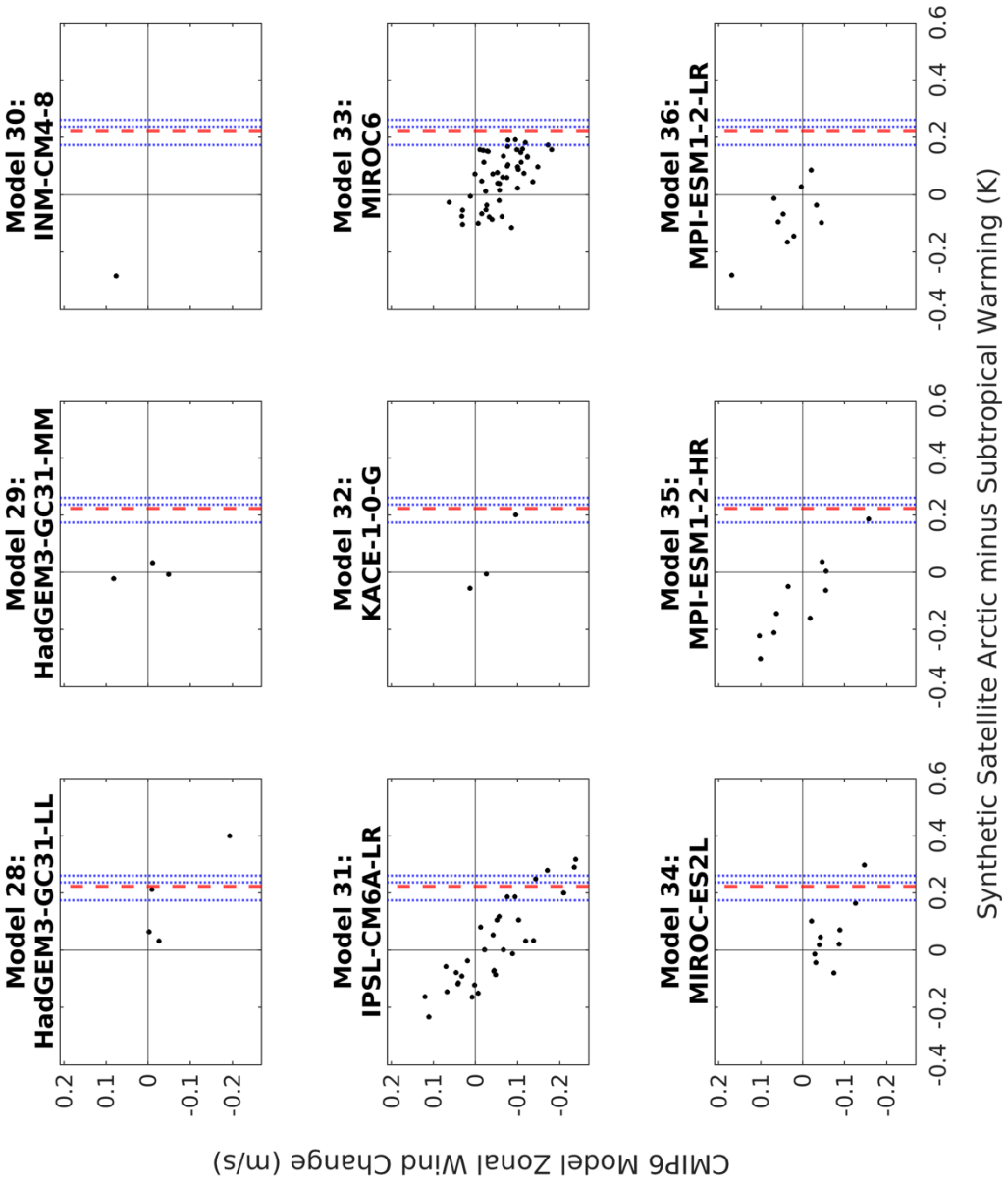

Figure 41: As in Figure 38, but for models 28 through 36 of 44.

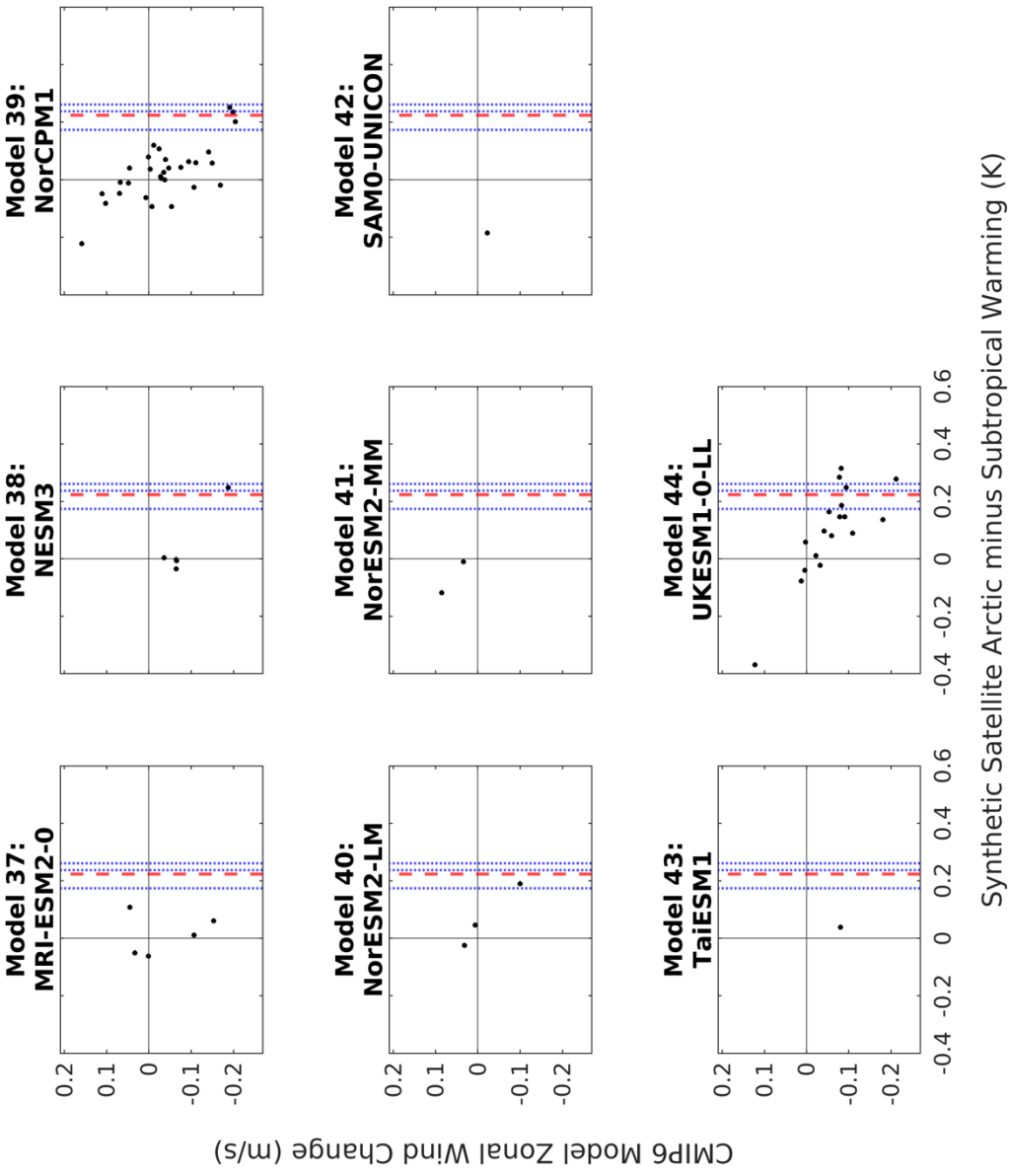

Figure 42: As in Figure 38, but for models 37 through 44.

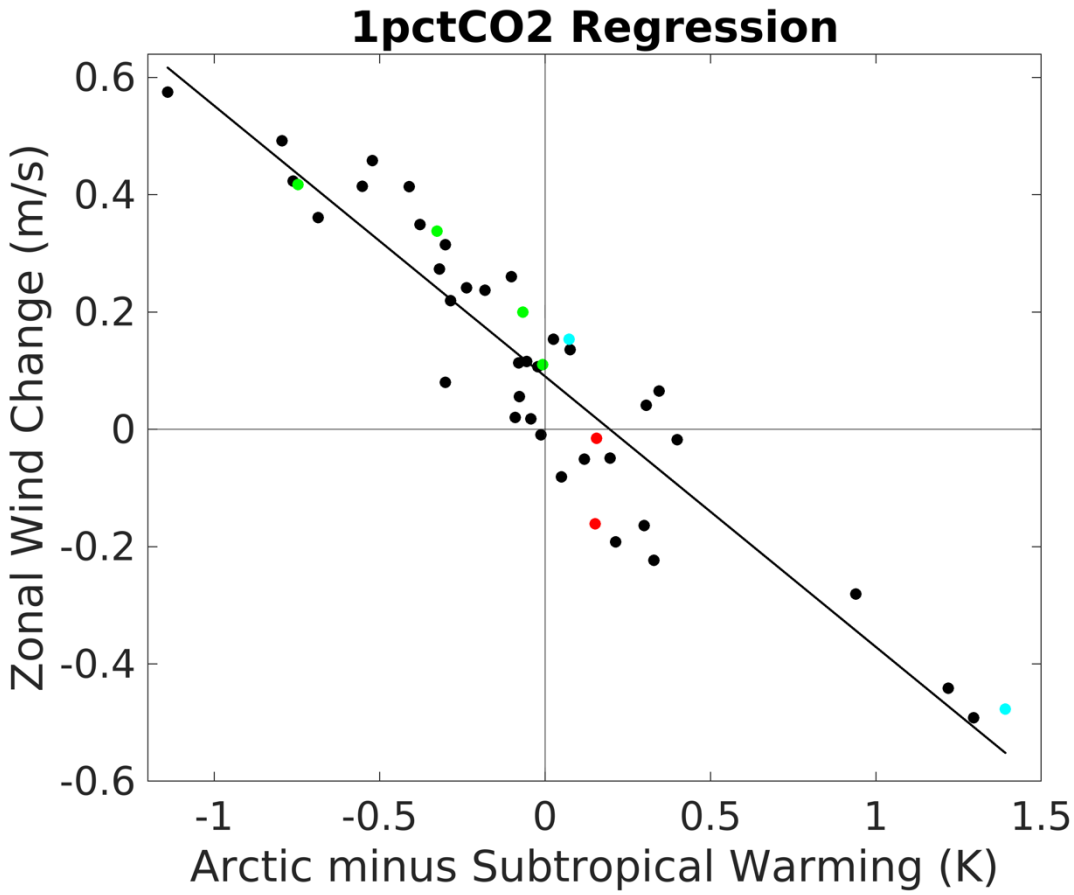

Figure 43: As in Figure 14, but with the models ruled out by reanalysis in red, the models ruled out by satellite MSU in cyan, and the models ruled out by both reanalysis and satellite MSU in green.

REFERENCES

Barnes, E.A., Dunn-Sigouin, E., Masato, E., Woolings, T., 2014: Exploring recent trends in Northern Hemisphere blocking. *Geophys. Res. Lett*., **41**, 638-644, https://doi.org/10.1002/2013GL058745.

Barnes, E. A. and Polvani, L., 2013: Response of the Midlatitude Jets, and of Their Variability, to Increased Greenhouse Gases in the CMIP5 Models, *J. Climate*, **26**, 7117-7135, https://doi.org/10.1175/JCLI-D-12-00536.1.

Barnes, E.A., and Polvani L.M., 2015: CMIP5 Projections of Arctic Amplification, of the North American/North Atlantic Circulation, and of Their Relationship. *J. Climate*, **28**, 5254-5271, https://doi.org/10.1175/JCLI-D-14-00589.1.

Barnes, E.A. and Screen, J.A., 2015: The impact of Arctic warming on the midlatitude jet-stream: Can it? Has it? Will it? *WIREs Clim. Change*, **6**, 277-286, https://doi.org/10.1002/wcc.337.

Berrisford, P and Coauthors (2011). ERA report series. The ERA-Interim archive Version 2.0. https://www.ecmwf.int/file/21498/download?token=cr31Wrx8.

Butler, A.H., Thompson, D.W.J., Heikes, R., 2010: The Steady-State Atmospheric Circulation Response to Climate Change–like Thermal Forcings in a Simple General Circulation Model. *J. Climate*, **23**, 3474-3496, https://doi.org/10.1175/2010JCLI3228.1.

Cattiaux, J., Peings, Y., Saint-Martin, D., Trou-Kechout, N., Vavrus, S.J., 2016: Sinuosity of midlatitude atmospheric flow in a warming world, *Geophys. Res. Lett*., **43**, 8259-8268, https://doi.org/10.1002/2016GL070309.

Ceppi, P., Hartmann, D.L., 2016: Clouds and the Atmospheric Circulation Response to Warming. *J. Climate*, **29**, 783-799, https://doi.org/10.1175/JCLI-D-15-0394.1.

Coumou, D., Petoukhov, V., Rahmstorf, S., Petri, S., and Schellnhuber, H., 2014: Quasi-resonant circulation regimes and hemispheric synchronization of extreme weather in boreal summer. *Proc. Natl. Acad. Sci. USA*, **111**, 12331-12336, https://doi.org/10.1073/pnas.1412797111.

Delcambre, S.C., Lorenz, D.J., Vimont, D.J., Martin, J.E., 2013: Diagnosing Northern Hemisphere Jet Portrayal in 17 CMIP3 Global Climate Models: Twenty-First-Century Projections. *J. Climate*, **26**, 4930-4946, https://doi.org/10.1175/JCLI-D-12-00359.1.

Deser, C., Tomas, R.A., Sun, L., 2015: The Role of Ocean–Atmosphere Coupling in the Zonal-Mean Atmospheric Response to Arctic Sea Ice Loss. *J. Climate*, **28**, 2168-2186, https://doi.org/10.1175/JCLI-D-15-0394.1.

Eyring, V. and Coauthors, 2016: Overview of the Coupled Model Intercomparison Project Phase 6 (CMIP6) experimental design and organization. *Geosci. Model Dev*., **9**, 1937-1958, https://doi.org/10.5194/gmd-9-1937-2016.

Feldstein, S.B., and Lee, S., 2014: Intraseasonal and Interdecadal Jet Shifts in the Northern Hemisphere: The Role of Warm Pool Tropical Convection and Sea Ice. *J. Climate*, **27**, 6497-6518, https://doi.org/10.1175/JCLI-D-14-00057.1.

Francis, J.A., 2015: The Arctic matters: extreme weather responds to diminished Arctic Sea ice. *Environ. Res. Lett*., **10**, 091002, https://doi.org/10.1088/1748-9326/10/9/091002.

Francis, J.A., 2017: Why Are Arctic Linkages to Extreme Weather Still Up in the Air? *Bull. Amer. Meteor. Soc*., **98**, 2551-2557, https://doi.org/10.1175/BAMS-D-17-0006.1.

Francis, J.A., and Vavrus, S.J., 2012: Evidence linking Arctic amplification to extreme weather in mid-latitudes. *Geophys. Res. Lett*., **39**, L06801, https://doi.org/10.1029/2012GL051000.

Francis, J.A. and Vavrus, S.J., 2015: Evidence for a wavier jet stream in response to rapid Arctic warming. *Environ. Res. Lett*., **10**, 014005, https://doi.org/10.1088/1748-9326/10/1/014005.

Fu, Q., Manabe, S., and Johanson, C.M., 2011: On the warming in the tropical upper troposphere: Models versus observations: ON TROPICAL UPPER TROPOSPHERIC WARMING. *Geophys. Res. Lett*., **38**, L15704, https://doi.org/10.1029/2011GL048101.

Gelaro, R., and Coauthors, 2017: The Modern-Era Retrospective Analysis for Research and Applications, Version 2 (MERRA-2). *J. Climate*, **30**, 5419-5454, https://doi.org/10.1175/JCLI-D-16-0758.1.

Golden, N., 2020: Very Strong Correlation Between Northern Hemisphere Jet Response and Arctic-minus-subtropical Warming Across CMIP5 Models. M.S. thesis, Dept. of Geography and Earth Sciences, University of North Carolina at Charlotte.

Graversen, R.G., Mauritsen, T., Tjernström, M., Kallen, E., Svensson, G., 2008: Vertical structure of recent Arctic warming. *Nature*, **451**, 53-56, https://doi.org/10.1038/nature06502.

Harvey, B.J., Cook, P., Shaffrey, L.C., Schiemann, R., 2020: The response of the northern hemisphere storm tracks and jet streams to climate change in the CMIP3, CMIP5, and CMIP6 climate models. *J. Geophys. Res. Atmos*., **125**, e2020JD032701, https://doi.org/10.1029/2020JD032701.

Harvey, B.J., Shaffrey, L.C. & Woollings, T.J, 2015: Deconstructing the climate change response of the Northern Hemisphere wintertime storm tracks. *Clim. Dyn.*, **45**, 2847-2860, https://doi.org/10.1007/s00382-015-2510-8.

Hassanzadeh, P., and Kuang, Z., 2015: Blocking variability: Arctic Amplification versus Arctic Oscillation. *Geophys. Res. Lett*., **42**, 8586-8595, https://doi.org/10.1002/2015GL065923.

Hersbach, H, Bell, B, Berrisford, P, et al., 2020: The ERA5 global reanalysis. *Q. J. R. Meteorol. Soc*., **146**, 1999-2049, https://doi.org/10.1002/qj.3803.

Jansen, E., Christensen, J.H., Dokken, T. et al., 2020: Past perspectives on the present era of abrupt Arctic climate change. *Nat. Clim. Chang.*, **10**, 714-721, https://doi.org/10.1038/s41558-020-0860-7.

Kobayashi, S., and Coauthors, 2015: The JRA-55 Reanalysis: General Specifications and Basic Characteristics. *J. Meteor. Soc. of Japan*, **93**, 5-48, https://doi.org/10.2151/jmsj.2015-001.

Lachmy, O. and Shaw, T., 2018: Connecting the Energy and Momentum Flux Response to Climate Change Using the Eliassen–Palm Relation. *J. Climate*, **31**, 7401-7416, https://doi.org/10.1175/JCLI-D-17-0792.1.

Li, Y., Thompson, D.W.J., Bony, S., Merlis, T.M., 2019: Thermodynamic Control on the Poleward Shift of the Extratropical Jet in Climate Change Simulations: The Role of Rising High Clouds and Their Radiative Effects, *J. Climate*, **32**, 917-934, https://doi.org/10.1175/JCLI-D-18-0417.1.

Lorenz, D. J., 2014: Understanding Midlatitude Jet Variability and Change Using Rossby Wave Chromatography: Poleward-Shifted Jets in Response to External Forcing. *J. Atmos. Sci*., **71**, 2370-2389, https://doi.org/10.1175/JAS-D-13-0200.1.

Lorenz, D.J. and DeWeaver, E.T., 2007: Tropopause height and zonal wind response to global warming in the IPCC scenario integrations, *J. Geophys. Res*., **112**, D10119, https://doi.org/10.1029/2006JD008087.

Manney, G.L. and Hegglin, M.I., 2018: Seasonal and Regional Variations of Long-Term Changes in Upper-Tropospheric Jets from Reanalyses. *J. Climate*, **31**, 423-448, https://doi.org/10.1175/JCLI-D-17-0303.1.

Matsumura, S., Ueki, S., & Horinouchi, T., 2019: Contrasting responses of midlatitude jets to the North Pacific and North Atlantic warming. *Geophys. Res. Lett.*, **46**, 3973-3981, https://doi.org/10.1029/2019GL082550.

Mears, C.A., Wentz, F.J., 2016: Sensitivity of satellite-derived tropospheric temperature trends to the diurnal cycle adjustment, *J. Clim.* **5**, 3629–3646, https://doi.org/10.1175/JCLI-D-15-0744.1.

Peings, Y., Cattiaux, J., Vavrus, S.J., Magnusdottir, G., 2018: Projected squeezing of the wintertime North-Atlantic jet. *Environ. Res. Lett.*, **13**, 1-11, https://doi.org/10.1088/1748-9326/aacc79.

Po-Chedley, S., and Coauthors, 2021: Natural variability contributes to model–satellite differences in tropical tropospheric warming. *Proc. Natl. Acad. Sci. U.S.A*, **118**, e2020962118, https://doi.org/10.1073/pnas.2020962118.

Po-Chedley, S., Thorsen, T.J., Fu, Q., 2015: Removing diurnal cycle contamination in satellite-derived tropospheric temperatures: Understanding tropical tropospheric trend discrepancies. *J. Clim.* **28**, 2274-2290, https://doi.org/10.1175/JCLI-D-13-00767.1.

Saha, S., and Coauthors, 2014: The NCEP Climate Forecast System Version 2. *J. Climate*, **27**, 2185-2208, https://doi.org/10.1175/JCLI-D-12-00823.1.

Santer, B.D. et al., 2013: Identifying human influences on atmospheric temperature. *Proc. Natl. Acad. Sci. USA*, **110**, 26-33, https://doi.org/10.1073/pnas.1210514109.

Santer, B.D. et al., 2018: Human influence on the seasonal cycle of tropospheric temperature. *Science*, **361**, 1-11, http://dx.doi.org/10.1126/science.aas8806.

Schneider, T., Bischoff, T., Plotka, H., 2014: Physics of changes in synoptic midlatitude temperature variability. *J. Clim.*, **28**, 2312-2331, https://doi.org/10.1175/JCLI-D-14-00632.1.

Screen, J.A., 2014: Arctic amplification decreases temperature variance in northern mid- to high-latitudes. *Nat Clim Change*, **4**, 577-582, https://doi.org/10.1038/nclimate2268.

Screen, J.A., Bracegirdle, T.J. & Simmonds, I., 2018: Polar Climate Change as Manifest in Atmospheric Circulation. *Curr. Clim. Change Rep.,* **4**, 383-395, https://doi.org/10.1007/s40641-018-0111-4.

Screen, J.A., Deser, C., Sun, L., 2014: Reduced risk of North American cold extremes due to continued Arctic sea ice loss. *Bull. Am. Meteorol. Soc*., **96**, 1489-1503, https://doi.org/10.1175/BAMS-D-14-00185.1.

Shaw, T.A., Tan, Z., 2018: Testing Latitudinally Dependent Explanations of the Circulation Response to Increased CO2 Using Aquaplanet Models. *Geophys. Res. Lett.*, **45**, 9861-9869. https://doi.org/10.1029/2018GL078974.

Slivinski, L. C., and Coauthors, 2019: Towards a more reliable historical reanalysis: Improvements for version 3 of the Twentieth Century Reanalysis system. *Q.J.R. Meteorol. Soc.*, qj.3598, https://doi.org/10.1002/qj.3598.

Spencer, R.W., Christy, J.R., Braswell, W.D, 2017: UAH Version 6 global satellite temperature products: Methodology and results. *Asia. Pac. J. Atmos. Sci.* **53**, 121-130, https://doi.org/10.1007/s13143-017-0010-y.

Staten, P.W., Lu, J., Grise, K.M., Davis, S.M., Birner, T., 2018: Re-examining tropical expansion. *Nature Clim. Change,* **8**, 768-775, https://doi.org/10.1038/s41558-018-0246-2.

Sun, L., Perlwitz, J., Hoerling, M., 2016: What caused the recent "Warm Arctic, Cold Continents" trend pattern in winter temperatures? *Geophys. Res. Lett*., **43**, 5345-5352, https://doi.org/10.1002/2016GL069024.

Thorne, P., 2008: Arctic tropospheric warming amplification? *Nature,* **455**, E1-E2, https://doi.org/10.1038/nature07256.

Trenberth, K.E., Fasullo, J.T., Branstator G., Phillips A.S., 2014: Seasonal aspects of the recent pause in surface warming. *Nat. Clim. Change*, **4**, 911-916, https://doi.org/10.1038/nclimate2341.

Wallace, J.M., Held, I.M., Thompson, D.W.J., Trenberth, K.E., Walsh, J.E., 2014: Global Warming and Winter Weather. *Science*, **343**, 729-730, https://doi.org/10.1126/science.343.6172.729.

Yim, B.Y., Min, H.S., and Kug, J.-S., 2016: Inter-model diversity in jet stream changes and its relation to Arctic climate in CMIP5. *Clim. Dyn.*, **47**, 235-248, https://doi.org/10.1007/s00382-015-2833-5.

Yin, J. H., 2005: A consistent poleward shift of the storm tracks in simulations of 21st century climate, *Geophys. Res. Lett*., **32**, L18701, https://doi.org/10.1029/2005GL023684.